CELL ENTRAPMENT FOR MITIGATING FOULING IN MEMBRANE BIOREACTORS TREATING DOMESTIC WASTEWATER

A Dissertation
Submitted to the Graduate Faculty
of the
North Dakota State University
of Agriculture and Applied Science

By

Chaipon Juntawang

In Partial Fulfillment of the Requirements
for the Degree of
DOCTOR OF PHILOSOPHY

Major Program:
Environmental and Conservation Sciences

October 2017

Fargo, North Dakota

North Dakota State University
Graduate School

Title

CELL ENTRAPMENT FOR MITIGATING FOULING IN MEMBRANE BIOREACTORS TREATING DOMESTIC WASTEWATER

By

Chaipon Juntawang

The Supervisory Committee certifies that this ***disquisition*** complies with North Dakota State University's regulations and meets the accepted standards for the degree of

DOCTOR OF PHILOSOPHY

SUPERVISORY COMMITTEE:

Dr. Eakalak Khan
Chair

Dr. Achintya Bezbaruah

Dr. Craig Stockwell

Dr. Chad Ulven

Approved:

April 5, 2018 — Date

Dr. Craig Stockwell — Department Chair

ABSTRACT

Membrane bioreactors (MBRs) have been a process of choice for wastewater treatment and reuse because of several advantages over conventional process (activated sludge) including superior quality effluent, less biomass yields and more compact design. However, membrane fouling is a major drawback that hampers widespread and full-scale applications of MBRs. Cell entrapment is a relatively new wastewater treatment process. It involves cells artificially entrapped in a porous polymer matrix. In this dissertation research, three versions of entrapped cells-based MBR processes, aerobic MBR, anaerobic MBR and anaerobic forward osmosis (FO) MBR, were developed by using polyvinyl alcohol as a cell entrapment matrix. Their domestic wastewater treatment performances and fouling characteristics were tested and compared with their suspended cells-based MBR counterparts. For aerobic and anaerobic MBRs, entrapped cells-based processes provided similar organic removal but experienced delayed fouling compared to suspended cells-based processes. The entrapment diminished bound extracellular polymeric substances (bEPS) and soluble microbial products (SMP), which are a main culprit of irreversible fouling through pore blocking. Entrapped cells-based aerobic and anaerobic processes had 5 and 8 times lower pore blocking resistance than corresponding suspended cells-based processes. For anaerobic FOMBR, the entrapment protected cells from reverse salt flux leading to slightly higher organic removal. Lower bEPS and SMP in entrapped cells-based FOMBR led to higher permeate flux compared to suspended cells-based FOMBR. The delayed membrane fouling in entrapped cells-based MBRs means lower costs associated with membrane cleaning processes and longer membrane lifespan. Another contribution of this study is novel knowledge on fouling conditions and mitigation for FOMBR, an emerging wastewater treatment process.

ACKNOWLEDGMENTS

My deepest gratitude goes first and foremost to my adviser, Dr. Eakalak Khan, for providing me the opportunity to work under his supervision. My sincere thanks go to him for constant encouragement and guidance during all phases of my graduate research and education. Throughout the years, I have learned so much from him about science and life, which will be greatly cherished, in my future life.

I would like to thank my committee members Dr. Achintya Bezbaruah, Dr. Craig Stockwell and Dr. Chad Ulven. Without their advices and help, this dissertation would not have been possible. I acknowledge Office of Education Affairs, the Royal Thai Embassy, Washington D.C.; Office of the Civil Service Commission, the Royal Thai Government; Environmental and Conservation Sciences Program and Graduate School of North Dakota State University for financial support.

My gratitude is extended to Chaiwat Rongsayamanont, Prince of Songkla University, Thailand for his guidance and friendly cooperation during my research. I could not have done this work without all my friends in the Environmental laboratory who shared their time, love, and lives. Last but not least, I am forever indebted to my parents, my brother, and my relatives. Without their continuous support and encouragements, I would have a much more difficult time. Knowing they were always behind me helped push me to complete this journey.

TABLE OF CONTENTS

LIST OF TABLES

LIST OF FIGURES

LIST OF ABBREVIATIONS

3DEEM .....Three-dimension excitation emission matrix

AMBR .....Aerobic membrane bioreactor

AG-MBR.....Attached growth membrane bioreactor

AnMBR.....Anaerobic membrane bioreactor

bEPS.....Bound extracellular polymeric substances

BNR .....Biological nutrient removal

BOD .....Biochemical oxygen demand

CAS .....Conventional activated sludge

CIP .....Chemically cleaned in place

COD .....Chemical oxygen demand

COP .....Chemically cleaned out of place

DI .....De-ionized

DO.....Dissolved oxygen

DS .....Draw solution

E-AnMBR.....Entrapped cells-based-anaerobic membrane bioreactor

E-FOMBR.....Entrapped cells-based-anaerobic forward osmosis membrane bioreactor

E-MBR.....Entrapped cells-based-membrane bioreactor

E_x/E_m .....Excitation/emission wavelengths

FI .....Filament index

F/M.....Food to microorganism ratio

FOMBR.....Forward osmosis membrane bioreactor

FS .....Flat sheet membrane

FTIR.....Fourier transform infrared

GPC.....Gel permeation chromatography

HF .....Hollow fiber membrane

HRT.....Hydraulic retention time

ICP .....Internal concentration polarization

iMBR .....Immersed membrane bioreactor

L_t .....The total flux decline in the FOMBR

L_f .....The flux decline due to membrane fouling

L_{in} .....The flux decline due to reversible membrane fouling

L_{in2}.....The flux decline due to irreversible membrane fouling

LMH .....Liter per square meter per hour

M_n.....Number-average molecular weight

M_w .....Weight-average molecular weight

M_w/M_n .....Dispersity index

MB-MBR .....Moving biofilm membrane bioreactor

MBRs .....Membrane bioreactors

MLSS .....Mixed liquor suspended solids

MW .....Molecular weight

MWD .....Molecular weight distribution

NaOCl .....Sodium hypochlorite

NH_3-N .....Ammonia

NO_2-N .....Nitrite

NO_3-N .....Nitrate

NF .....Nanofiltration

OLR.....Organic loading rate

ORP.....Oxidation reduction potential

PSD .....Particles size distribution

PVA.....Polyvinyl alcohol

R_t .....Total resistance

R_m.....Membrane resistance

R_p.....Pore blocking resistance

R_c.....Cake filtration resistance

RO .....Reverse osmosis

RSD .....Reverse solute diffusion

S-AnMBR .....Suspended cells-based-anaerobic membrane bioreactor

S-FOMBR.....Suspended cells-based-anaerobic forward osmosis membrane bioreactor

SCOD.....Soluble chemical oxygen demand

SEM-EDX.....Scanning electron microscopy-energy dispersive X-ray spectroscopy

SMP.....Soluble microbial products

SRT .....Solids retention time

sMBR .....Side-stream membrane bioreactor

S-MBR.....Suspended-cells-based MBR

SS .....Suspended solids

SVI .....Sludge volume index

T .....Tubular membrane

TFC .....Thin film composite

THF .....Tetrahydrofuran

TMP .....Transmembrane pressure

TSS .....Total suspended solids

UF .....Ultrafiltration

WWTP .....Wastewater treatment plant

LIST OF APPENDIX FIGURES

CHAPTER 1: INTRODUCTION

1.1. Background

Membrane bioreactor (MBR) has been a process of choice for wastewater treatment and reuse since the last decade. MBR provides several advantages over conventional activated sludge process (CAS) including superior quality effluent, less biomass yields and more compact design. CAS needs filtration and disinfection after sedimentation tank to produce effluent quality at a similar level given by MBR. This means more space requirements for CAS which already has larger footprints compared to MBR. Thus, MBR is considered as a suitable option for urban areas when stringent regulations for effluent quality have to be met and space is limited or costly.

However, membrane fouling is still a major drawback that hampers widespread and full-scale applications of MBR. Fouling is a reduction of membrane permeability that is originated by adsorption or accumulation of deposits on the surface and/or in the pores of membrane during operation. Loss of membrane permeability results in higher transmembrane pressure (TMP) leading to increase in an operating cost of MBR for keeping a constant permeate flux with an increased applied pressure and frequent chemical cleaning (Verrecht *et al*., 2010; Judd, 2010; Cornel *et al.*, 2003; Zhang *et al.*, 2003).

Fouling, commonly found in submerged MBR operation, is deposition of sludge cake onto membrane surface (cake deposition) and clogging of small deposits within membrane pore (pore blocking). Microbial products including bound extracellular polymeric substances (bEPS) and soluble microbial products (SMP) that are released during utilization, growth and decay of active cells in sludge are currently considered as the predominant cause of cake deposition and pore blocking in MBRs (Wang *et al.*, 2009). bEPS consist of proteins, polysaccharides, nucleic acids, lipids, and humic acids, which are located at or outside the cell surface. SMP are soluble organic

pools that occur during substrate metabolism, cell disintegration/lysis and bEPS hydrolysis (Lee & Rittman, 2002). The primary concern of fouling in long term operation is irreversible fouling as chemical cleaning cannot remove all accumulation from membrane pores. Another concern is more chemical use will damage the membrane texture and shorten the membrane lifetime. Thus, finding a strategy to prevent accumulation of bEPS and SMP on membrane surface is therefore worthy for investigation.

Forward osmosis membrane bioreactor (FOMBR) is an emerging MBR system which can provide the benefits over traditional MBR including less energy requirements, less fouling propensity and better effluent quality. The FOMBR system is driven by the difference in osmotic pressure between the bioreactor and draw solution compartments. However, the main drawback of FOMBR remains as the same as that of MBR which is fouling. Fouling condition found in FOMBR rather differs from MBR because fouling in FOMBR can occur on both sides of the membrane (active layer and support layer sides).

The attached-growth MBR (AG-MBR) has less bEPS and SMP in the system compared to suspended-growth MBR (S-MBR) (Hu *et. al*., 2012), because AG-MBR produced less proteins and less carbohydrates than S-MBR. Khan *et al.* (2012, 2011) compared AG-MBR and moving biofilm membrane bioreactor (MB-MBR) with S-MBR and found that SMP (proteins and carbohydrates) concentration in S-MBR was higher than AG-MBR and MB-MBR resulting in more severe fouling in S-MBR. In addition, Di Trapani *et al*. (2014) and Rodríguez-Hernández *et al*. (2014) reported less fouling in MB-MBR compared to S-MBR. Ng *et al.* (2014, 2012, 2011) reported lower bEPS and SMP in entrapped cell MBRs than those in S-MBR. These previous

studies are in agreement that entrapped cell/biofilm/attached growth MBR have less/slower fouling condition compared to S-MBR. Previous research on fouling in entrapped cell/biofilm/attached growth MBRs is summarized in Table 1-1.

1.2. Research justification

Cell entrapment has potential to reduce fouling in MBR systems (Ng *et al.*, 2014, 2012, 2011). Cell entrapment in polymeric gel is a promising technology which has been widely applied (Konsoula *et al*., 2006) to prevent biomass washout in biological wastewater treatment systems, and to gain improved tolerance or protection of cells from substrate and end product inhibition. Tsen *et al.* (2004) reported the advantages of the entrapment matrices that can provide protection to the cells against unsuitable environment such as toxic compounds or low pH. Moreover, the porosity within the entrapment allows the diffusion of substrates and products across the matrix but prevents the release of cells into the bulk liquid. Polyvinyl alcohol (PVA) has been successfully used as cell entrapment media for wastewater treatment because of high durability and nontoxicity to bacteria. It provides higher specific growth and specific substrate utilization rates than alginate and carrageenan (Pramanik & Khan, 2008). Entrapped cells-based MBR has been investigated but none of the studies specifically explored on how entrapped cells can reduce/delay fouling in MBR systems (Ng *et al*., 2014, 2012, 2011).

This study combines MBR with a cell entrapment technique to produce new wastewater treatment processes. These entrapped cell processes should be able to effectively maintain bacteria in the bioreactor tank preventing cell washout. In addition, they should reduce deposition on membrane surface, which is the main cause of all fouling mechanisms. They are expected to (1) delay fouling of the membrane and (2) be more efficient at removing organic matters and nutrients.

Table 1-1: Previous research on fouling in entrapped cell/biofilm/attached growth MBRs.

System	Media/Carrier	Type of wastewater	Experimental scale	Flux (LMH[1])	COD[2] removal (%)	Test/observed	References
Entrapment/ Immobilization	Cellulose triacetate	Pharmaceutical Synthetic	Lab scale	5-20	30-50%	COD; biomass level; bEPS and SMP; TMP	Ng *et al*., 2014
Entrapment/ Immobilization	Cellulose triacetate	Real industrial	Lab scale	20	85-93%	COD; ammonia; SMP; TMP	Ng *et al*., 2012
Entrapment/ Immobilization	Cellulose triacetate	Real food processing	Lab scale	20	>90%	COD; ammonia; SMP-fractionation; TMP	Ng *et al*., 2011
MB-MBR/Biofilm	AnoxKaldnes K1 carrier	Real municipal	Pilot scale	15	>80%	COD; total suspended solids (TSS); ammonia; bEPS and SMP; membrane resistance	Di Trapani *et al*., 2014
MB-MBR/Biofilm	AnoxKaldnes K1 carrier	Real + synthetic	Pilot scale	10.3	70%	COD; TSS; ammonia; particle size distribution (PSD); TMP; zeta potential	Sun *et al*., 2012
MB-MBR/Biofilm	Polyurethane sponge	Synthetic municipal	Lab scale	8.75	85%	COD; PSD; membrane resistance; TMP; bEPS	Khan *et al*., 2012
MB-MBR/Biofilm	Polyurethane sponge	Synthetic municipal	Lab scale	8.75	98%	COD; total nitrogen; total phosphorus; TSS; PSD; TMP	Khan *et al*., 2011
MB-MBR/Biofilm	Polyurethane square mesh	Real municipal	Pilot scale	10	>80%	COD; ammonia; PSD; TMP	Rodríguez-Hernández *et al*., 2014
MB-MBR/Biofilm	Plastic square carrier	Synthetic municipal	Lab scale	15	NA	COD; ammonia; TSS; PSD; FI[3], SVI[4], membrane resistance; bEPS and SMP; TMP	Hu *et al*., 2012
MB-MBR/Biofilm	Nonwoven carrier	Synthetic municipal	Lab scale	6.25	95%	COD; ammonia; bacteria community; TMP	Yang *et al*., 2009

LMH[1] = L/m^2-h; COD[2] = Chemical oxygen demand; FI[3] = Filament index; SVI[4] = Sludge volume index

1.3. Research objectives

The broad objectives of this dissertation research are to develop entrapped cells-based MBR processes and test their performances and fouling propensity. The processes are aerobic MBR (Task I), anaerobic MBR (Task II), and anaerobic FOMBR (Task III). Specific objectives of the research include:

(1) Quantify and analyze fouling severity and mechanism(s) between suspended cells-based MBRs and entrapped cells-based MBRs.

(2) Compare system performances between suspended cells-based MBRs and entrapped cells-based MBRs.

(3) Quantify biofouling and inorganic fouling severity from reverse salt flux between two draw solutions (only for Task 3 anaerobic FOMBRs)

1.4. Research hypotheses

(1) Entrapped cells-based MBRs experience less fouling than suspended cells-based MBRs.

(2) Entrapped cells-based MBRs and suspended cells-based MBRs provide comparable treatment performances.

(3) Effect of reverse salt flux from draw solution on the system performances is less in entrapped cells-based FOMBR compared to suspended cells-based FOMBR.

1.5. Dissertation organization

This dissertation is divided into 6 chapters. This chapter includes background, research justification, objectives, hypotheses, and dissertation organization (this section). Chapter 2 provides a literature review on MBRs and FOMBR focusing on fouling. Chapter 3 presents an application of entrapped cells in aerobic MBR system to delay fouling. It is based on a manuscript titled “Fouling Characterization in Entrapped Cells-Based-Membrane Bioreactor Treating

Wastewater." This manuscript has been published in *Separation and Purification Technology* (Juntawang *et al*., 2017a). Chapter 4 is derived from a manuscript titled "Entrapped Cells-Based-Anaerobic Membrane Bioreactor Treating Domestic Wastewater: Performances, Fouling, and Bacterial Community Structure." This manuscript has been published in *Chemosphere* (Juntawang *et al*., 2017b). Chapter 5 is based on a manuscript titled "Entrapped-Cells-Based Anaerobic Forward Osmosis Membrane Bioreactor Treating Medium-Strength Domestic Wastewater: Fouling Characterizations and Performance Evaluation" This manuscript will be submitted for publication in a peer reviewed journal. Chapter 6 presents conclusions and recommendations for future work.

CHAPTER 2: LITERATURE REVIEW

2.1. MBR

2.1.1. Overview of MBR

MBR is one of the most effective wastewater treatment systems. It combines a conventional biological treatment process with membrane filtration to provide an advanced level of organic and suspended solids removal from wastewater. Currently, MBR is widely used in treating municipal and industrial wastewater for different applications, including removal of nutrients, organic matter and micropollutants. MBR can be operated aerobically or anaerobically. A simple schematic diagram which describes aerobic MBR process is shown in Figure 2-1. The process configuration for anaerobic MBR (AnMBR) is essentially the same as that for aerobic MBR (AMBR); however, aeration is not provided (Judd, 2010).

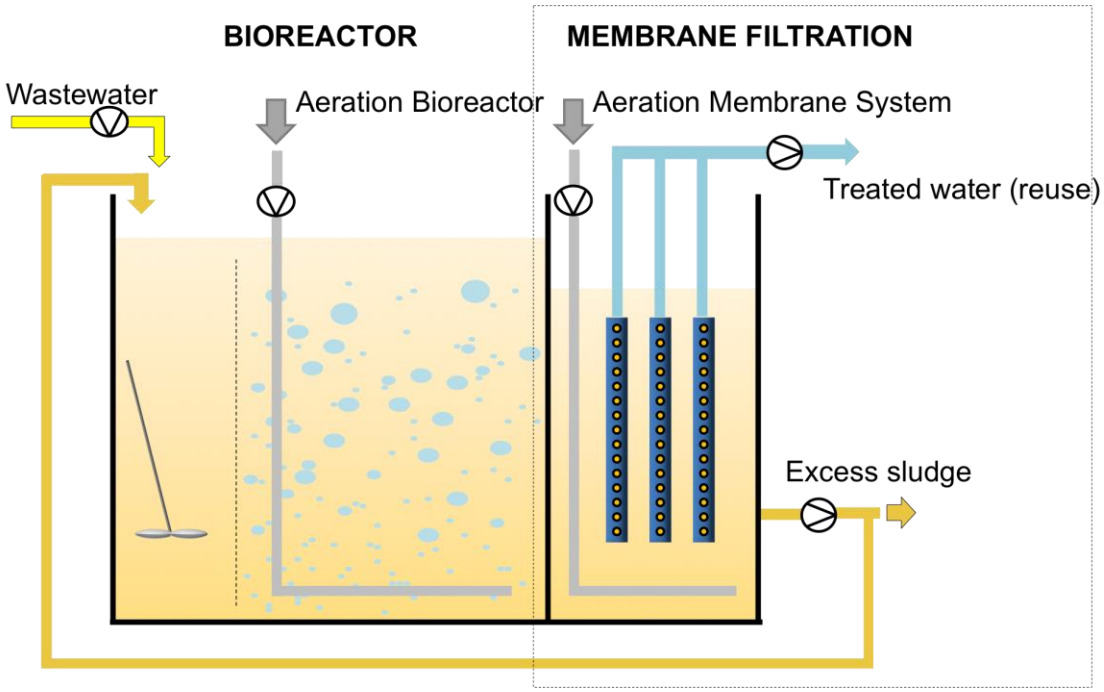

Figure 2-1: Simple schematic describing aerobic MBR process (modified from http://www.triqua.eu).

In a MBR system, the membranes are submerged in a biological reactor. The membranes have a pore size ranging from 35 nm to 400 nm (depending on the type and manufacturer). There are two types of membrane pore size (1) microfiltration (> 50 nm), and (2) ultrafiltration (35-50 nm) (Chung *et al*., 2008; Nissinen *et al*., 2001). These two types of filtration produce high quality effluent and eliminate the sedimentation process typically required for conventional wastewater treatment. Because the need for sedimentation is eliminated, this biological process can operate at a much higher mixed liquor concentration than other wastewater treatment systems (Rosesenberger *et al*., 2006; Gao *et al.*, 2004; Gander *et al*., 2000). The MBR system dramatically reduces the number and size of tanks required and allows many existing plants to be upgraded for better effluent quality. In the MBR system, the mixed liquor is typically kept in the 1.0-1.2% solids range, which is 4 times that of a conventional activated sludge plant (Rosesenberger *et al*., 2006).

Advantages of the MBR process include smaller footprint, rapid startup, complete retention of biomass inside the bioreactor, independent control of the solids retention time (SRT) from the hydraulic retention time (HRT), and better and reliable effluent quality that makes most regulatory agencies look favorably on the process (Smith *et al*., 2003). The most outstanding benefit of MBRs includes its shorten HRT to 4-8 hours compared with those of conventional systems (16-24 hours). The SRT can be flexible from 15 to 365 days without negative process impact. In addition, MBR can operate at higher mixed liquor suspended solids (MLSS) of 8,000-25,000 mg/L compared with 3,000-7,000 mg/L for conventional systems. It produces 20-40% less sludge yield and requires 25% of the footprint of conventional plants (Yeom *et al*., 1999; Van & Roncken, 1997). The MBRs also offer better nutrient removal, and have less susceptibility to flow variations and less odor than conventional systems (Zheng *et al.*, 2003).

It is possible to upgrade existing wastewater treatment plants (WWTPs) to MBR systems. In this case, old WWTPs can both improve their effluent for higher quality and save money for constructing whole new plants. Figure 2-2 shows flow diagrams of conventional activated sludge and aerobic MBR plants. Figure 2-3 presents the working principles of membrane treatment process in MBR systems.

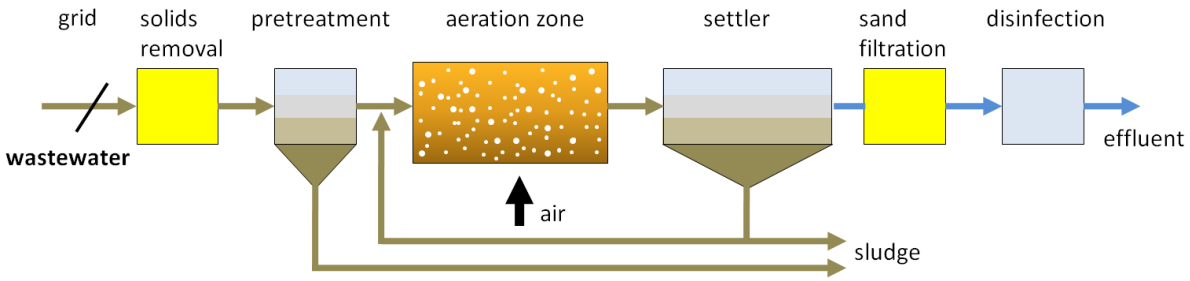

(a) Conventional activated sludge process

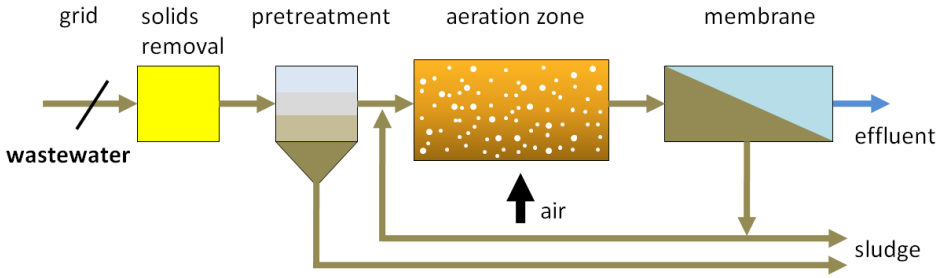

(b) Aerobic MBR

Figure 2-2: Schematic of (a) conventional activated sludge process and (b) aerobic MBR (modified from http://www.en.wikipedia.org).

The high costs of aeration and sludge handling associated with AMBR are concerns. Thus, AnMBR that can address these issues has been studied. The operation costs dealing with aeration and sludge handling are lower in anaerobic treatment as no oxygen is needed and the production of sludge is lower. In addition, greenhouse gas emissions during anaerobic treatment are lower than aerobic treatment if methane, byproduct, is used as an energy source (Lew *et al.*, 2009). The main challenge for AnMBR is retaining slow-growth anaerobic microorganisms in a relatively short HRT (Huang *et al.*, 2011).

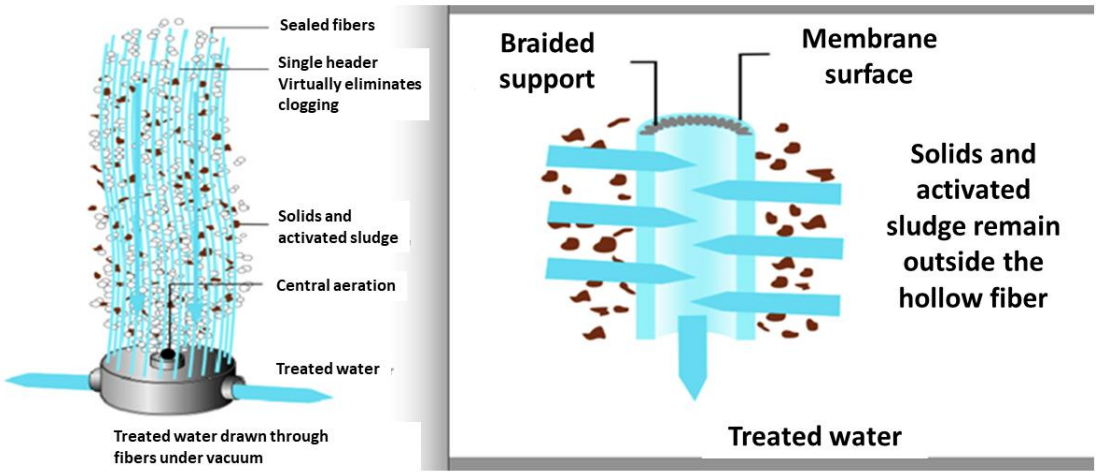

Figure 2-3: Working principles of membrane treatment process in MBR systems (modified from http://www.filtsep.com).

2.1.2. MBR definition

The term MBR applies to all water and wastewater treatment processes integrating a permeable selective membrane with a biological process. A traditional MBR is comprised of CAS coupled with membrane separation to retain the biomass. Since the effective pore size is generally below 0.1 μm, the MBR produces a clarified and disinfected effluent. In addition, membrane condenses the biomass and reduces the required tank size and also increases the efficiency of the biological treatment process. All currently available commercial MBR processes employ the membrane as a filter, rejecting the solid materials developed by the biological process (Judd, 2010). The outstanding performances of MBR in treating organic matter, nitrogen, phosphorus, and pharmaceuticals and personal care products in municipal wastewater are widely known (Chon *et al.*, 2012). The quality of the MBR permeates conforms largely with the microbiological standards for urban or agricultural reuse. In comparison with CAS, MBR presents many advantages, such as faster activation of WWTP, elimination of the sedimentation unit, ability to operate at high concentrations of suspended solids, and less sludge production (Zanetti *et al*., 2010).

2.1.3. MBR types

MBR can be divided based on the types of membrane modules, biological processes, and process configurations. The type of modules refers to the packing of the membrane in the module. Common membrane modules include plate and frame/flat sheet (FS), tubular (T), spiral-wound, hollow fiber (HF), capillary tube, and pleated filter cartridge. Generally, HF is widely used in WWTPs (Judd, 2010; Ren *et al*., 2005) because its high packing density of membrane per membrane module offers a compact and cost-effective solution for filtering large volumes of liquid and utilizes minimal space and energy. The HF module and flows pattern are shown in Figure 2-4. The FS membrane and T membrane have low packing density and are not commonly used for municipal wastewater treatment because municipal wastewater has a wide range of water conditions. Therefore, T and FS are appropriate for certain wastewater or food processing applications where there is a high fouling tendency (Judd, 2010; Stephenson, 2000). Ideally, membranes should be configured to have characteristics such as a high membrane area to module bulk volume ratio, a high degree of turbulence for mass transfer promotion on the feed side, a low energy expenditure per unit product water volume, a low cost per unit membrane area, a design that facilitates cleaning, and a design that permits modularization.

MBR systems can be divided into two types based on biological processes: AMBR and AnMBR. Oxygen is usually supplied as atmospheric air via immersed air-bubble diffusers in AMBR, while there is no aeration and only mixing is provided in AnMBR. Compared with AMBR, AnMBR has a lower energy demand (due to the absence of aeration), slower microbial growth, lower COD removal (generally 60-90%), no nitrification, greater potential for odor generation, longer start-up, higher alkalinity, lower sludge production, and biogas (methane) generation.

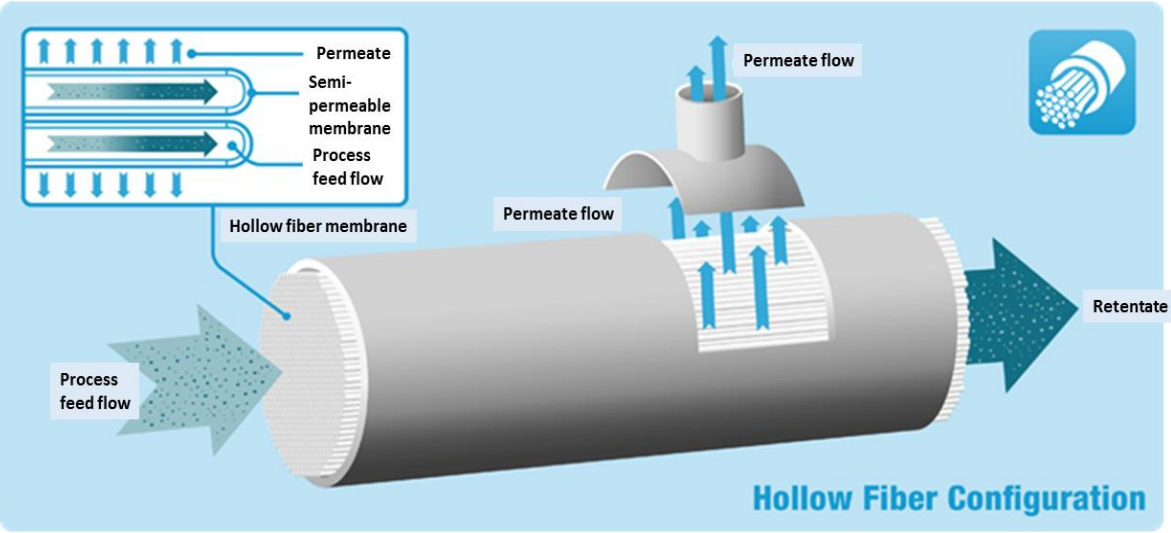

Figure 2-4: Hollow fiber membrane module (modified from www.kochmembrane.com).

Generally, anaerobic biological systems work well with high-strength wastewater and have difficulty in maintaining treatment efficiency when treating low-strength wastewater. The low-strength wastewater feed leads to low biomass growth yield and growth rate, such that the biomass concentration in the reactor is more difficult to sustain, particularly when substantial biomass wash-out from the reactor can occur. MBR systems can fix this problem through the retention of the biomass in the reactor by the membrane independent of the HRT (Judd, 2010).

Another way to categorize MBRs is by the process configuration. The MBR can be divided into two main configurations (Figure 2-5): side-stream (sMBR), and submerged or immersed (iMBR) (Judd, 2010).

In sMBR, the membrane modules are installed externally to the reactor, often in a plant room. The biomass is either pumped directly through a number of membrane modules in series and back to the bioreactor, or the biomass is pumped to a bank of modules, from which a second pump circulates the biomass through the modules in series. Cleaning and soaking of the membranes can be conducted with use of an installed cleaning tank, pump and pipework (Ren *et al.,* 2005). In iMBR, the principle of MBR process remains the same as sMBR except the

membrane modules are installed directly in the bioreactor tank. Cleaning and soaking of the membranes modules in iMBR can be done by removing membrane modules from the vessel and transferring them to an offline cleaning tank.

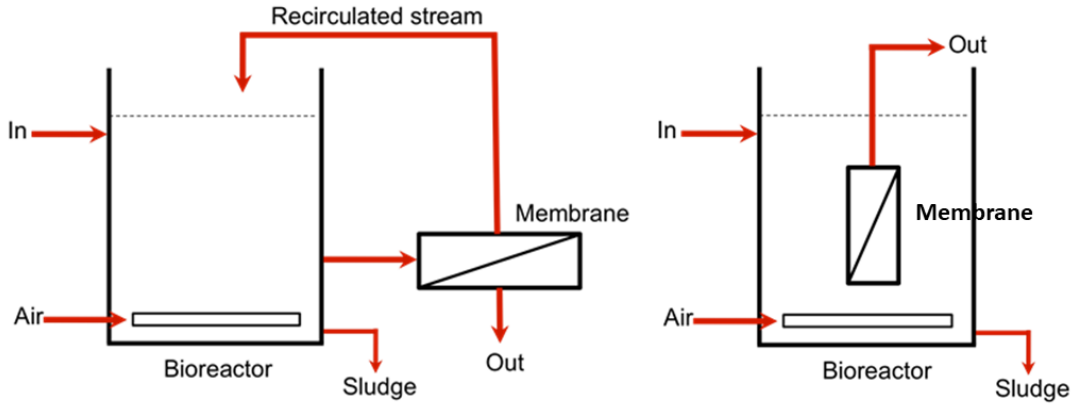

Figure 2-5: (a) Side-Stream MBRs and (b) Immersed MBRs (modified from Ng *et al.*, 2007).

sMBRs have a higher fouling tendency than iMBRs as higher flux operation always results in lower permeability because fouling itself increases with increasing flux, particularly above the critical flux (Stephenson, 2000; Tardieu *et al.*, 1999). Moreover, iMBRs are superior in energy efficiency, expressed as a specific energy demand in kWh/m^3 permeate product than sMBRs. The membrane module is placed directly in the bioreactors for iMBRs, resulting in less numbers of pumps required compared to sMBRs. Although sMBRs cannot provide the same low energy demand as the immersed configuration, they have some advantages over iMBRs: (1) The membranes in sMBRs system can be chemically cleaned in place (CIP) without any chemical risk to the biomass, and (2) it is generally possible to operate sMBRs at higher MLSS levels than in iMBRs.

The process configuration options for AnMBR are essentially the same as for aerobic one: pumped and gas-lift side-stream (Figure 2-2 (a)) and immersed (Figure 2-2 (b)). However, for AnMBR membrane, scouring with air is obviously not an option. Instead, scouring and lifting of the sludge through the membrane channels must use either liquid pumping or the generated biogas (Judd, 2010).

2.1.4. MBR limitations

The main drawbacks of MBR technology in comparison to CAS are its high cost and the requirement of a skill technician to control the system. While membrane module costs have decreased dramatically, leading to a decrease in capital costs, membrane fouling abatement leads to elevated energy demands and has become the main contributor to the overall MBR operating cost. Fouling has been a major issue in membrane and particularly MBR for more than a decade. Approximately 30% of all MBR related publications deal with fouling (Judd, 2010).

2.1.4.1. Fouling

The main drawback of MBR technology in comparison to the CAS is high capital, and operation and maintenance costs. However, the dramatic reduction in the price of membrane module costs has led to lower capital costs. The remaining obstacle of MBR is fouling abatement that leads to elevated energy demands and has contributed substantially to the overall MBR operating costs (Bouhabila *et al*., 2001). Fouling condition results from the local breakdown of cross-flow conditions and the subsequent dewatering of the biomass which leaves a solid deposit in the voids of the modules. Since deposits are brought to the membrane mainly by convective transport, it is clear that the rate of fouling depends on the velocity orthogonal to the surface – the permeate flux (Reid *et al*., 2008).

The main disadvantages of fouling conditions in MBR systems are:

- Decreased plant productivity/permeate yield due to filtration breaks and backflush. To remove the deposit layer, backflushing from the permeate side (hollow fiber modules) or relaxation (flat-sheet modules) is commonly applied.
- Frequent cleanings (maintenance cleanings approximately every 2–7 days, main cleanings once or twice a year). This also leads to environmental hazards through the formation of chemical cleaning by-products such as absorbable organic halogens.
- Damaging, and inefficient or late chemical cleaning which might reduce the lifespan of the modules and result in higher replacement costs.

All of the disadvantages mentioned above come from various types of fouling mechanisms consisting of (a) Complete blocking, (b) Standard blocking, (c) Intermediate blocking and (d) Cake filtration as shown in Figure 2-6. Basically, fouling mechanisms for AnMBR may be similar to those of AMBR but the nature of the foulants can be expected to be different. The difference in the nature of foulants can occur from various conditions including feed water characteristics, membrane surface, membrane module properties and process operating conditions.

Traditionally, the term reversible fouling refers to fouling that can be removed by physical cleaning such as backflushing or relaxation under cross-flow conditions, while irreversible fouling refers to fouling which can only be removed by chemical cleaning. Reversible fouling occurs due to external deposition of material (cake filtration) and is mostly removed during filtration breaks or backflush cycles (Verrecht *et al*., 2010; Brepols *et al*., 2008). Finally, over long periods irreversible fouling cannot be removed by any cleaning (irrecoverable fouling). Figure 2-7 shows the cleaning procedure of membrane fouling.

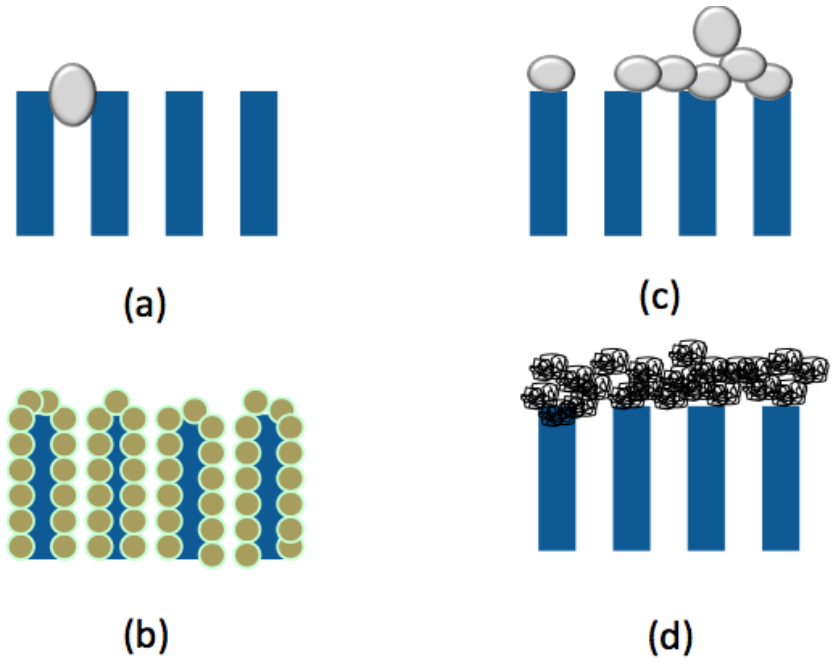

Figure 2-6: Fouling mechanisms: (a) Complete blocking; (b) Standard blocking; (c) Intermediate blocking; (d) Cake filtration (modified from Radjenović *et al*., 2007).

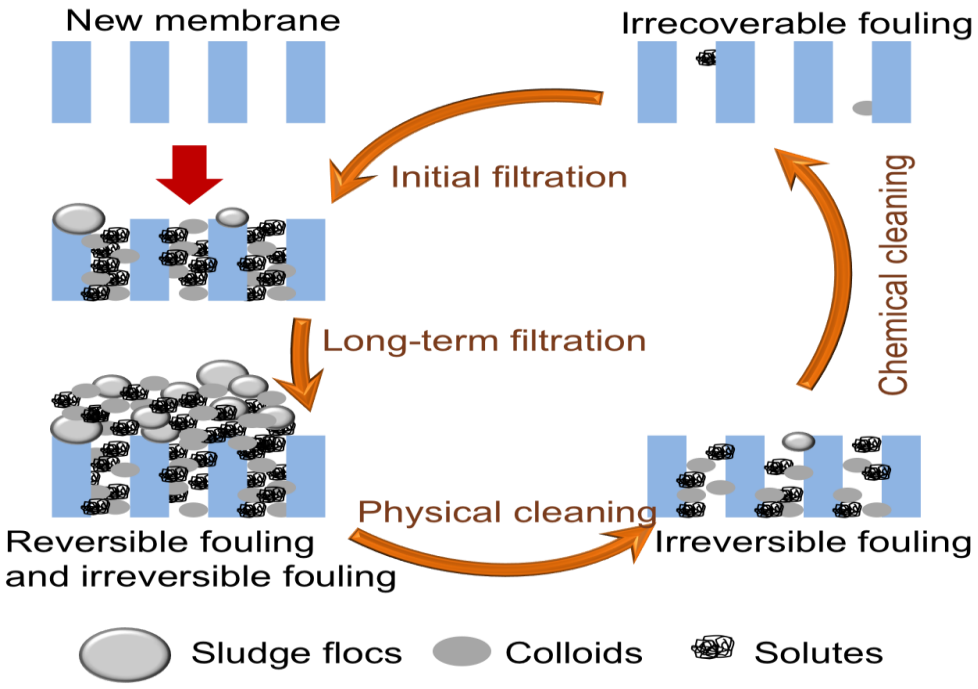

Figure 2-7: Fouling and cleaning procedure (modified from Meng *et al.*, 2009).

Due to economic considerations, fouling has been a major issue in membrane and particularly MBR research with a steady increase in published articles (Judd, 2010). Traditionally, three factors have direct effects on fouling: membrane module characteristics, biomass characteristics and system operation. Fouling is inevitable but can be controlled to a certain extent when the mechanisms and responsible substances are known. The factor "operation" needs to be divided into biological and membrane operation parameters. Aeration ports and module dimensions have been added to the original three factors and make up the group of design parameters. Apart from fouling and clogging, cleaning also affects permeability loss by aging of the membrane. Cleaning chemicals might also alter the foulant attachment susceptibility of the membrane (Zhang *et al.*, 2003). Fouling analyses depend on the detection of the onset of fouling itself or on factors related to fouling. A large variety of methods have been established, ranging from sampling of laboratory- to full-scale plants and from analyzing sample constituents to performing various filtration experiments. System size and selection of analytical methods can lead to different results of fouling conditions. Figure 2-8 shows the inter-relationships between MBR parameters and fouling.

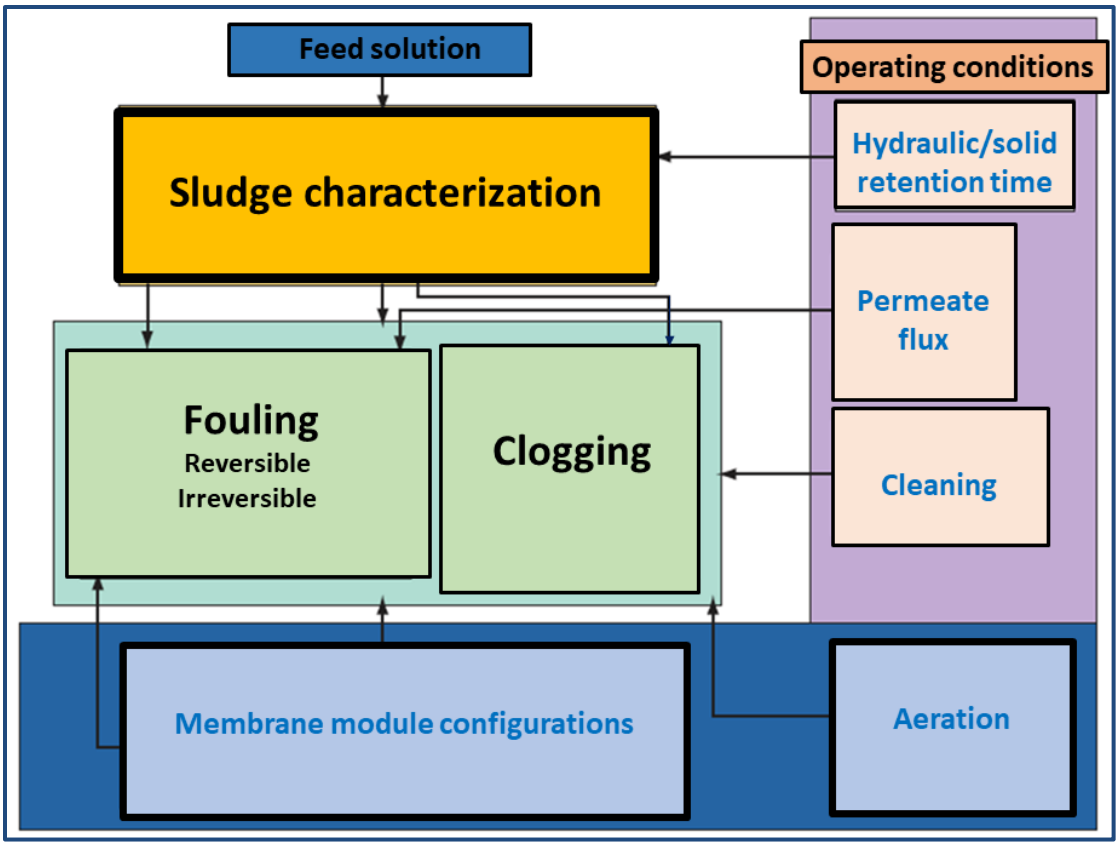

Figure 2-8: Inter-relationship between MBR parameters and fouling (modified from Judd, 2010).

2.1.4.2. Cost of system

Over the last two decades, implementation of MBRs has increased due to their superior effluent quality and small plant footprint (Judd, 2010). However, they are still viewed as a high-cost option, both in capital and operating expenditures. The main expenses are due to membrane installation and replacement costs and higher energy demand compared to conventional activated sludge systems.

2.1.4.2.1. Capital costs

The construction cost for MBR plants varies with membrane module manufacturer and/or membrane type. Other expenditures include tanks, piping system, and the system equipment (Verrecht *et al.*, 2010). The overall construction cost of the MBR system is still higher when

compared with the CAS system (approximately 2-4 times). The main expenditure comes from the price of the membrane module, pumps and number of blowers to generate a satisfactory amount of oxygen for the bioreactor tank in AMBR system.

2.4.1.2.2. Operational costs

An ongoing cost to run MBR systems, the operational expenditure, could be estimated by considering the following issues:

- Chemical consumption: NaOCl and citric acid are two main chemicals for cleaning membrane modules, both CIP and cleaning out of place (COP). The MBR systems need to do CIP weekly and do COP twice a year (Verrecht *et al*., 2010).
- Sludge production: The costs for sludge handling and disposal, which account for chemicals, labor, treatment (collection, thickening, digestion, dewatering) and disposal need to be considered for MBR systems. The differences in sludge characteristics from aerobic and anaerobic conditions are mostly attributed to different mechanisms involved in the biological process. Aerobic biological suspensions mainly include microorganisms and decay products which result from the high specific growth rates and biomass yields. Both high specific growth rate and biomass yields impact the sludge property. For anaerobic biological with low hydrolysis rates and low biomass yield, the reactor solid inventory is considered to be mainly constituted by influent particles that have reduced particle size and density (Lant & Hartley, 2007).

- Membrane replacement: When CIP and COP cannot retain the efficiency or required effluent water quality, then the MBR systems need a membrane module replacement. The worst case lifetime of a membrane module is 5 years while typical MBR membrane module replacement is every 10 years (Judd, 2010).

The rapidly decreasing membrane cost is the important driving force for the widespread application of MBR (Judd, 2010). However, under the present circumstances the total energy consumption by MBR in some cases reach values between 6 and 8 kWh/m^3 (Zhang *et al.*, 2003). The energy demand of MBR in municipal wastewater treatment is reported to be a factor of 2–4 times higher compared to the CAS (Cornel *et al*., 2003). Overall, it is shown that the energy demand for MBR treating municipal wastewater could be as low as 0.7–0.8 kWh/m^3 (Cornel *et al*., 2003), which is still higher than 0.3–0.4 kWh/m^3 by traditional wastewater treatment system. Aeration of a bioreactor unit to maintain a satisfactory amount of oxygen in the system is the main cost for submerged-MBR.

2.1.5. MBR applications

2.1.5.1. Organic matter and suspended solids removal

There have been several investigations on treatment efficiencies of MBR and CAS operating under comparable conditions that showed significantly improved performance of an MBR in terms of COD and suspended solids (SS) removal (Wisniewski & Grasmick, 1998). There are several factors that may contribute to the lower organic carbon content of MBR effluent as compared to that of CAS, such as longer retention times and smaller floc sizes.

Côté *et al*. (1998) attributed the improved COD removal to the avoidance of biomass washout problems commonly encountered in the activated sludge process, as well as complete particulate retention by the membrane. Membrane module rejection of a significant amount of

soluble organic molecules and colloids makes their removal more efficient. Higher sludge ages that are achieved by long SRT allow more complete mineralization of biodegradable raw water organics and an adaptation of microorganisms to less biodegradable compounds. Therefore, biomass can acclimatize to wastewater without being restricted to fast-growing and floc-forming microorganisms.

In a study of Al-Malack (2006), COD removal efficiency by iMBR was found to increase significantly with increase in MLSS concentration. However, the effect of SRT on permeate COD became insignificant for MLSS concentrations above 3,000 mg/L, which probably means that the organic loading rate was not high enough to show a significant difference at higher biomass concentrations. Since typical sludge concentrations for iMBR are between 15,000 and 25,000 mg/L, elimination of organic matter and turbidity is almost independent of SRT, and average removal efficiencies normally achieved for COD and SS are over 90 and nearly 100%, respectively (De Wever *et al*., 2004).

Concerning turbidity removal, due to a complete retention of particulate matter by the membrane, there are no suspended solids found in the MBR effluent, unlike the effluent of a conventional process. The UF/MF membrane can capture all SS in the reactor because of its fine pore size (Chu & Li, 2006). Therefore, non-biodegradable organic compounds are removed through filtration of particulates and discharged with the sludge. Gander *et al*. (2000) reported that the membrane module in MBR systems contributes to organic matter removal around 30%. In another study with an external membrane module, total COD removal was 97% on average, where 85% was removed by the bioreactor and only 12% resulted from membrane separation (Xing *et al*., 2000).

Ujang *et al*. (2002) found no significant difference in COD removal efficiency by MBR during vary aeration/non-aeration time. This implies that in intermittently aerated MBR the organic matter can be degraded both under aerobic and anaerobic conditions. Another study conducted by Kim *et al*. (2005) reported that over aeration in MBR can lead to poor sludge characteristics including bad floc structure, poor settling and relatively high sludge volume index, which promote fouling and high effluent solid concentrations. iMBR is strongly capable of resisting shock loadings and variations in the inflow turbidity, and organic matter content has no effect on their removal efficiencies. The removal of organic pollutants in terms of COD and SS has been proven to be very high and good quality effluent can be achieved during long-term operation.

2.1.5.2. Nutrient removal

Biological nitrogen and phosphorus removal from wastewater is widely practiced. Nitrogen removal requires aerobic–anoxic stages, while phosphorus removal requires alternating anaerobic-aerobic stages. Typical conventional biological nutrient removal (BNR) systems include three sequential separated stages: anaerobic-anoxic-aerobic, concluding with a secondary clarifier. However, removal efficiencies of nitrogen and phosphorus by biological processes are limited. The nitrogen removal efficiency in biological process depends on the recirculation ratio that transfers the nitrate produced by nitrification in the aerated zone back to the anoxic zone, and is therefore limited to 75–90%. Phosphorus removal efficiency is considerably affected by the effluent TSS concentration, and therefore directly dependent on the secondary clarifier efficiency. The MBR system is recommended for nitrogen and phosphorus removal because (1) it can retain nitrifiers and prolong SRT, resulting in complete nitrification process (Tchobanaglous *et al.*, 2003), and (2) the complete retention of suspended solids in MBR systems results in less total phosphorus in the effluent than BNR (Monti *et al.*, 2006).

Galil *et al*. (2009) reported that optimal nitrification could be achieved in the MBR system, because long SRT prevents nitrifying bacteria from being washed out from the bioreactors. Other studies on MBR have focused on nutrient removal and indicated high removal efficiency and several advantages over the conventional BNR systems (Kraume *et al*., 2005; Patel *et al*., 2005; Ramphao *et al*., 2005; Lesjean *et al*., 2003) which include:

- Insensitivity to sludge settleability and filamentous bulking.
- Insensitivity to activated sludge (AS) flocculation characteristics and hydraulic shear in the reactor.
- High-quality effluent, free of particles: the effluent solids from an enhanced biological phosphorus removal system have an average phosphorus content of 3 to 6% on a dry solids basis, and therefore contribute significantly to the effluent total phosphorus levels.
- Optimization beyond AS process performance at even slowly growing microorganisms, such as the nitrification population, can be established.

Thus, the MBR system provides high quality effluents with low concentrations of organic matter and SS (Galil *et al*., 2009), as well as almost complete absence of (pathogenic) bacteria.

2.2. FOMBR

2.2.1. Overview of FOMBR

FOMBR combining forward osmosis (FO) with activated sludge process has attracted interests in the field of wastewater treatment and reclamation (Yap *et al*., 2012; Achilli *et al*., 2009). In FOMBR, wastewater flows across a selectively permeable membrane from an activated sludge side to a draw solution side by an osmotic driving force (Figure 2-9). Compared to MBR, FOMBR has a lower fouling propensity due to the use of osmotic pressure instead of hydraulic

pressure as a driving force (Yap *et al*., 2012; Achilli *et al*., 2009). In addition, FOMBR provides higher quality effluent water compared to traditional MBR because most of the contaminants are effectively rejected by the FO membrane (Yap *et al*., 2012; Qin *et al*., 2010).

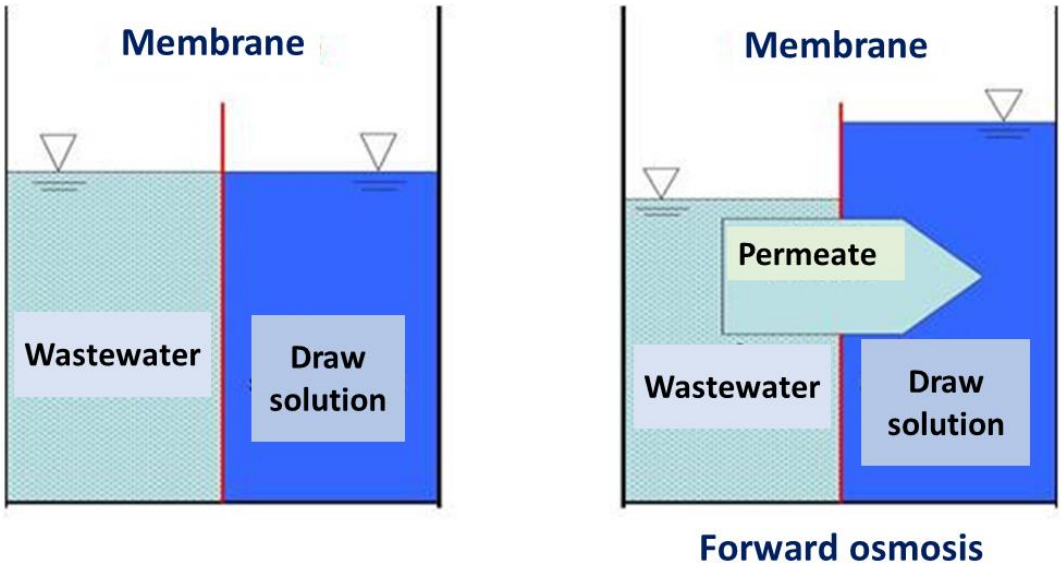

Figure 2-9: Forward osmosis diagram. (modified from www.freedrinkingwater.com).

2.2.2. FOMBR definition

FOMBR is an emerging MBR technology with water being spontaneously drawn by a solution with high salt concentration, with most microorganisms and impurities being retained in the feed side (mixed liquor) (Wang *et al*., 2014). FOMBR has some advantages over traditional MBR technologies, including its low fouling propensity, low energy consumption, and high effluent quality (Qiu & Ting, 2014). However, reverse salt flux from higher salt concentration (draw solution side) to lower salt concentration (bioreactor side) leads to salt accumulation in FOMBR which can deteriorate nitrification activity (Qiu & Ting, 2013). Qiu & Ting (2014) noted that elevated salinity in mixed liquor could alter surface hydrophobicity of sludge particles and increase the amount of bEPS produced so membrane can become severely fouled.

2.2.3. FOMBR configurations

Similar to conventional MBR, FOMBR can be designed and operated in submerged or side-stream configuration (Figure 2-10). In practical application, an additional separation process is required to recover the draw solutes and generate high quality product water. Compared to conventional MBR, membrane fouling in FOMBR is potentially less severe due to its relatively low water flux and the smooth and hydrophilic nature of typical FO membranes. Lately, there are two types of FO membrane available: cellulose triacetate by HTI and thin-film composite by Oasys Water.

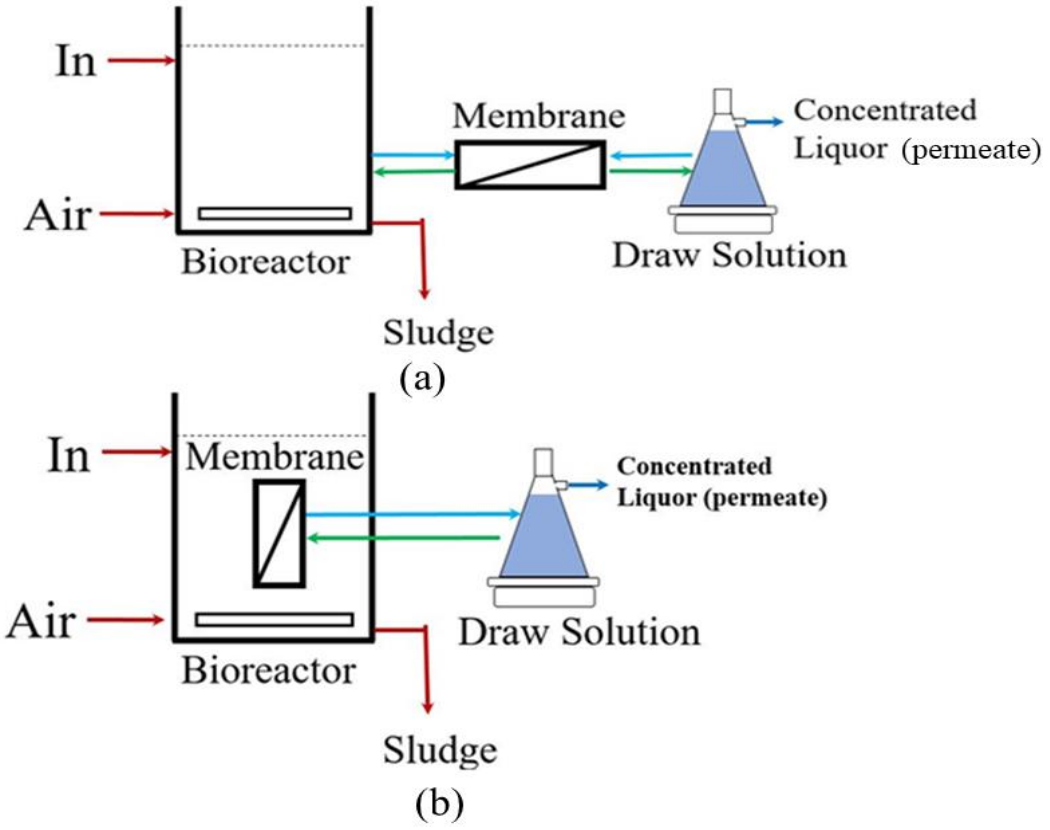

Figure 2-10: (a) Side-Stream FOMBR and (b) Immersed FOMBR (modified from Yuan *et al.*, 2015).

2.2.4. Draw solution

2.2.4.1. Ideal draw solution

An appropriate draw solution not only promotes the efficiency of the FO process, but also saves costs of the subsequent steps in recovering and replenishing the draw solute. In addition to having minimal toxicity and low cost, an ideal draw solution has the following conditions:

- Able to generate high osmotic pressure: As the osmotic pressure difference between the draw solution and feed solution across the membrane is the driving force for the FO process, the osmotic pressure of a draw solution must be higher than that of the feed solution to ensure a positive permeate flux. According to the Morse equation derived from the Van't Hoff equation by considering dilute ionic solutions (Ge *et al.*, 2013), the osmotic pressure of a solution, π, can be expressed as follows:

$$\pi = iMRT = i(n/V)RT$$

  where i is the Van't Hoff factor, M is the molarity of the solute which is equal to the ratio of the number of solute moles (n) to the volume of the solution (V), R is the gas constant, and T is the absolute temperature. Hence, to achieve a high osmotic pressure, a good solubility of the draw solute in water is required to get a high n or M value. In addition, an ionic compound which is able to fully dissociate to produce more ionic species is preferred because it may result in a high i value. This indicates that multivalent ionic solutes are the most favorable. Therefore, compounds with a high water solubility and a high degree of dissociation are potential candidates as draw solutes.

- Minimum reverse flux of draw solution: The occurrence of reverse draw solute flux adversely affects the FO and subsequent processes. It not only reduces the driving

force and contaminates the feed solution, but also increases the replenishment cost of the draw solute. For example, if FO is applied to enrich proteins or pharmaceuticals, the reverse flux may degrade these products and even denature them because they may be sensitive to salt (Morão *et al.*, 2011; Yang *et al.*, 2009). For the production of potable water, trace amounts of draw solutes in the final product water must be less than the maximum allowable values for potable water. In FOMBR system, the reverse flux makes the draw solute accumulate in the bioreactor, which may impose toxic effects on the microbial community (Alterki *et al.*, 2012; Achilli *et al.*, 2009). Therefore, a minimum reverse flux of the draw solute is vital for a FOMBR process.

- Easy to regenerate: Usually, FO is coupled with another process to produce clean water. For example, FO based seawater desalination involves at least two steps: (1) extraction of water from the seawater by a draw solution, and (2) separation of the product water from the diluted draw solution by means of reverse osmosis (RO), nanofiltration (NF), ultrafiltration (UF), membrane distillation (MD) or other thermal methods (Ge *et al.*, 2012; Ling & Chung, 2011; Tan & Ng, 2010). These processes consume energy, as either hydraulic pressure or heating is required to re-concentrate the diluted draw solution. Hence, easy regeneration of draw solutions is highly desirable to lower energy consumption and overall operation costs.
- Small molecular weight (MW) and low viscosity: Concentration polarization is inevitable in the FO process. Concentration polarization, especially internal concentration polarization (ICP), is partially caused by the low diffusion coefficient of the draw solute. The diffusion coefficient of a draw solute is inversely

proportional to its MW and solution viscosity. A draw solute with a large MW and high viscosity would have a low diffusion coefficient, hence, significant ICP. Therefore, a draw solute with a small MW and low viscosity is favorable.

2.2.4.2. Types of draw solution

- Inorganic salts: The first type is thermal recoverable inorganic draw solutes such as ammonium bicarbonate (NH_4HCO_3). A high water flux and a high water recovery are achieved because of the high osmotic pressure generated by the NH_4HCO_3 solution. A thermal method can be applied to recover NH_4HCO_3 from the diluted draw solution (permeate flux) by heating the diluted draw solution under atmospheric pressure at 60°C (using distillation column). Then, the gases obtained from heating can be dissolved in water to regenerate a NH_4HCO_3 draw solution. In view of the low decomposition temperature of NH_4HCO_3, the energy required in its recovery can be tapped from low-grade waste heat in industries. Therefore, a NH_4HCO_3-promoted FO seawater desalination process was claimed to save up to 85% energy when compared with other desalination technologies (McGinnis & Elimelech, 2007).

  The second type of inorganic salts includes those compounds which can function as fertilizers. If the diluted draw solution after FO is for irrigation, the separation of permeate water from draw solution is unnecessary. Therefore, the only required energy in this approach is for running the two pumps that do not exert much hydraulic pressure. As the draw solute recovery process after FO is regarded as the most energy-intensive step for seawater desalination (McGinnis & Elimelech, 2007; Cath *et al.,* 2006), the absence of draw solute recovery in FO

process will ensure energy savings. Draw solutions containing larger hydrated anions such as $MgSO_4$, $KHCO_3$, $NaHCO_3$, Na_2SO_4, $(NH_4)_2SO_4$, and K_2SO_4 show lower reverse salt fluxes. However, based on the overall evaluation of water flux, reverse salt flux and RO permeate concentration, none of these draw solutions rank high among available draw solutions.

- Organic salts: The advantage of using biodegradable organic salts is to mitigate the accumulation of draw solutes in FOMBR. An organic salt is defined as an organic anion combined with an organic or inorganic cation (Bowden *et al*., 2012).

  Generally, an organic salt with a shorter carbon chain outperforms that with a longer carbon chain when they have the same cationic species at the same osmotic pressure. This is because the former has less ICP than the latter due to a higher diffusion coefficient. Organic salts prove their advantages over their inorganic counterparts in terms of higher salt rejection in the RO re-concentration process and biodegradation potential required in a FOMBR system. However, the FO water fluxes of the organic salts are much lower than those of their inorganic counterparts (Ge *et al*., 2013). This may be because organic sodium salts with larger molecules when compared to NaCl have lower diffusion coefficients and are more affected by ICP.

- Synthetic materials: To advance FO technology, many researchers have been exploring the viability of using synthetic materials as draw solutes, and a variety of synthetic compounds have been proposed and applied. Some of them exhibit great potential as draw solutes. Hydrophilic magnetic nanoparticles (MNPs) are considered promising draw solutes and have generated a fair amount of interest

(Bai *et al*., 2011; Ling *et al*., 2010). Furthermore, to lower the material cost and reduce the reverse flux, polyelectrolytes of polyacrylic acid sodium (PAA-Na) salts were also investigated as draw solutes by Ge *et al*. (2013). The PAA-Na salts have high water solubility and structurally expanded configuration that potentially provide high osmotic pressure. Experimental results confirmed a high water flux with an insignificant reverse salt flux when using PAA-Na salts as the draw solutes. In addition, a high salt rejection was achieved when recycling PAA-Na by UF process. The multi-ionic PAA-Na outperforms conventional ionic salts, such as NaCl, when comparing their FO performance via the same membranes (Gray *et al*., 2006). Other synthetic materials such as MNPs and MNPs capped by poly acrylic acid were also investigated as draw solutes to get the best match with specific uses.

Although some of the draw solutions tested have shown promises, NaCl is still widely used as an effective draw solute in FO due to its high solubility, low cost and the relative ease of regeneration using conventional desalination processes without risk of scaling. NaCl exhibits relatively high reverse salt diffusion and results in a moderate water flux (Achilli *et al*., 2010). Ammonium carbonate ($(NH_4)_2CO_3$) has also been widely used as the draw solute, but the carbonate ions (CO_3^{2-}) may potentially cause mineral scaling on the membrane surface when the feed solution is concentrated by FO. It should be noted that not all the FO draw solutions have been tested for their application in FOMBR.

Ideally, a semi-permeable membrane should prevent all draw solute particles from undergoing reverse transport. However, a small amount of draw solute passes the membrane and moves into the feed side. This phenomenon may affect the FOMBR in two ways: (i) if the draw solute is toxic to the bacterial species present in the bioreactor, it can negatively affect the

biological process(es) and in turn treatment efficiency, (ii) if draw solute is harmful to the aquatic environment, an additional treatment step for the feed solution concentrate would be required prior to discharge.

The reverse draw solute, if trapped by the fouling layer, can contribute to enhanced osmotic pressure on the feed side. This enhanced osmotic pressure within the fouling layer reduces the net driving force, consequently resulting in a net flux decline (Li *et al.,* 2012). Reverse draw solute transport is an important factor which affects flux through an FO membrane (Hancock & Cath, 2009). This occurs due to the big difference in solute concentrations between the feed and draw solution sides. The reverse solute transport is governed by Fick's law:

$$Js = B\Delta C$$

where "Js" is reverse salt flux, "Jw" is water flux, ''B'' is solute permeability coefficient and ''C'' is the solute concentration difference across the membrane. To avoid reverse solute diffusion, multivalent ions with lower diffusivity are preferred in the draw solution. The Js/Jw value is the third important criterion for FO membrane selection after permeate flux and salt rejection (Zhao *et al.,* 2012). Figure 2-11 shows the reverse solute transport direction, which is opposite to the water flux. The negative impact of concentration polarization and reverse solute transport on net driving force reduce osmotic pressure of FO. This is attributed to the difference between free energy and mole fraction of water on either side of the membrane.

In FOMBR, the draw solutes play an imperative role as they provide the driving force for the transport of water across the membrane, while the reverse diffusion of the solute through the membrane should be considered in their selection. The draw solutes for osmotic driven processes must have high osmotic pressure, zero toxicity, low cost and easy recovery (Chung *et al.,* 2012).

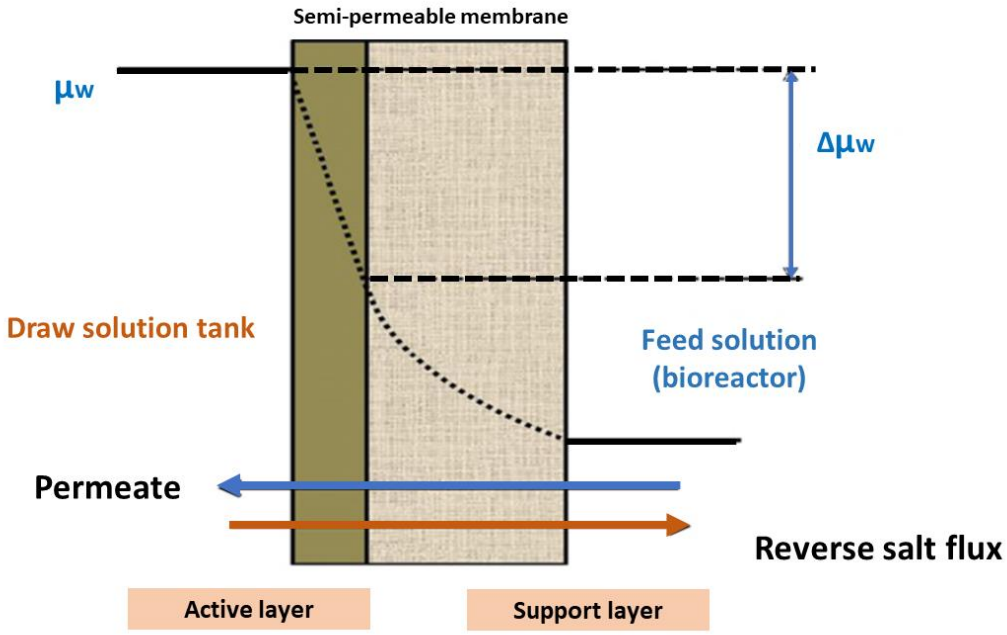

Figure 2-11: Asymmetric FO membrane with active layer facing draw solution (modified from Nawaz *et al*., 2013)

2.2.5. FOMBR limitations

A major drawback associated with FO membrane is its severe ICP (Tang et al., 2010; Cath et al., 2006). An asymmetric FO membrane consists of an active layer and a porous support layer, hence leading to two different membrane orientations. If the porous support layer faces the feed solution, a polarized layer is established inside the dense layer as water and solutes diffuse through the porous layer. This phenomenon is known as concentrative ICP, and cannot be controlled by cross flow-associated hydrodynamic shear. In the other scenario where the active layer faces the feed solution, the draw solution within the porous support layer becomes diluted due to the permeation of water through the active layer. This is called dilutive ICP. The FO flux and ICP have been modeled by the coupling solution–diffusion theory for the rejection layer and the less severe for membrane with thinner and more porous support layers due to their reduced mass transfer resistance.

The reverse salt transport in FOMBR enhances salt accumulation, and further impacts on the performance of bioreactor, while reducing the effective driving force due to lowered net osmotic pressure across membrane and increased ICP (Hancock *et al.,* 2011; Hancock & Cath, 2009). In order to overcome low water flux and high salt accumulation often observed in FOMBR, extensive research has been conducted on the selection of draw solutes and development of an ideal FO membrane (Lay *et al*., 2011, 2010; Cornelissen *et al*., 2008). Cost-effective draw solutes are required to lower the operational costs and economically compete with existing MBR.

Factors affecting the fouling in FO and FOMBR are as follows:

- Changes in operating conditions such as increases of initial water flux and cross flow velocity can increase fouling rate while increases of spacer, aeration rate and temperature can reduce fouling.
- Feed water characteristics, including foulant type, foulant physicochemical properties (e.g., shape, size, charge, and functional group), foulant concentration, solution pH, ionic strength, and ionic composition (e.g., divalent cation);
- Draw solution composition, such as draw solution concentration and draw solute type;
- Membrane properties, including membrane separation and structural properties, and membrane surface properties (e.g., hydrophilicity/hydrophobicity, roughness, charge density, and surface functional group).

Types of FOMBR fouling are as follows:

- Inorganic scaling: In FO, inorganic scaling occurs with the deposition and growth of the sparingly soluble inorganic scale on the osmotic membranes. Particularly, the occurrence and severity of scaling are strongly dependent on the concentration

and solubility of potential scalants (or their precursors) in the feed solution. The kinetics of precipitation determines the severity of scaling and can be sped up with a high concentration of nucleation sites. In addition, the reverse diffusion of scaling precursor ions from draw solution (DS) into feed solution (FS) can further enhance the scaling. When scaling precursor ions (i.e., Ca^{2+} or SO_4^{2-}) diffuse into FS, the precipitation of gypsum as inorganic scaling on membrane surfaces substantially increases on the feed side, especially within the support layer where ICP plays an important role. In reality, typical inorganic scaling can be caused by alkaline scale (e.g., calcium carbonate ($CaCO_3$) and calcium phosphate ($Ca_3(PO_4)_2$) and silica-based scale. In FO, the H^+ and OH^- can diffuse through the membrane bidirectional between DS and FS, which can potentially alter pH near the membrane surface and thus the scaling tendency of those alkaline and silica-based scales on the membrane.

- Biofouling: Compared to organic and inorganic fouling where the foulants are non-living substances, biofouling is much more complicated. When the live microorganisms attach to the membrane surface, they start to propagate utilizing the nutrients from the surrounding environments to form the aggregated "biofilm" and are capable of colonizing almost all of the surface (Al-Juboori & Yusaf, 2012; Baker & Dudley, 1998).

Biofouling intensity is influenced by the number of microorganisms and nutrient concentrations. Even small amounts of microorganisms in the initial feed solution can induce severe biofouling due to biofilm development if sufficient nutrients are provided for their growth. This is different from organic and inorganic fouling which can be well controlled by simply reducing the foulant concentration in the feed solution. In the FO and FOMBR, the nutrients for

biofilm growth can be obtained from three major sources: (1) the contaminants in the original bulk feed water, (2) the leached material from the substratum that could be the membrane material itself, and (3) the solutes with nutrient elements in the draw solution (that can reversely diffuse into feed water).

bEPS from the microbial metabolism is another essential factor affecting the biofouling. bEPS is important constituting materials for biofilm (Meng *et al*., 2010; Le-Clech & Fane, 2006), and consists of polysaccharides, proteins, lipids, and nucleic acids (Meng *et al.*, 2010; Le-Clech & Fane, 2006; Baker & Dudley, 1998). These materials are sticky and can enhance the adhesive interaction between the microorganisms and the membrane surface (Le-Clech & Fane, 2006). Figure 2-12 shows a schematic illustration of the role of reverse solute diffusion on enhanced membrane fouling in FOMBR.

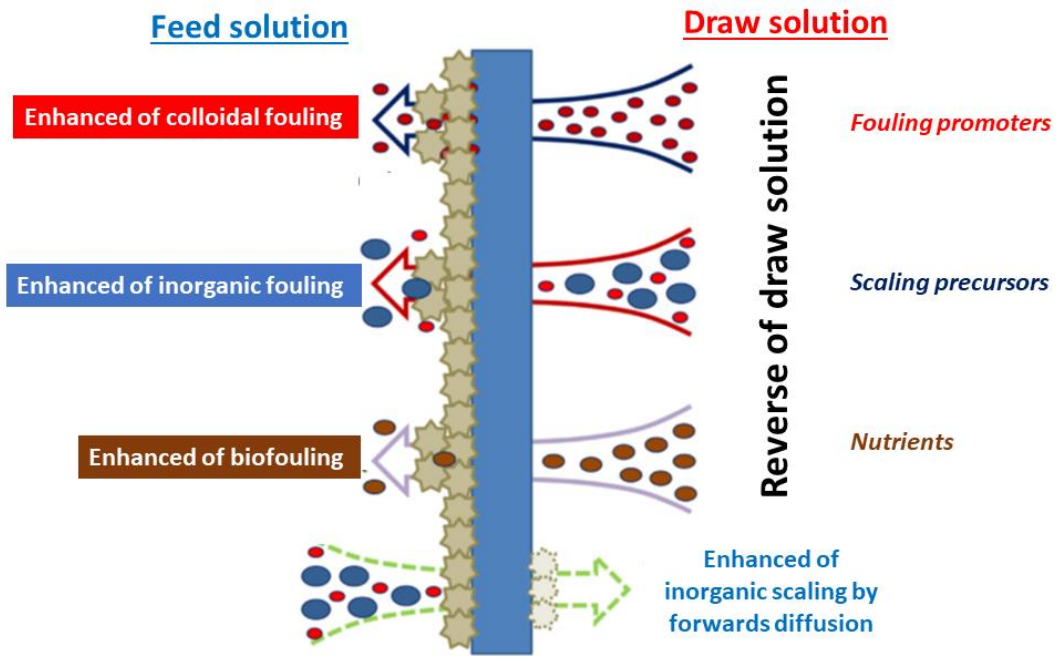

Figure 2-12: Schematic illustration of the role of reverse solute diffusion (RSD) on enhanced membrane fouling in FOMBR. (modified from She *et al.*, 2016).

2.2.6. FOMBR applications

In recent years, there have been a number of studies on FOMBR applications (Goh *et al*., 2013; Lay *et al*., 2010). Smaller size contaminants such as hydrolyzed organic matter could be effectively retained by membrane, prolonging its residence time in the reactor and potentially leading to improved biodegradation efficiency and effluent quality (Goh *et al*., 2013; Cornelissen *et al.*, 2008). The application of FOMBR in wastewater treatment can achieve better effluent quality and less energy consumption compared to traditional MBR, due to prolonged retention time with high rejection property of FO membranes (Qin *et al*., 2010; Achilli *et al*., 2009; Cornelissen *et al.*, 2008). When compared to aerobic FOMBR, anaerobic FOMBR has lower aeration costs and biomass yields (Gu *et al.*, 2015); however, the application of anaerobic FOMBR is rather limited since the process has been introduced just recently by Chen *et al*. (2014). Due to high rejection of inorganic matters by FO membrane, FOMBR can be used to recover PO_3^{4-}. Huang *et al*. (2015) enriched PO_3^{4-} in high strength domestic wastewater (COD of 1,500 mg/L) in the bioreactor of FOMBR. The enriched PO_3^{4-} could be efficiently recovered by adding $MgCl_2$ and adjusting pH to 8.5 or higher.

CHAPTER 3: RESEARCH TASK I–FOULING CHARACTERIZATION IN ENTRAPPED CELLS-BASED-MEMBRANE BIOREACTOR TREATING WASTEWATER

3.1. Introduction

With more stringent standard for treated effluents, MBRs have been a process of choice for wastewater treatment and reuse. MBRs provide several advantages over conventional treatment process (activated sludge) including superior quality effluent, less biomass yields and more compact design (Judd, 2010). Therefore, MBRs are currently used as a secondary treatment unit for numerous full-scale municipal wastewater treatment and reclamation facilities in the United States and Europe (Judd, 2010). At biochemical oxygen demand (BOD) and ammonia loading rates of 0.2–0.7 kg/m^3·d and 0.05–0.17 kg N/m^3·d, the treatment efficiencies of MBRs were excellent achieving effluent BOD, ammonia and total suspended solids of 0.7–3.0 mg/L, 0.5–2.0 mg N/L, and 1–2.5 mg/L, respectively (AWWA, 2013; GE Power &Water, 2012). However, membrane fouling is a major drawback that hampers widespread and full-scale applications of MBRs. Fouling is a reduction of membrane permeability that is originated by adsorption or accumulation of deposits on the surface and/or in the pores of membrane during operation. Loss of membrane permeability results in higher TMP leading to a higher operating cost of MBRs for keeping a constant permeate flux with increased applied pressure and frequent chemical cleaning (Judd, 2010; Verrecht *et al*., 2010).

Fouling, commonly found in submerged MBRs operation, is deposition of sludge cake onto membrane surface (cake deposition) and clogging of small deposits within membrane pores (pore blocking). Microbial products including bEPS and SMP that are released during utilization, growth and decay of active cells in sludge are currently considered as the predominant cause of cake

deposition and pore blocking in MBRs (Wang *et al*., 2009). bEPS consist of proteins, polysaccharides, nucleic acids, lipids, and humic acids, which are located at or outside the cell surface. SMP are soluble organic pools that occur during substrate metabolism, and cell decay and bEPS hydrolysis (Liang *et al*., 2007; Lee & Rittmann, 2002). Cake resistance is often contributed by hydrophobic SMP which have MW in a range of 10–100 kDa (Arabi & Nakhla, 2010).

The primary concern of fouling in long term operation is irreversible fouling as chemical cleaning cannot remove all accumulation from membrane pores. Another concern is high chemical use will damage the membrane texture and shorten the membrane lifetime. Thus, finding a strategy to prevent accumulation of bEPS and SMP on membrane surface is worthy of investigation.

A study on S-MBR, in which bacteria can grow freely, showed higher bEPS and SMP (in terms of proteins and carbohydrates) in the system when compared with AG-MBR, which is a MBR containing biofilm carriers (Hu *et al*., 2012; Khan *et al*., 2012, 2011). Khan *et al.* (2012, 2011) compared AG-MBR and MB-MBR, which is a specific type of AG-MBR containing free-floating biofilm carriers, with S-MBR. They found that SMP concentration in S-MBR was higher than those in AG-MBR and MB-MBR indicating more severe fouling in S-MBR. In addition, Di Trapani *et al*. (2014) and Rodríguez-Hernández *et al*. (2014) reported less fouling in MB-MBR than S-MBR. These previous studies are in agreement that biofilm-based MBR have less/slower fouling condition compared to S-MBR.

The concept of attached-growth/biofilm is similar to cell entrapment/immobilization principle. Entrapped cells-based-MBR (E-MBR) reduces the concentrations of bEPS and SMP leading to less fouling compared to S-MBR (Hu *et al*., 2012; Khan *et al*., 2011; Ng *et al*., 2010). Tsen *et al.* (2004) reported that entrapment matrices can provide protection to the cells against unsatisfied environment such as toxic compounds or low pH. Moreover, the porosity within the

entrapment cells allows the diffusion of substrates and products across the matrix but prevent the release of cells into the bulk liquid. Polyvinyl alcohol has been successfully used as an entrapment matrix for wastewater treatment because of high durability, applicability in a wide range of pH (4–10), nontoxicity to bacteria, and higher specific growth and specific substrate utilization rates when compared to alginate and carrageenan (Pramanik & Khan, 2008; Siripattanakul *et al*., 2008; Chen *et al.*, 2003). Gel entrapped cells-based-MBR has been studied but none of them specifically explored on how entrapped cells can reduce/delay fouling in MBR system (Ng *et al*., 2014, 2012).

The objective of this research task was to investigate the role of entrapped cells on membrane fouling and fouling mechanism in E-MBR treating medium-strength domestic wastewater through analysis of membrane resistance and characterizations of bEPS and SMP. A fouling condition in E-MBR was observed in parallel with S-MBR. S-MBR was used for comparison in this research task because it is widely used while attached-growth MBR has not been applied at full-scale. It is expected that the porous gel matrix can prevent not only cells but also bEPS and SMP releases into bulk liquid resulting in lower membrane fouling because of reduction in cake deposition and pore blocking.

3.2. Materials and methods

3.2.1. Synthetic wastewater and chemicals

Synthetic medium-strength domestic wastewater, which has a soluble chemical oxygen demand (SCOD):N:P ratio of 100:5:0.7 (Nagaoka, 1999), was prepared by adding 0.5 mL of concentrated CH_3COOH (as 500 mg/L SCOD), 100 mg of NH_4Cl, 16 mg of KH_2PO_4, 4 mg of $FeCl_3 \cdot 6H_2O$, 11 mg of $CaCl_2$, 17 mg of $MgSO_4$, 8 mg of KCl, 8 mg of NaCl and 350 mg of

$NaHCO_3$ into one liter of de-ionized water. Polyvinyl alcohol (99.0–99.8% fully hydrolyzed, J.T. Baker, USA) was used as a gel entrapment matrix. All chemicals used are the American Chemical Society reagent grade.

3.2.2. Preparation of entrapped cells

Mixed liquor taken from an aeration tank of the Moorhead wastewater treatment facility (Minnesota, USA) was inoculated to start up S-MBR and E-MBR. Entrapped cells in E-MBR were prepared using a procedure described in Chen & Lin (1994). In brief, the concentrated sludge (80 g wet weight) was thoroughly mixed with 535 mL of a 10% polyvinyl alcohol gel solution (w/v). The mixture was then dropped into a saturated boric acid solution to form spherical beads. The formed gel beads (diameter of 2.4 ± 0.15 mm) were transferred and incubated for 4 h in a saturated orthophosphate solution for hardening resulting in phosphorylated polyvinyl alcohol (PPVA) gel beads. Both boric acid and orthophosphate were not adsorbed onto the polyvinyl alcohol gel but rather incorporated into the gel structure (Pramanik & Khan, 2008; Chen & Lin, 1994). The beads were washed thoroughly with de-ionized water and inoculated into E-MBR.

3.2.3. Membrane bioreactor setup and operation

For S-MBR and E-MBR setups, two rectangular acrylic tanks with working volume of 10 L were used. Each tank consisted of two compartments divided by an acrylic plate. One compartment was for aeration zone (7 L) and the other was for filtration zone (3 L) (Figure 3-1). Both E-MBR and S-MBR had the same configuration and operation conditions except that E-MBR was inoculated with entrapped cells instead of mixed liquor. A hollow fiber membrane module (ZW-1, GE Water& Power, Canada) with a pore diameter of 0.04 μm and an effective surface area of 0.047 m^2 was submerged in the filtration zone of MBR.

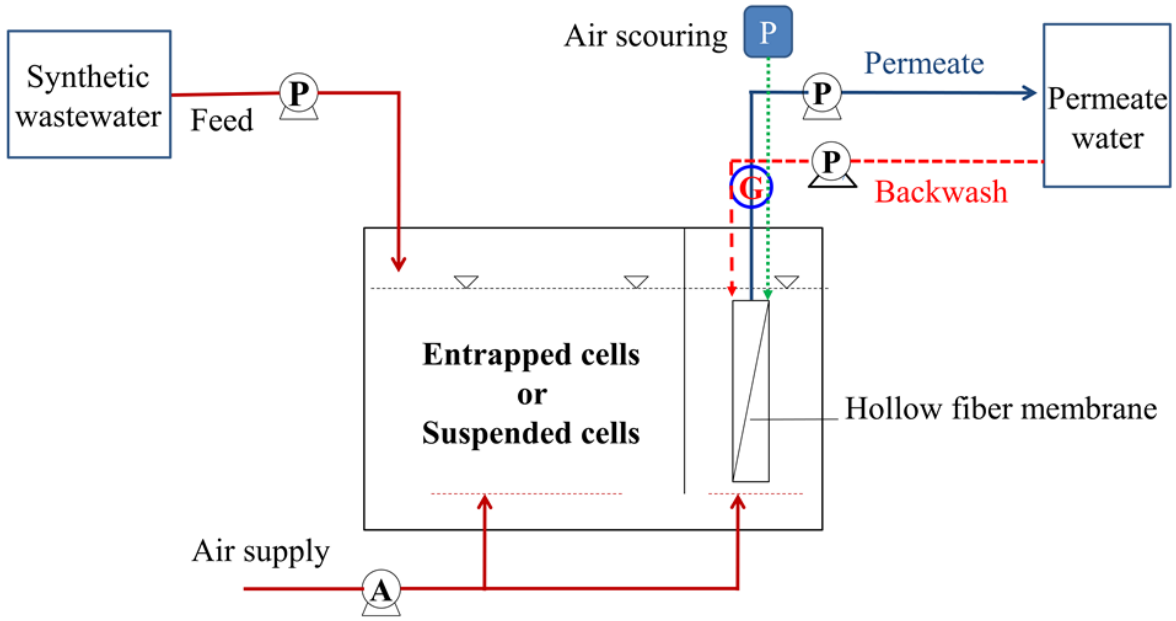

Figure 3-1: Schematic diagrams of E-MBR and S-MBR.

Oxygen was supplied using a laboratory air system and diffused through small stone diffusers to maintain sufficient mixing and aerobic condition in the reactors. Two peristaltic pumps were used as influent and permeate pumps (Model 7553-60, Barnant, USA and Model 7554-90, Thermo Fisher Scientific, USA). TMP was monitored during filtration via a vacuum gauge (Model 14902.5, Ashcroft, USA). Under a 1-day HRT, a constant permeate flux at 10.63 LMH was maintained through 15 min backflushing and air scouring for every 3 h. Permeate water was pumped from the permeate tank to backflush membrane while air was blown through an air pump (Whisper 100, Tetra, USA) to scour cake deposited on the membranes. An electronic timer (ODT309-M2, Smart Electrician, USA) was used to control the backflush pump and air scouring system. Membrane was cleaned when TMP reached 55 kPa or it was not possible to maintain a constant permeate flux by soaking under 200 ppm sodium hypochlorite for a minimum of 5 h and then moving to a 5 g/L citric acid solution for a minimum of 5 h. The reactors were operated at room temperature (22.2 ± 0.9 °C) after steady state for 90 days without wasting sludge. Conditions for the reactor operation are summarized in Table 3-1.

3.2.4. Characterizations of feed, reactor fluid, permeate, sludge, bound extracellular polymeric substances (bEPS), and soluble microbial products (SMP)

3.2.4.1. Feed, reactor fluid, and permeate characterizations

During steady state operation, when SCOD removal varied less than 10% (Tchobanoglous *et al*., 2003), the concentrations of SCOD, ammonia (NH_3-N), nitrite (NO^-_2-N) and nitrate (NO^-_3-N), dissolved oxygen (DO), and pH in the feed water, permeate and reactor (DO and pH) were monitored weekly. Samples were taken from the feed and permeate tanks then filtered using GF/C microfiber filters with a nominal pore size of 1.2 µm (Whatman, USA). SCOD was measured by the Reaction Digestion method, NH_3-N was measured by the Salicylate method, NO^-_2-N was measured by the Diazotization method, and NO^-_3-N was measured following the UV screening method at wavelengths of 220 and 275 nm (APHA *et al.*, 2005). A DR 5000 spectrophotometer (HACH, USA) was used for SCOD, NH_3-N, NO^-_2-N and NO^-_3-N determinations. DO was measured by a dissolved oxygen meter (model 850, Thermo Scientific, USA). pH was measured by a pH meter (model 250, Thermo Scientific, USA). All these analyses were conducted in triplicate by splitting each sample into three portions.

3.2.4.2. Particles size distribution

The particle size distribution (PSD) of activated sludge taken from E-MBR and S-MBR tanks was determined by a particle characterization device with 2 detection ranges: 1 nm–2 µm (Nicomp 380, Particle Sizing Systems, USA) and 1–400 µm (Nicomp 780A, Particle Sizing Systems, USA). The PSD was measured in triplicate using one sample from each type of MBRs.

Table 3-1: Operational conditions and performances of E-MBR and S-MBR.

Parameters	E-MBR	S-MBR
Influent soluble organic (mg SCOD/L)	547±11	547±11
Effluent soluble organic (mg SCOD/L)	25±6	23±5
Soluble organic removal (% SCOD removal)	95.6±0.9	95.8±0.8
Influent NH_3 (mg N/L)	25.45±0.22	25.45±0.22
Effluent NH_3 (mg N/L)	1.71±0.21	1.81±0.54
NH_3 removal (%)	92.62±2.09	93.28±0.80
Nitrification (as NO_3^-/ NH_3 removed, %)	85.14±0.78	86.15±0.42
Total operation period (days)	120	120
Organic loading rate (OLR)(kg SCOD/m^3·d)	0.5	0.5
Temperature (°C)	22.17±0.89	22.17±0.89
pH (bioreactor)	7.23±0.22	7.23±0.05
Feed concentration (mg SCOD/L)	500	500
DO (mg O_2/L)	8.03±0.07	8.04±0.07
Permeate flux (LMH)	10.63	10.63
HRT (hrs.)	24	24
MLSS (g/L)	-	8
Entrapped biomass (g/L)	8	-
Resistance:		
- Membrane (R_m) (m^{-1})	2.52×10^5	2.52×10^5
- Pore blocking (R_p) (m^{-1})	1.00×10^6	5.03×10^6
- Cake filtration (R_c) (m^{-1})	8.80×1^{05}	5.03×10^5
bEPS and SMP (g/L):		
- bEPS (Protein)	0.465±0.116	2.107±0.327
- bEPS (Carbohydrate)	0.213±0.038	0.272±0.051
- SMP (Protein)	0.858±0.175	3.737±0.809
- SMP (Carbohydrate)	0.467±0.134	0.511±0.010

3.2.4.3. bEPS and SMP characterizations

3.2.4.3.1. Extraction and quantification

Samples of mixed liquor, entrapped cells, and membrane deposited biomass taken from the aeration tank of the reactors were extracted for bEPS and SMP. The extraction procedure for entrapped cells was the same as that for mixed liquor and membrane deposit biomass according to Judd (2010). The entrapment gel matrix was completely dissolved at 80 °C and then centrifuged to obtain the sediment which contained cells as well as bEPS and SMP. Heating at 80 °C does not affect bEPS and SMP as it is a well-established method for extracting and quantifying them (Judd, 2010; Le-Clech *et al*., 2006). bEPS and SMP in the sediment were measured for proteins and carbohydrates by the Lowry method (Lowry *et al*., 1951) and the Anthrone method (Ludwig *et al*., 1956), respectively. Proteins and carbohydrates in bEPS and SMP were measured in triplicate by splitting each sample into three portions.

3.2.4.3.2. Gel permeation chromatography

The samples representing bEPS from E-MBR and S-MBR as described in the preceding subsection were freeze dried at -50 °C for 48 h. (Freezone 4.5, Labconco, USA). The dried samples were dissolved in tetrahydrofuran at a ratio of 1 mg dry sludge/1 mL tetrahydrofuran, at room temperature, for 2 h. Then, the mixture was filtered through a polytetrafluoroethylene syringe filter (diameter of 13 mm and pore size of 0.45 µm). The filtrate was subjected to gel permeation chromatography (GPC) (TSKgel SuperHM-L 6.00 mm ID × 15 cm columns, EcoSEC HLC-8320GPC, Tosoh Bioscience, Japan), at an effluent flow rate of 0.6 mL/min and a differential refractometer detector to obtain molecular weight distribution (MWD) of bEPS. The GPC was conducted once per sample.

3.2.4.3.3. Three-dimension fluorescence excitation emission matrix spectroscopy

The SMP samples from E-MBR and S-MBR were filtered through a 0.45 μm pore-size cellulose acetate membrane filter (Whatman, USA), and then analyzed by using fluorescence spectroscopy (FP-8200, JASCO, USA). The three-dimension fluorescence excitation emission matrix spectra (3DEEM) were collected by scanning excitation wavelengths in the range from 200 nm to 500 nm in 2 nm steps, and detecting the emitted fluorescence in 2 nm steps between 250 nm to 600 nm. The excitation and emission slits were maintained at 5 nm and the scanning speed was 2000 nm/min. The spectrum of de-ionized water was recorded as a blank. The structure of organic molecules in SMP was interpreted following the five regions of 3DEEM divided by Chen *et al.* (2003). The 3DEEM was conducted once per sample.

3.2.4.3.4. Fourier transform infrared spectroscopy

Fourier transform infrared (FTIR) analysis was used to characterize the major functional groups of organic matters and to predict the major components (Maruyama *et al.*, 2001). bEPS samples from E-MBR and S-MBR were freeze dried at -50 °C for 48 h. (Freezone 4.5, Labconco, USA). Then, the dried sample was mixed with potassium bromide powder and pressure of 1.8 tons was applied by using a manual hydraulic press (Specac, USA) for 5 min to obtain a transparent pellet. The pellet was analyzed by a FTIR spectrometer (Nicolet 8700, Thermo Fisher Scientific, USA). The FTIR analysis was conducted in triplicate using one bEPS sample from each type of MBRs.

3.2.5. Membrane resistance analysis

The analysis of membrane fouling was based on membrane permeability monitoring which was performed by measuring the hydraulic resistances to permeation. The total resistance is contributed by three types of resistance (Judd, 2010; Maximous *et al*., 2009).

$$R_t = R_m + R_p + R_c$$

where R_t, R_m, R_p, and R_c are total resistance, membrane resistance, pore blocking resistance and cake filtration resistance (m^{-1}), respectively. A resistance test was conducted by filtering with de-ionized water through membrane under a constant permeate flux at 10.63 LMH and TMP, which represents resistance, was recorded. R_m and R_t were obtained based on TMP from resistance tests with new and fouled membranes, respectively. The fouled membrane was washed to remove cake layer and then tested for resistance to obtain $R_m + R_p$. R_p was obtained by subtracting R_m from $R_m + R_p$ while R_c was obtained by subtracting $R_m + R_p$ from R_t.

3.2.6. Statistical analysis

A paired sample *t*-test was conducted to statistically compare the results from different conditions and treatment based on a 5% significance level. The PSPP program (version 0.10.2, GNU, the Free Software Foundation, USA) was used for this statistical analysis.

3.3. Results and discussion

3.3.1. Treatment performances

Table 3-1 and, Figure 3-2 (a) and 3-2 (b) show high removal efficiencies for SCOD and NH_3-N in E-MBR and S-MBR. These high efficiencies were a result of operating under low food to microorganism (F/M) ratio (0.06 kg COD/kg MLSS·d) compared to a range of F/M for activated sludge treating domestic wastewater (0.04–1.00 kg COD/kg MLSS·d (Khan *et al*., 2011; Ng *et al.*, 2010; Tchobanoglous *et al*., 2003)). Moreover, the removal efficiencies of the two MBRs were also comparable ($p > 0.05$), suggesting that the gel entrapment did not affect treatment performances (gel matrix of PPVA did not limit the treatment ability of bacteria inside the gel). The oxygen uptake rate of the entrapped cells was not negatively affected by gel entrapment because of sufficient bulk DO in the solution (8.0 mg O_2/L) leading to high oxygen transfer from

the bulk solution into the gel matrix. The estimated oxygen uptake rates for S-MBR and E-MBR during steady state were not different (2.73×10^{-3} and 5.63×10^{-4} g O_2/g SS·h for carbon oxidation and nitrification in S-MBR versus 2.72×10^{-3} and 5.65×10^{-4} g O_2/g SS·h in E-MBR). It should be noted that for some datasets the error bars corresponding to the triplicate analyses cannot be seen because they are so small (contained within the data legend).

During the first 34 days of operation, heterotrophic and nitrifying bacteria originated from municipal sludge were acclimating to new growth conditions in MBRs (i.e. new wastewater, reactor configuration, and dilution rate), resulting in gradual improvements on the SCOD and ammonia removal efficiencies. After 34 days of operation, the bacteria became acclimated leading to steady and high treatment performances. The SCOD and ammonia removal efficiencies of E-MBR were 95.6 ± 0.9% and 92.6 ± 2.1% while those of S-MBR were 95.8 ± 0.8% and 93.3 ± 0.8% during steady state from day 34 to 111. These results agree with the findings by Ng *et al*. (2014), which compared entrapped cell MBR with suspended cell MBR, along with Di Trapani *et al.* (2014), Hu *et al.* (2012) and Khan *et al.* (2011) which compared biofilm/attached-growth MBR with suspended-growth MBR. All of these studies found comparable performances between biofilm-based MBR and suspended growth MBR. E-MBR showed high (>93%) and comparable organic removal performance with full-scale conventional MBRs (submerged hollow fiber suspended-growth MBRs) in the United States, Europe and Singapore (Judd, 2010). However, it was operated at lower values of F/M and OLR (Table 3-1, 0.06 kg COD/kg MLSS·d and 0.5 kg COD/m^3·d) compared to what are typically used in full-scale conventional MBRs (0.13–0.35 kg COD/kg MLSS·d for F/M and 0.8–1.7 kg COD/m^3·d for OLR) (Delrue *et al*., 2011; Judd, 2010).

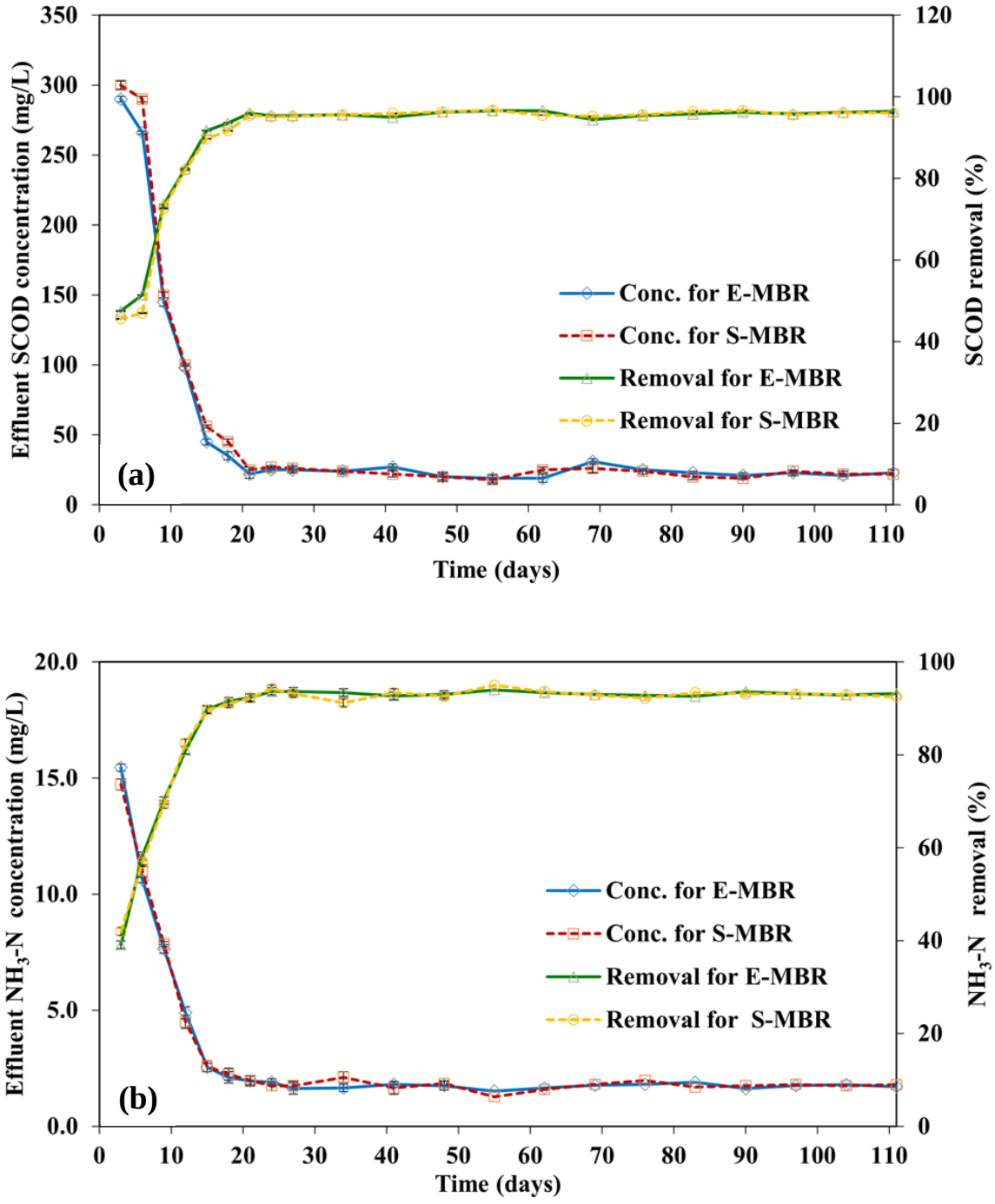

Figure 3-2: System performances: (a) SCOD removal and (b) NH_3 removal for E-MBR and S-MBR.

3.3.2. Permeate flux and transmembrane pressure

In order to investigate the fouling behavior, the change in TMP with operation time was monitored at a constant flux of 10.63 LMH for both MBRs. Figure 3-3 shows the change of TMP in E-MBR and SMBR. TMP increased slightly for the first few days of the operation and then abruptly climbed to reach the allowable level at 55 kPa (criterion for fouling) in both systems. This observation agrees with a previous study by Deng *et al.* (2015) which reported a two-step pattern for TMP profile associated with fouling. At the beginning, TMP rises smoothly and slowly. Then, after more severe fouling, TMP rises sharply and quickly. The TMP increasing rate of E-MBR was slower than that of S-MBR indicating that entrapped cells can delay membrane fouling.

Average periods to reach fouling were 16 days for E-MBR and 9 days for S-MBR at the same permeate flux. Chemical cleaning was required after these periods. The clean membrane was then put in operation and monitoring of TMP continued. The TMP profile shows that the magnitude of TMP increase within each physical cleaning cycle (air scouring and 15 min backflushing for every 3 h) for S-MBR was higher after the chemical cleaning. This phenomenon, which was much less pronounced in E-MBR, was caused by irreversible fouling that remained on membrane modules after the chemical cleaning. S-MBR exhibited higher irreversible fouling than E-MBR. This deduction is supported by the membrane resistance test discussed below. The filtration duration before reaching the allowable TMP was almost double for E-MBR compared to S-MBR.

Previous research reported similar findings that attached growth-MBR and entrapped-cells-based MBR are better than suspended growth-MBR on mitigating fouling by reducing the chemical cleaning frequency (Ng *et al.*, 2014; Huang *et al*., 2008; Lee *et al*., 2006). For example, a study of Khan *et al*. (2012, 2011), which investigated fouling conditions in MBRs at a

comparable range of permeate flux used in this research task (8.75 LMH for Khan *et al*. (2012, 2011) versus 10.63 LMH for this research task), reported the chemical cleaning frequencies were every 1.5–4 days for suspended growth-MBR and 4–8 days for attached growth-MBR. While in this research task, the chemical cleaning frequencies were every 9 days for S-MBR and every 16 days for E-MBR. However, it should be noted that the higher frequency of the chemical cleaning in Khan *et al.* (2012, 2011) is a result of using six times higher OLR (3 kg SCOD/m^3·d) than that used in this research task (0.5 kg SCOD/m^3·d).

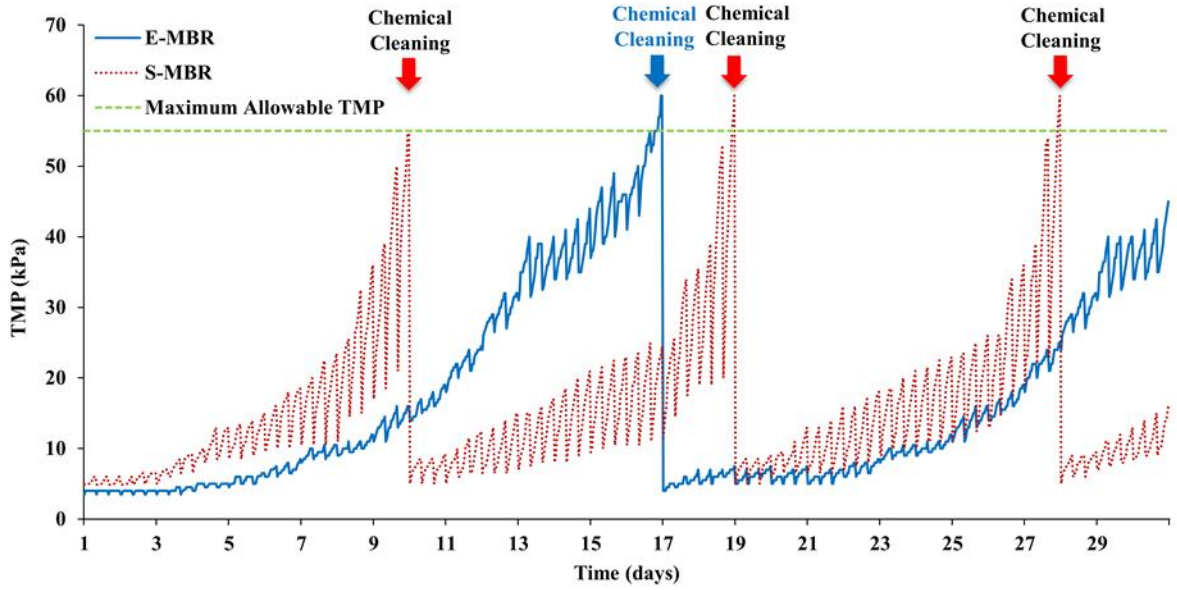

Figure 3-3: Observed TMP during the operations of E-MBR and S-MBR.

The resistance-in-series model was used to evaluate the membrane filtration characteristics and the results are reported in Table 3-1. Results of the membrane resistance test revealed that R_p was a key fouling mechanism for membranes in both E-MBR and S-MBR; R_p was 1.00×10^6 m^{-1} for E-MBR and 5.03×10^6 m^{-1} for S-MBR. Accumulation of SMP, mainly proteins, in the membrane pores caused by particles or colloids with equal or smaller size than the membrane pores, is considered to be the major cause of irreversible fouling and was likely the main cause of

pore blocking resistance in MBR (Ng *et al*., 2014). The proteins likely narrowed membrane pores via adsorption and caused more pore blocking resistance (Deng *et al.*, 2015; Ng *et al*., 2010). Previous research on bEPS and fouling suggests that fouling increases when bEPS increases but a mathematic correlation between bEPS and fouling resistance could not be established (Liu & Mi, 2012; Wang *et al*., 2009). As shown in Table 3-1, the significantly lower contents of SMP (Cosenza *et al*., 2013) were observed in E-MBR than in S-MBR ($p < 0.01$), corresponding to five times lower R_p in E-MBR. The significant decline of R_p in E-MBR can be attributed to the changes in biopolymer concentration, as well as the changes in sludge floc morphology (Khan *et al*., 2012). E-MBR can achieve longer operation time and membrane lifetime because it can lower pore blocking, which is a culprit for irreversible fouling, when compared with S-MBR. The results imply that R_p is the major contributor towards membrane fouling in this research task.

Cake filtration resistances of E-MBR and S-MBR were 8.80×10^5 m^{-1} and 5.03×10^5 m^{-1}, respectively. The reason that E-MBR had slightly higher cake filtration resistance than S-MBR is because smaller floc size in E-MBR system increased the specific energy barrier adhesion of floc to the membrane surface. Su *et al.* (2013) and Lin *et al.* (2011) observed that the formed cake layer possessed a higher fraction of small sludge floc compared with bulk sludge because of strong adhesion tendency of small flocs to membrane surface. Floc size apparently affects cake layer structure and therefore, may take roles in the osmotic pressure mechanism and cake resistance. This indicates that detachment of the small floc from the membrane surface is much more difficult once it adheres to the surface (Shen *et al*., 2015)

3.3.3. Bound extracellular polymeric substances (bEPS) and soluble microbial products (SMP) accumulation in entrapped cells-based-membrane bioreactor (E-MBR) and suspended-cells-based MBR (S-MBR)

The TMP monitoring and membrane resistance test indicated that E-MBR experienced less fouling than S-MBR. This finding clearly supported by bEPS and SMP concentrations in E-MBR and S-MBR as shown in Table 3-1. E-MBR produced significantly less SMP and bEPS ($p \leq 0.01$), in terms of protein and carbohydrate concentrations, than S-MBR. Previous studies on bench scale MBRs reported that membrane fouling is highly related to the concentrations of bEPS and SMP in the system (Wang *et al*., 2014, 2013; Luna *et al*., 2014); increases of bEPS and SMP concentrations result in increases of membrane fouling. Cosenza *et al.* (2013) reported that bEPS cause reversible fouling through cake layer deposition and SMP contribute to irreversible fouling mainly through pore blocking. Less bEPS and SMP in E-MBR were mainly due to a decrease in proteins. Thus, lowering bEPS and SMP concentrations in wastewater by using cell entrapment will mitigate membrane fouling.

3.3.4. Sludge characterizations

3.3.4.1. Particles size distribution

The PSD of mixed liquor is evaluated on the basis of particle diameter and reported as percentage of sludge volume. The PSD of sludge in a steady state indicates that the sludge of E-MBR had smaller particles size than S-MBR for both detection ranges (1 nm – 2 µm and 1 µm – 400 µm) as shown in Figure 3-4 (a, b). The smaller size of sludge particles in E-MBR was due to collisions between sludge particles and cell entrapment matrix (Huang *et al.*, 2008; Lee *et al*., 2006).

The mean particle sizes of sludge of the E-MBR and S-MBR obtained from a detection range of 1–2 µm were 768 nm and 1420 nm, respectively. The mean particle sizes of sludge of the EMBR and S-MBR obtained from a detection range of 1–400 µm were 192 µm and 271 µm, respectively. Traditionally, sludge suspension with particles sizes that are smaller than membrane pores shows a strong tendency to be deposited into membranes pores (Li *et al.*, 2012); however, both E-MBR and S-MBR had particle sizes that were larger than the membrane pore size of 0.04 µm. Therefore, membrane pore blocking in both E-MBR and S-MBR was not caused by the sludge particles but SMP as discussed in Section 3.3.3. The floc sizes of E-MBR were smaller than those of S-MBR leading to higher sludge adhesion on membrane surface (Shen *et al.*, 2015) of E-MBR compared to S-MBR. This resulted in higher cake resistance in E-MBR than that in S-MBR (cake resistance of E-MBR and S-MBR was 8.80×10^{5} m^{-1} and 5.03×10^{5} m^{-1}, respectively).

3.3.4.2. Molecular weight distribution

The MWDs of bEPS in E-MBR and S-MBR were analyzed by GPC. In principle, large molecular weight molecules are excluded earlier than smaller ones because they are unable to travel through the chromatography gel pores. The correlation between the exclusion time and the molecular weight of bEPS in E-MBR and S-MBR is shown in Figure 3-6. There are 4 peaks for bEPS in E-MBR (70 kDa, 609 Da, 454 Da, 309 Da) and 4 peaks for bEPS in S-MBR (86 kDa, 568 Da, 451 Da, and 307 Da). The GPC results also provided the values of the number-average molecular weight (M_n), weight-average molecular weight (M_w) and the dispersity index (M_w/M_n). The dispersity index is used as a measure of the broadness of molecular weight distribution that the larger dispersity index means the boarder molecular weight (Wang *et al.*, 2009). The M_w, M_n and M_w/M_n ratio of bEPS in E-MBR were 8313 Da, 435 Da and 19.0, respectively, while those in S-MBR were 2776 Da, 397 Da and 7.0, respectively. The dispersity index indicated that bEPS in

E-MBR had a much broader molecular weight distribution than that in S-MBR. The difference in molecular weight distributions of these two systems were expected due to different chemical natures and different biodegradation kinetics (Ni *et al.*, 2010). An equation by Erickson (2009) was used to convert the molecular weight distribution data to molecular size range. bEPS in E-MBR and S-MBR had molecular size ranges of 0.45×10^{-3}-2.72×10^{-3} µm and 0.44×10^{-3}-2.93×10^{-3} µm, respectively.

The molecular sizes of bEPS observed indicate that proteins and carbohydrates, as the main components of bEPS, can enter the membrane pore (0.04 µm) and possibly get deposited on the wall of the pores leading to partial or full pore blocking and in turn less permeate flux. In addition, when comparing the molecular size of bEPS in E-MBR to the PPVA gel matrix pore size (0.02-10 µm) found in previous studies (Siripattanakul *et al*., 2008; Zhang *et al*., 2007), it is clear that the PPVA gel matrix could not retain bEPS (proteins and carbohydrates) in EMBR. This confirms that less bEPS production observed in E-MBR compared to S-MBR was true and not attributed to the retention in the matrix.

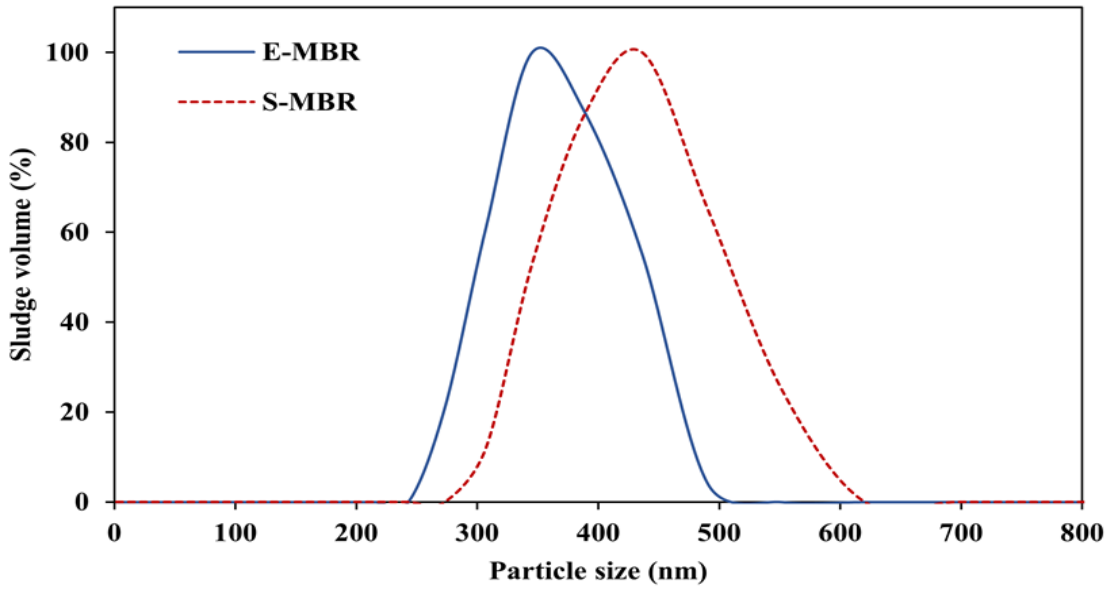

(a)

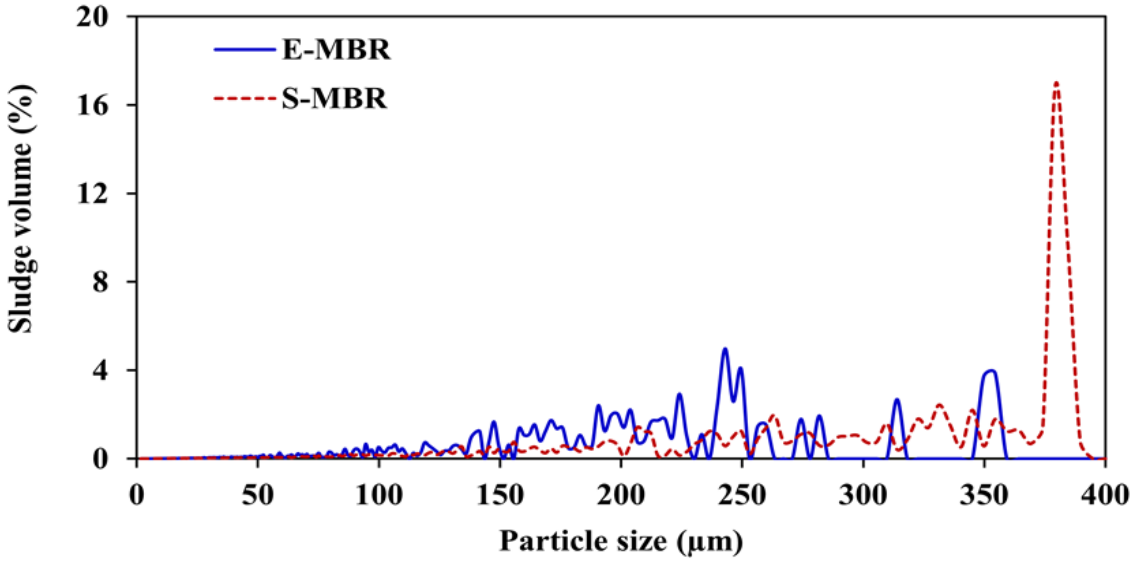

(b)

Figure 3-4: Particles size distribution for E-MBR and S-MBR sludge: (a) Range I: 1 nm – 2 µm and (b) Range II: 2 µm – 400 µm.

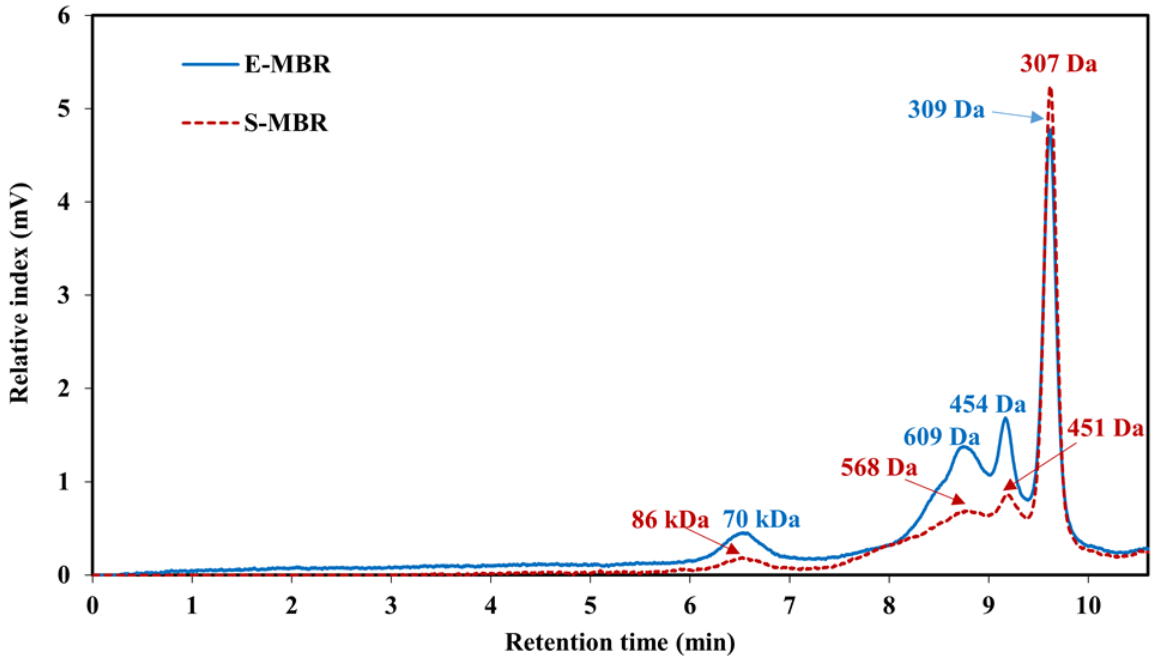

Figure 3-5: Molecular weight distribution of bEPS in E-MBR and S-MBR.

3.3.4.3. 3DEEM spectroscopy

The 3DEEM results were analyzed in order to characterize dissolved organic matter in SMP of both E-MBR and S-MBR. The fluorescence spectra of SMP in E-MBR had three major peaks as shown in Figure 3-6 (a), at the excitation/emission wavelengths (E_x/E_m) of 275/370 nm (peak A), 320/380 nm (peak B) and 380/460 nm (peak C). According to five regions of 3DEEM divided by Chen *et al*. (2003), peak A indicated as tryptophan substances, peak B indicated as protein-like substances and peak C indicated as humic acid-like substances. The fluorescence spectra of SMP in S-MBR had three major peaks as shown in Figure 3-6 (b), at the E_x/E_m of 220/410 nm (peak D), 250/410 nm (peak E) and 345/415 nm (peak F). These spectra results suggest hydrophobic acid substances for peak D, fulvic acid substances for peak E, and humic acid-like substances for peak F. The dominant organic substances in SMP of E-MBR were protein-like substances, tryptophan substances and humic acid-like substances with the intensity of 700, 620 and 380, respectively.

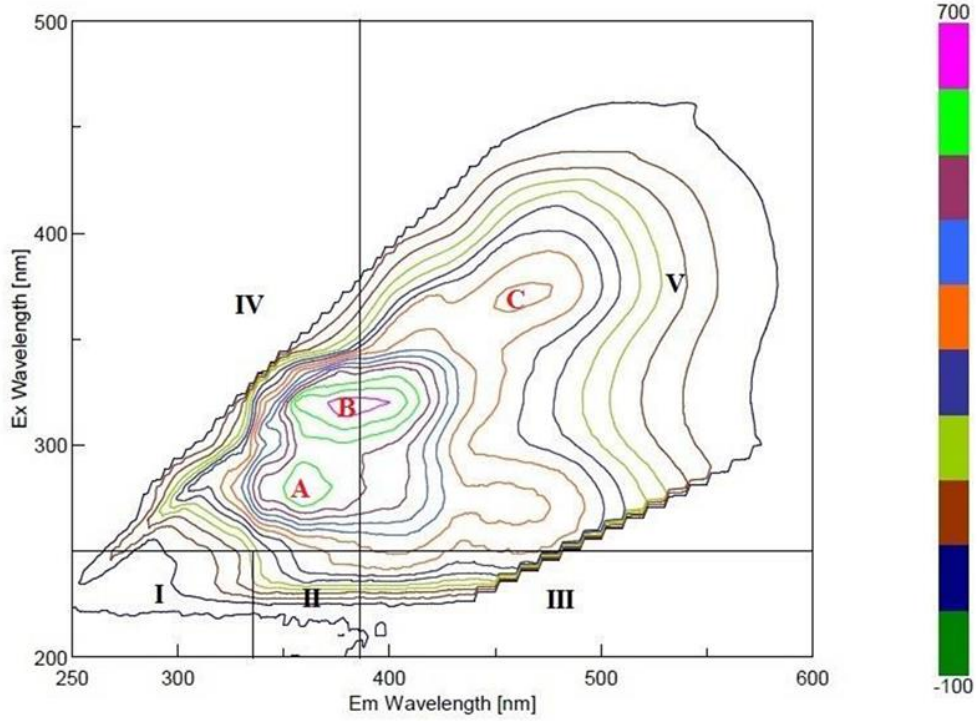

(a)

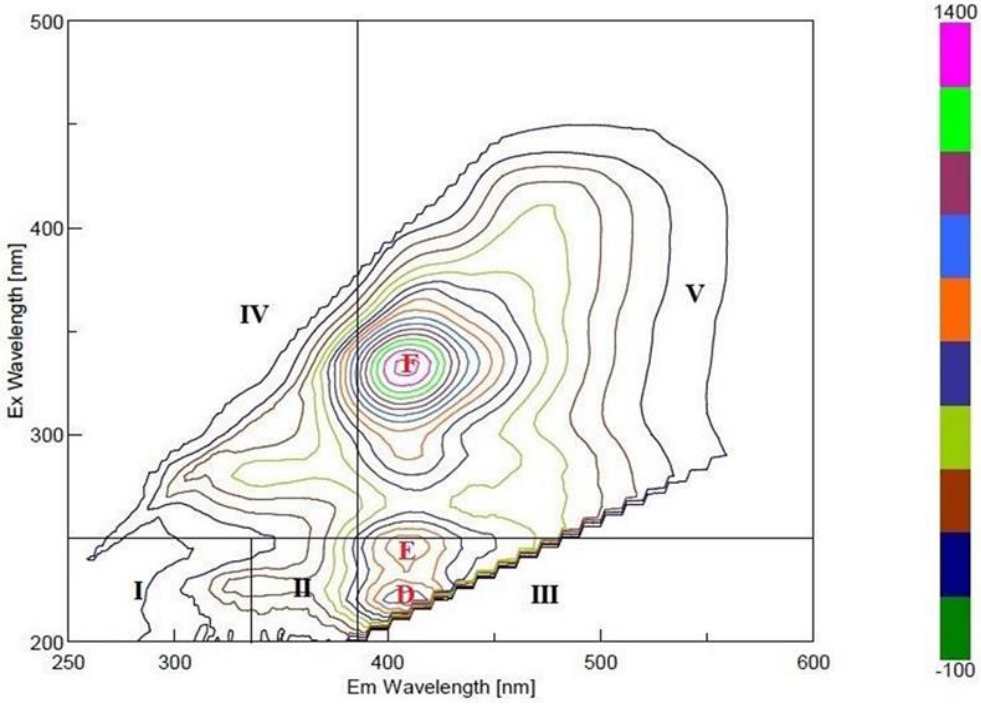

(b)

Figure 3-6: Three-dimension fluorescence excitation-emission matric spectra of SMP in (a) E-MBR and (b) S-MBR.

The dominant organic substances in SMP of S-MBR were humic acid-like substances, hydrophobic acid substances and fluvic acid substances with the intensity of 1400, 880 and 740, respectively. It can be seen that the intensity of humic acid-like substances of S-MBR was almost 4 times higher than of E-MBR, corresponding to the ratio of suspended solids in both systems. S-MBR had higher concentrations of suspended solids compared to E-MBR leading to higher numbers of dead cells in S-MBR.

3.3.4.4. FTIR spectroscopy

The FTIR spectra of bEPS in E-MBR and S-MBR are illustrated in Figure 3-7. The spectra for the two systems were similar except for the peak at 1558 cm^{-1} for S-MBR which is not identifiable. The peaks of adsorption around 3392–3420 cm^{-1} are attributed to stretching of the N-H bond in amines (Kumar *et al*., 2006). The peak at 2924–2926 cm^{-1} suggests the C-H bond of alkyl. The three peaks at 1653, 1540 and 1418 cm^{-1} are unique to the protein secondary structures, amides I and II (Maruyama *et al*., 2001), confirming that proteins were one of the components of bEPS. The peak at 1238–1240 cm^{-1} could be due to the presence of $-CH_3$ and C-H bond in methyl group (Maruyama *et al*., 2001). In addition, a broad peak at 1075 cm^{-1} exhibits the character of carbohydrates or carbohydrates-like substances (Croue *et al.,* 2003), verifying that carbohydrates were present in the bEPS. The organic structures identified are known to be sticky and can enhance the adhesive interaction between bacteria and the membrane surface (Meng *et al.,* 2009) leading to fouling.

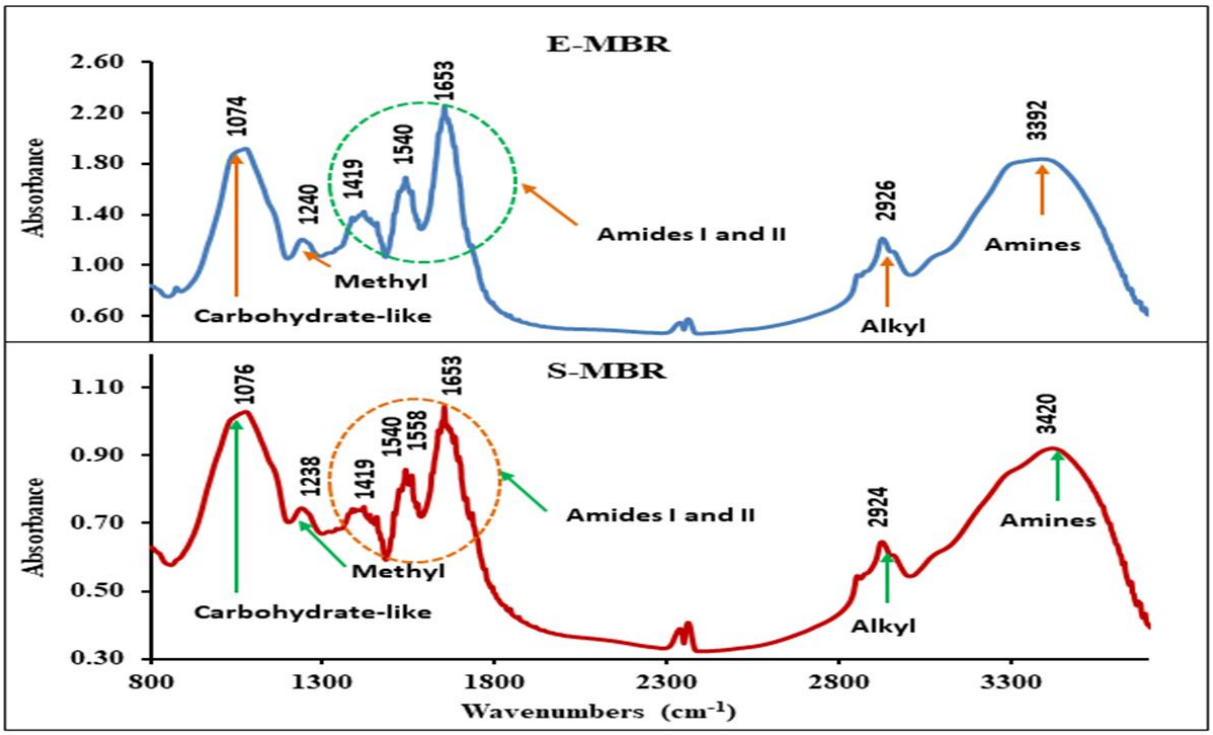

Figure 3-7: FTIR spectra of bEPS in the E-MBR and S-MBR.

3.4. Summary

Laboratory scale E-MBR and S-MBR were operated side by side for treatment of medium-strength synthetic wastewater. The results demonstrated that both E-MBR and S-MBR achieved high SCOD and ammonia nitrogen removal, indicating that PPVA gel matrix did not limit the treatment ability of bacteria inside the gel. Lower biomass concentration, and lower bEPS and SMP concentrations (in terms of proteins and carbohydrates) in E-MBR extended the membrane filtration time as E-MBR sustained a longer service duration of 16 days compared to only 9 days for S-MBR at a flux of 10.63 LMH. The membrane resistance test shows that pore blocking resistance, which is a main culprit for fouling in MBR, is greatly reduced in E-MBR. The higher pore blocking resistance in S-MBR was influenced by more bEPS and SMP deposition and adsorption on membrane and within membrane pores, accelerating the fouling rate. The results of PSD, GPC, 3DEEM and FTIR analyses provided a better understanding of sludge characteristics

in E-MBR and S-MBR systems. The PSD data showed that E-MBR had smaller particle sizes compared to S-MBR. The molecular sizes of bEPS observed by GPC indicated that proteins and carbohydrates, as the main components of bEPS, can enter the membrane pore and get blocked into the pores. Based on 3DEEM results, the intensity of humic acid-like substances in SMP was 4 times higher in S-MBR than E-MBR, corresponding to the ratio of suspended solids in S-MBR and E-MBR. The organic structures identified by FTIR are known to be sticky and can induce cake layer on the membrane surface, leading to fouling. The results from this research task suggest that the application of E-MBR can alleviate fouling leading to less frequent chemical cleaning and in turn the operating cost.

CHAPTER 4: RESEARCH TASK II–ENTRAPPED CELLS-BASED-ANAEROBIC MEMBRANE BIOREACTOR TREATING DOMESTIC WASTEWATER: PERFORMANCES, FOULING, AND BACTERIAL COMMUNITY STRUCTURE

4.1. Introduction

Research and developments on AnMBR have been carried out widely in recent years. AnMBR is a promising treatment technology for domestic wastewater because of its ability for energy recovery, high biomass retention and effluent quality (Charfi *et al*., 2015; Lin *et al*., 2013; Ozgun *et al*., 2013; Smith *et al*., 2013). However, AnMBR requires longer time to reach stable operation compared to aerobic MBR. This is because bacteria in AnMBR have lower substrate consumption rates which are associated with slower growth rates. Therefore, organic removal in AnMBR is normally lower than that in aerobic MBR (Liu *et al*., 2016, 2015; Salazar-Pelaez *et al*., 2011).

Higher biomass concentration is required for AnMBR compared to aerobic MBR due to slow growing and low substrate consumption rates of anaerobic bacteria (Liu *et al*., 2016, 2015; Salazar-Pelaez *et al*., 2011). The higher biomass concentration leads to faster and more severe fouling in AnMBR (Liu *et al*., 2016; Ding *et al*., 2015; Dereli *et al*., 2015). Fouling mitigation in aerobic MBR has been well studied including new approaches such as cellular quorum quenching and immobilization of alginate lyase on membrane (for reduction of fouling associated with alginate) (Waheed *et al*., 2017; Meshram *et al*., 2016). That is not the case for AnMBRs. Recently, several attached growth AnMBRs have been developed to retain slow growing anaerobic microorganisms and lower membrane fouling. Kim *et al*. (2014) combined rotary disks with sponge carriers (5 mm cube polyurethane sponge with 97.9% voids) to sustain microbial growth

as well as to control membrane fouling in attached-growth AnMBR. They suggested that the developed process can save 90% of the electricity costs compared to traditional AnMBR.

Gao *et al*. (2014, 2010) suggested that collision and scouring between biofilm carriers and membrane surfaces reduce cake filtration resistance in attached-growth AnMBR. The lower cake filtration resistance in attached-growth AnMBR contributes to less suspended sludge concentration compared to suspended-growth AnMBRs (Kim *et al.*, 2011; McCarty *et al*., 2011). Another study on biofilm carriers by Ng *et al*. (2014) indicated higher bEPS and SMP, major culprits for membrane fouling, in suspended-growth AnMBR compared to biofilm carrier AnMBR. However, membrane fouling in attached growth AnMBRs, particularly foulant characteristics, is not well understood and remains unclear (Yue *et al*., 2015; Charfi *et al*., 2012; Stuckey, 2012).

Cell entrapment, a technique that artificially entraps cells in a porous polymer matrix, is a relatively new wastewater treatment process. Compared to suspended cells, entrapped cells are more resistant to cell washout and toxicity, and have higher specific growth and substrate utilization rates (Pramanik & Khan, 2008). Recently, phosphorylated-polyvinyl alcohol entrapped cells have been applied in order to retard membrane fouling in aerobic MBR (Juntawang *et al*., 2017a). The E-MBR can delay fouling due to lower biomass, bEPS, and SMP compared to the traditional S-MBR.

It is widely known that the amount and characteristics of membrane foulants generated by bacterial metabolism is partly influenced by the community structure. Yu *et al.* (2012) suggested that an attachment to membrane surface by some groups of bacteria in AnMBR results in the production of bEPS leading to cake layer formation. It is reasonable to expect different bacteria species to differ in their relative contributions to fouling due to differences in the nature and quantity of bEPS and SMP. High amounts of polysaccharide EPS in anaerobic sludge were tied to

an abundance of fermentative bacteria (*Clostridium butyricum*) which were as high as 30% of total biomass concentrations (Gao *et al.*, 2010). Nevertheless, information about the contributions of different bacterial populations to bEPS and SMP secretion in AnMBR is very rare (Ma *et al*., 2013). Bacteria communities involved in biofouling are useful knowledge for AnMBR operation and design for effective fouling control.

In this research task, a new submerged AnMBR process called entrapped-cells-based AnMBR (E-AnMBR) was developed to treat medium-strength domestic wastewater. E-AnMBR was operated in parallel with a suspended-cells-based AnMBR (S-AnMBR) to investigate the influences of cell entrapment on the system performance and membrane fouling. It was expected that the entrapped cells in E-AnMBR can lower biomass, bEPS and SMP concentrations in similar ways as E-MBR (Juntawang *et al*., 2017a). In addition, the Illumina high-throughput sequencing of 16S rRNA genes was used to characterize the bacterial communities in cake layers of both MBRs. The knowledge of fouling mechanisms and bacteria community gained from this research task will be useful for future AnMBR system design and operation.

4.2. Materials and methods

4.2.1. Synthetic wastewater and chemicals

Synthetic wastewater was prepared according to the formula listed in Subsection 3.2.1.

4.2.2. Preparation of entrapped cells

The preparation of entrapped cells followed the procedure in Subsection 3.2.2. However, in this research task, anaerobic sludge taken from an anaerobic digester (Moorhead wastewater treatment facility, Moorhead, MN) was the cell source instead of mixed liquor taken from an aeration tank mentioned in Subsection 3.2.2.

4.2.3. Anaerobic membrane bioreactor setup and operation

Laboratory-scale E-AnMBR and S-AnMBR systems consisted of (1) bioreactors, (2) membrane modules, (3) feed tank, (4) backwash tank, (5) gas collection units, (6) nitrogen gas tank, (7) peristaltic pumps, (8) stirrers and (9) vacuum gauges as shown in Figure 4-1. The two systems had the same configuration and operation except that E-AnMBR was inoculated with entrapped anaerobic sludge while S-AnMBR was inoculated with suspended anaerobic sludge (8 g/L). Each bioreactor was made of acrylic and had a working volume of 6.0 L. A hollow fiber membrane module (ZW-1, GE Water & Power, Canada) with a pore diameter of 0.04 μm and an effective surface area of 0.047 m^2 was submerged in the bioreactor. Nitrogen gas from a gas tank was supplied through fine stone diffusers to achieve and maintain anaerobic condition in the feed tank, backwash tank and bioreactors. Three peristaltic pumps (Model 7553-60, Barnant, USA and Model 7554-90, Thermo Fisher Scientific, USA) were used as influent, permeate and backwash pumps.

TMP was monitored during the filtration via vacuum gauges on the permeate sides (Model 14902.5, Ashcroft, USA). Under 24 h HRT, a constant permeate flux at 10.63 LMH was maintained through 15 min backflushing by deoxygenated water from the backwash tank every 1.5 h. An electronic timer (ODT309-M2, Smart Electrician, USA) was used to control the backflush pump system. When TMP reached 55 kPa or it was not possible to maintain constant permeate flux, the membrane was cleaned by soaking in 200 ppm sodium hypochlorite for a minimum of 5 h and then 5 g/L citric acid for a minimum of 5 h. E-AnMBR and S-AnMBR were operated at room temperature for 90 days after reaching steady state, based on less than 10% SCOD removal variation (Burton *et al*., 2003), without wasting sludge (a total of 120 days including a 30 days startup period). A magnetic stirrer located at the bottom of the reactor provided constant

mixing at 200 rpm. Biogas production was measured by the water replacement method. Daily feed flow and membrane flux were manually measured. Reactor operational conditions of both systems are summarized in Table 4-1.

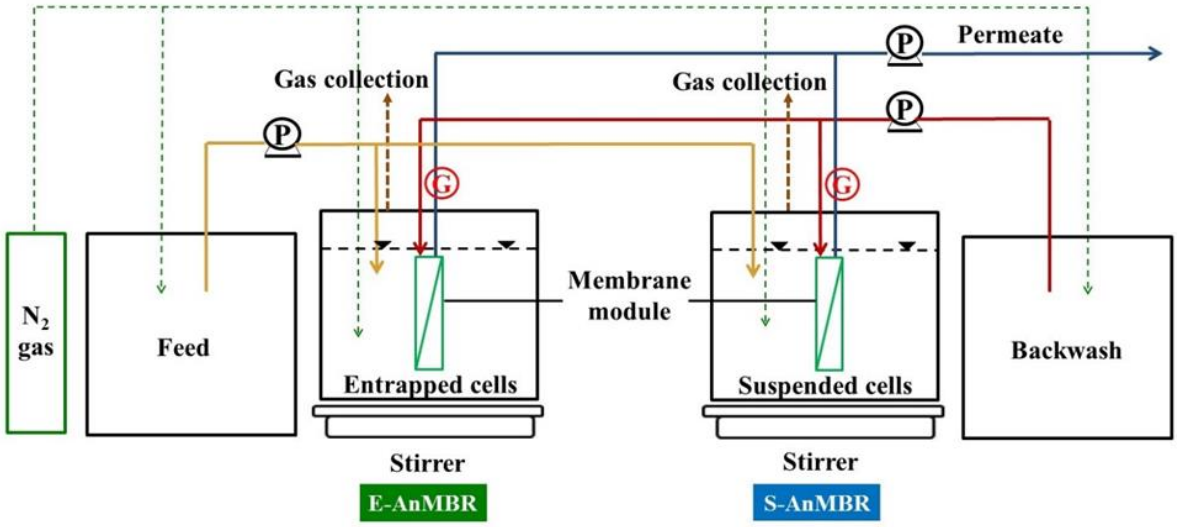

Figure 4-1: Experimental setups of E-AnMBR and S-AnMBR systems.

Table 4-1: Operational conditions of E-AnMBR and S-AnMBR (mean ± standard deviation)

Parameters	E-AnMBR	S-AnMBR
[a] Influent soluble organic (mg SCOD/L)	565±11	565±11
[a] Influent NH_3 (mg N/L)	25.14±0.20	25.14±0.20
[a] Organic loading rate (kg SCOD/m^3·d)	0.57±0.01	0.57±0.01
[a] Food-to-microorganisms ratio (kg SCOD/kg MLSS·d)	0.071±0.001	0.071±0.001
[b] Permeate flux (LMH)	10.63	10.63
[b] HRT (h)	24	24
[c] Temperature (°C)	27.42±0.61	27.64±0.54
[c] pH (in bioreactor)	7.38±0.24	7.43±0.09
[c] Oxidation reduction potential (mV)	-312±11	-325±8

[a] n = 30; [b] n = 120 and [c] n = 24

4.2.4. Characterizations of feed, reactor fluid, permeate, sludge, bEPS, and SMP

4.2.4.1. Feed, reactor fluid, and permeate characterizations

During steady state operation, SCOD, NH_3-N, NO_2^--N, NO_3^--N, DO, oxidation reduction potential (ORP) and pH in the feed water, permeate water and reactor fluid were monitored every 4 days. Samples were taken from the feed and permeate tanks then filtered through a GF/C microfiber filter (Whatman, USA). COD was measured by the Reaction Digestion method. NH_3-N was measured by the Salicylate method. NO_2^--N was measured by the Diazotization method. NO_3^--N was measured following the UV screening method at wavelengths of 220 and 275 nm. The procedures for these four analytical methods were according to APHA *et al.* (2005). A DR 5000 spectrophotometer (HACH, USA) was used for SCOD, NH_3-N, NO_2^--N and NO_3^--N determinations. DO was measured by a DO meter (model 850, Thermo Scientific, USA). ORP and pH were measured by an ORP-pH meter (model 250, Thermo Scientific, USA). All these analyses were conducted in triplicate by splitting each sample into three portions.

4.2.4.2. Particles size distribution

Particle size distribution was determined according to the procedure described in Subsection 3.2.4.2.

4.2.4.3. bEPS and SMP characterizations

4.2.4.3.1. Extraction and quantification

The methods for bEPS and SMP extractions and quantification are described in Subsection 3.2.4.3.1.

4.2.4.3.2. Gel permeation chromatography

The procedure for gel permeation chromatography is described in Subsection 3.2.4.3.2.

4.2.4.3.3. Three-dimension fluorescence excitation emission matrix spectroscopy

For 3DEEM spectroscopy, the procedure was the same as that listed in Subsection 3.2.4.3.3.

4.2.4.3.4. Fourier transform infrared spectroscopy

The method for FTIR analysis is in Subsection 3.2.4.3.4.

4.2.5. Membrane resistance analysis

Membrane resistance analysis was conducted according to the procedure in Subsection 3.2.5.

4.2.6. Biogas monitoring and analysis

Biogas volume was monitored daily through a biogas collection tank. In addition, biogas was sampled during the last 45 days of the operation on days 75, 90, 105 and 120 from the overhead space of E-AnMBR and S-AnMBR bioreactors using syringes. The sample was analyzed for CH_4 and CO_2 using a gas chromatograph (GC) (Model No. 8610C, SRI Instruments, USA) equipped with a flame ionization detector (temperature set at 300°C). The GC column temperature was programmed to maintain a temperature of 100°C for 15 min. Compound peaks were recorded and analyzed with Peak Simple Chromatography Data System Software (Ver. 3.72; SRI Instruments, Torrance, CA, USA).

4.2.7. Bacteria community

Total genomic DNA was extracted from 2 mg of cake sludge (as total solids) deposited on the membrane surface using a Fast DNA™ SPIN kit for soil (MP Biomedicals, Solon, OH, USA). Two milligrams of sludge are adequate for DNA extraction for sludge from biological wastewater treatment systems according to Karst *et al.* (2016). DNA quality was assessed by using agarose gel electrophoresis. Thereafter, 12 ng of the extracted DNA was used as a template for PCR using

the Illumina primer pair (Forward 5'-TCGTCGGCAGCGTCAGATGTGTATAAGAGACAGCC TACGGGNGGCWGCAG3', Reverse 5'-TCTCGTGGGCTCGGAGATGTGTATAAGAGACAG GACTACHVGGGTATCTAATCC3', Klindworth *et al*., 2013) to amplify the V3 and V4 regions of the 16S rRNA gene. PCR amplification was carried out in a 25 µl reaction containing 2X KAPA hot-start ready mix and 200 nM of each primer. The amplification condition included an initial denaturation step for 3 min at 94°C, followed by 25 cycles of 98°C for 20 s, 55°C for 30 s, and 72°C for 30 s, followed by a single step final extension step at 72°C for 5 min. The 16S amplicon products were purified using AMPure XP beads. Subsequently, the purified 16S amplicon was indexed using 2X KAPA hot-start ready mix and 5 µl of each Nextera XT index primer in a 50 µl PCR reaction, followed by 8-10 cycles of PCR condition as described above. The indexed 16S amplicon was purified using AMPure XP beads, pooled and diluted to a final loading concentration of 4 pM. Cluster generation and 250-bp paired-end read sequencing were performed on an Illumina MiSeq at Omics Sciences and Bioinformatics Center (Chulalongkorn University, Bangkok, Thailand).

The pair-end sequencing reads were de-multiplexed, and stitched together. Low quality reads were filtered out using FASTX-Toolkit. In addition, chimeric reads were removed using VSEARCH software. The automated pipeline *pick_open_reference_otu.py* in QIIME 1.9.0 was implemented for operational taxonomic unit (OTU) picking, taxonomy assignment, and sequences alignment against the Greengenes reference database. The uclust algorithm was used as executed in USEARCH option to perform the open reference OTU picking. To ensure even sequencing depth across samples, 10,000 sequences per sample were randomly subsampled for the analysis of bacterial communities. Alpha diversity estimates were computed for phylogenetic diversity, and

rarefaction curve was generated. Beta diversity was estimated by computing weighted and unweighted UniFrac distances between samples in order to create principal component analyses. These downstream analyses were performed using QIIME.

4.2.8. Statistical analysis

For statistical analysis, a *t*-test was performed according to the details in Subsection 3.2.6.

4.3. Results and discussion

4.3.1. Treatment performances

The influent SCOD concentration for both E-AnMBR and S-AnMBR was 565±11 mg/L (same feed tank). The average SCOD removal in both reactors is shown in Figure 4-2. Permeate SCOD concentrations were 87±9 mg/L for E-AnMBR and 89±11 mg/L for S-AnMBR. SCOD removal efficiency remained high throughout the operation time of 90 days after steady state (from day 30 to 120) at 84.7±2.1% for E-AnMBR and 84.3±2.4% for S-AnMBR at an average organic OLR of 0.57±0.01 kg SCOD/m^3·d. The results suggest that the treatment efficiency of E-AnMBR was comparable to that of S-AnMBR (p = 0.714) suggesting that gel entrapment had no effect on treatment performance.

The SCOD removal efficiency of S-AnMBR in this research task is comparable to values reported for AnMBRs in previous studies except for biofilm-AnMBRs (Table 4-2). The lower SCOD removal efficiency reported by Gao *et al*. (2014) compared to this research task might be from higher OLR applied in their research. The higher SCOD removal efficiency reported by Kim *et al*. (2014) compared to this research task is because of a pretreatment unit, anaerobic expanded bed reactor, in their system. The SCOD removal efficiency of E-AnMBR was comparable to those of S-AnMBR and other suspended cells-AnMBRs in previous research (Table 4-2). This suggests sufficient transfer of substrate in and out of the entrapment matrix (Juntawang *et al*., 2017a).

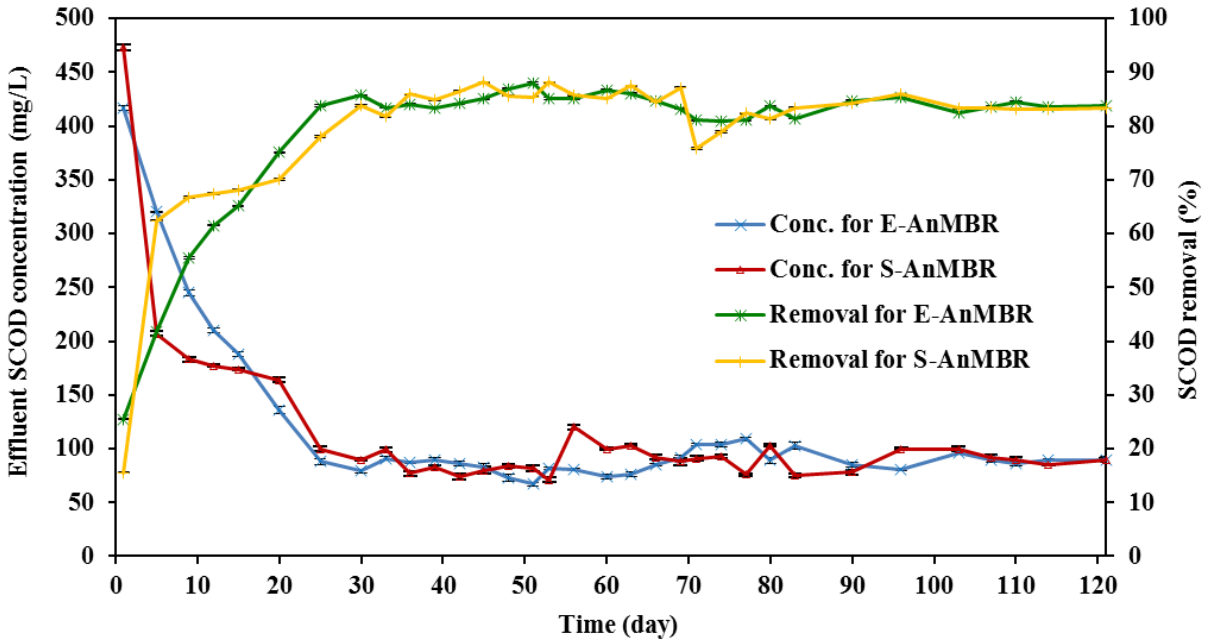

Figure 4-2: Influent and effluent SCOD concentrations and removal efficiency of E-AnMBR and S-AnMBR.

Table 4-2: AnMBR operational and treatment performances for domestic wastewater.

AnMBRs	Influent COD (mg/L)	COD removal (%)	OLR (kg COD/ m^3·d)	F/M (kg COD/ kg sludge·d)	CH_4 produced (L/d)	Flux (LMH)	References
Suspended cells	398 ± 70	87.9±7.4	1.00±0.2	0.297±0.014	0.3±0.01	5.00	Yue et al., 2015
	500±10	84.6±2.4	3.8	0.1±0.001	NA	5.30	Liu et al., 2012
	500	85	1.00	1.0	0.391±0.003	10.00	Ho et al., 2010
	565±11	84.3±2.4	0.57±0.01	0.071±0.001	0.28±0.03	10.63	This research task
Biofilm	700 ± 79	67.1±2.9	1.21± 0.14	1.03 ± 0.04	0.211±0.02	5.00	Gao et al., 2014
	343±17	96.3±0.9	1.20 ±0.14	0.24 ±0.01	0.241±0.002	5.00	Kim et al., 2014
Entrapped cells	565±11	84.7±2.1	0.57±0.01	0.071±0.001	0.23±0.02	10.63	This research Task

4.3.2. Permeate flux and transmembrane pressure

In order to investigate the fouling behavior, TMP was monitored with operation time at constant flux of 10.63 LMH in both AnMBRs (Figure 4-3). When TMP reached 55 kPa, chemical cleaning was required as represented by the red and blue arrows in Figure 4-3 for S-AnMBRs and E-AnMBRs, respectively. In this research task, both S-AnMBRs and E-AnMBRs were operated at higher permeate flux compared to other suspended cells AnMBRs and biofilm-AnMBRs shown in Table 4-2. The flux in this research task was targeted to achieve the permeate flux required for domestic wastewater treatment plants, 10-25 LMH (Judd, 2010). Average periods to reach fouling (55 kPa) were 11 days for E-AnMBR and 7 days for S-AnMBR at the same permeate flux. This observation agrees with Ng *et al.* (2014) and Kim *et al.* (2014) that reported longer operation time before chemical cleaning is required for biofilm-AnMBRs compared to suspended cells-AnMBRs. The superiority of biofilm-AnMBRs over suspended cells-AnMBRs was due to collisions between the biofilm-carrier and membrane surface resulting in reduced R_c and lower SMP concentrations leading to less R_p (Kim *et al*., 2014; Ng *et al*., 2014). When comparing with laboratory scale biofilm-AnMBRs treating synthetic wastewater, E-AnMBR can provide longer operation time before chemical cleaning is required, 11 days for E-AnMBR versus 4-10 days for biofilm-AnMBRs (Gao *et al*., 2014; Kim *et al*., 2014).

The TMP profile in Figure 4-3 shows higher difference in TMP magnitude for S-AnMBR compared to E-AnMBR, before and after physical cleaning through 15 min backflushing by deoxygenated water from the backwash tank every 1.5 h (lines a and b in Figure 4-3). This suggests more severe fouling in S-AnMBR compared to that in E-AnMBR, because higher hydraulic pressure was required by S-AnMBR to maintain the same permeate flux as E-AnMBR. Due to the higher fouling rate, more chemical reagents are needed for S-AnMBR membrane cleaning.

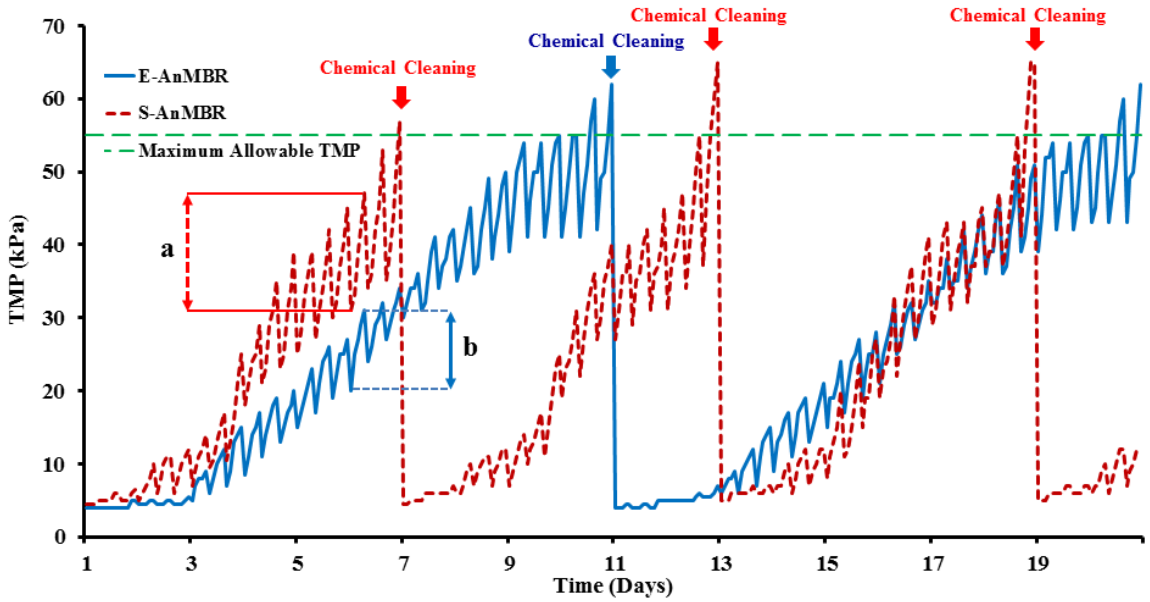

a: Difference of TMP magnitude in S-AnMBR before and after physical cleaning
b: Difference of TMP magnitude in E-AnMBR before and after physical cleaning

Figure 4-3: Observed TMP during the operations of E-AnMBR and S-AnMBR.

4.3.3. Membrane resistance

The membrane resistance tests indicate that R_p values of S-AnMBR and E-AnMBR were 2.54×10^6 m^{-1} and 0.32×10^6 m^{-1} while R_c values of S-AnMBR and E-AnMBR were 1.69×10^6 m^{-1} and 1.06×10^6 m^{-1}, respectively. These resistance values suggest pore blocking and cake layer as the key fouling mechanisms in S-AnMBR and E-AnMBR. Both R_p and R_c of S-AnMBR were higher than those of E-AnMBR agreeing with longer operation time prior to chemical cleaning achieved by E-AnMBR.

The higher R_c in S-AnMBR compared to E-AnMBR agrees with the PSD results (see Subsection 4.3.5.1), showing that particles in S-AnMBR had smaller sizes. The smaller floc size in S-AnMBR was influenced by adhesion force between particles and membrane surface leading to cake layer formation (Shen *et al*., 2015). Su *et al*. (2013) and Lin *et al*. (2011) observed that the formed cake layer possesses a higher fraction of small particles compared to suspended sludge

because of a strong adhesion tendency of small particles to the membrane surface. Detachment of the smaller particles from the membrane surface is more difficult once it adheres (Shen *et al*., 2015).

4.3.4. bEPS and SMP accumulations in E-AnMBR and S-AnMBR

bEPS and SMP contents in anaerobic sludge including proteins, carbohydrates, nucleic acids, lipids and humic acids are known to be the main causes of membrane fouling (Liu *et al*., 2015; Meng *et al*., 2009). The bEPS and SMP concentrations (Figure 4-4) measured as proteins and carbohydrates in E-AnMBR were significantly less than S-AnMBR ($p < 0.01$), (67–75% less carbohydrates and 72–84% less proteins for SMP and 75–81% less carbohydrates and 25–32% less proteins for bEPS). Previous research on MBRs shows that membrane fouling is highly related to bEPS and SMP concentrations in the systems (Juntawang *et al*., 2017a; Wang *et al*., 2013; Yun *et al*., 2006). Studies on the distribution of biopolymers in fouling layers revealed that the bottom part of the cake layer which attaches to the membrane surface is rich in proteins (Gao *et al*., 2011; Metzger *et al*., 2007). This suggests that proteins can form a sticky layer on the membrane surface which accelerates fouling as cake filtration resistance.

Previous studies indicated that increases in bEPS result in decreases in membrane permeability (Juntawang *et al*., 2017a; Wang *et al*., 2013; Yun *et al.*, 2006). In addition, Cho *et al.* (2005) found that an increase in bEPS leads to an increase in the membrane resistance. When bEPS rises, the cake resistance increases contributing to TMP. The accumulation of SMP in the membrane pores leads to pore blockage and induces faster long-term fouling rates. Eight times lower R_p in E-AnMBR compared to S-AnMBR are likely because of lower contents of bEPS and

SMP. The results in this research task suggest that entrapped cells in E-AnMBR mitigated membrane fouling and provided longer operation time before chemical cleaning was required by lowering bEPS and SMP especially in term of proteins compared to suspended cells in S-AnMBR.

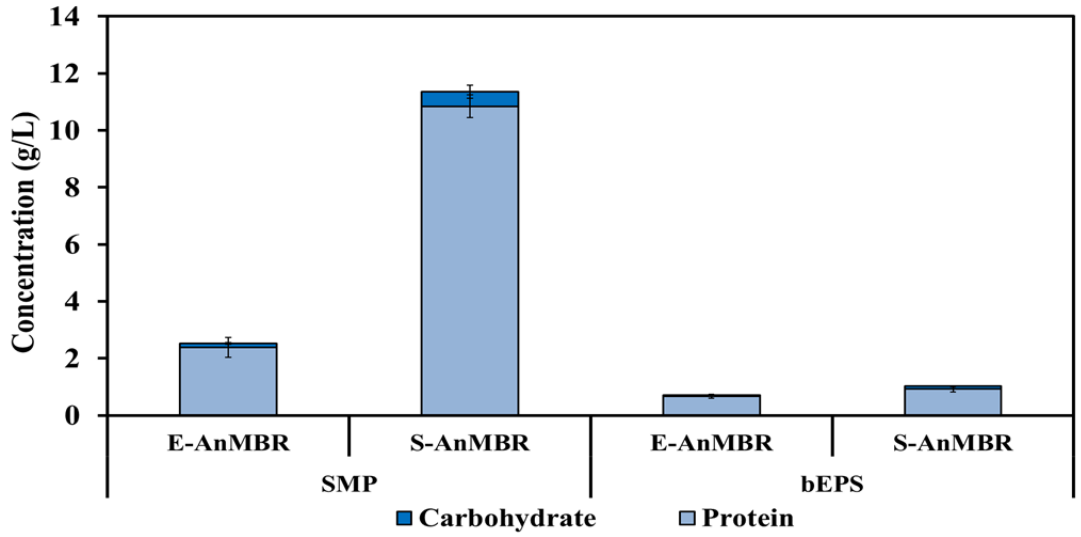

Figure 4-4: Concentrations of bEPS and SMP in E-AnMBR and S-AnMBR during steady state operations.

4.3.5. Sludge characterizations

4.3.5.1. Particles size distribution

The mean particle sizes of the sludge of the E-AnMBR and S-AnMBR for a detection range of 1- 400 µm were 59 and 49 µm for the cake layer (Appendix A, Figure A-1(a)), and were 88 and 55 µm for the suspended sludge (Appendix A, Figure A-1(b)), respectively. The results indicate larger average particle sizes of both the cake layer and suspended sludge in E-AnMBR compared to S-AnMBR. Most of the particles in E-AnMBR and S-AnMBR were in a range of 1-400 µm. The instabilities such as sudden organic load, temperature and pH changes, may cause floc breakage, resulting in decreases in particle size in AnMBRs (Gao *et al*., 2011, 2010; Akram & Stuckey, 2008). The PSD results correspond well with the membrane resistance test results that show higher cake filtration resistance in S-AnMBR (1.69×10^{6} m^{-1}) compared to E-AnMBR

(1.06×10^6 m^{-1}), because of smaller particles in S-AnMBR (Shen *et al.*, 2015). In addition, the PSD results indicated less chance of pore blocking in this research task because most of the particles were larger than membrane pores size (0.04 µm).

4.3.5.2. Molecular weight distribution

The GPC peaks (Appendix A, Figure A-2) of bEPS in E-AnMBR and S-AnMBRs indicate the molecular weights of >10 kDa, suggesting existence of carbohydrates and proteins in both systems (Gao *et al*., 2011). According to Wang *et al*. (2008), the bEPS components in suspended sludge of both systems that were greater than 500 kDa (831 kDa for E-AnMBR and 968 kDa for S-AnMBR) were from substrate metabolism and/or release from cell lysis and decay. The GPC peaks with molecular weight heavier than 500 kDa are present for bEPS of suspended sludge but absent for bEPS of cake layer (Appendix A, Figure A-2). This is because heavier molecular weight organic matters have less adhesion forces to membrane surface compared to lighter ones (Shen *et al*., 2015).

The broadness of MW distribution, Mw/Mn, was obtained from the ratio of Mw and Mn. The Mw/Mn ratios of bEPS from the suspended sludge in E-AnMBR and S-AnMBR were 2.74 and 1.78, respectively. The Mw/Mn ratios of bEPS from the cake layer in E-AnMBR and S-AnMBR were 17.6 and 8.5, respectively. The Mw/Mn ratios indicated that bEPS in both suspended sludge and cake layer of E-AnMBR had broader molecular weight distributions compared to those in S-AnMBR. This suggests that the degradation of substrate and cell lysis in E-AnMBR resulted to a wider range of molecular weight compared to S-AnMBR (Ni *et al*., 2010). The broader molecular weight distributions of bEPS in E-AnMBR led to lower R_p and R_c (see Subsection 4.3.3) compared to S-AnMBR (Wang *et al*., 2008; Laspidou & Rittmann, 2004).

4.3.5.3. 3DEEM spectroscopy

The 3DEEM analysis was applied to investigate characteristics of SMP from cake layer and suspended sludge (Appendix A, Figure A-3). The analysis is a reliable tool for characterizing membrane foulants (Juntawang *et al*., 2017a; Wang *et al*., 2017). Two major peaks were identified by the fluorescence spectrum of SMP from the cake layer of E-AnMBR: aromatic protein and protein-like substances containing tryptophan (Chen *et al*., 2003) at Ex/Em of 225/330 nm and 282/330 nm, respectively (Appendix A, Figure A-3(a)). The fluorescence spectrum of SMP from the suspended sludge in E-AnMBR suggests tryptophan and protein-like substances at Ex/Em of 250/350 nm and 300/350 nm, respectively (Appendix A, Figure A-3(b)).

SMP from the cake layer in S-AnMBR consisted of aromatic protein substances, protein-like substances containing tryptophan and protein-like substances based on Ex/Em of 225/330 nm, 275/330 nm and 310/350 nm, respectively (Appendix A, Figure A-3(c)). Four major peaks at Ex/Em of 275/440 nm, 360/410 nm, 365/520 nm and 440/520 nm indicate fulvic acid-like, hydrophobic acid, humic acid polymer and humic acid-like, respectively in SMP from the suspended sludge of S-AnMBR (Appendix A, Figure A-3(d)).

Organic substances in the suspended sludge and cake layer in E-AnMBR were similar, mainly protein functional groups. This supports the results of bEPS and SMP accumulations in E-AnMBR and S-AnMBR (see Subsection 4.3.4) which indicate that protein-like substances played a more vital role in membrane fouling than other organic substances. The organic substances in S-AnMBR in the suspended sludge and those in the cake layer were different. This was due to only organic substances with sticky nature, protein functional groups, in S-AnMBR can attach and form a cake layer on membrane surface (Meng *et al*., 2009) while other organic substances, humic acid polymer and humic acid-like, remained in the suspended sludge. The organic substances in the

suspended sludge in S-AnMBR were different from those in E-AnMBR. Higher suspended biomass concentrations in S-AnMBR resulted in higher accumulation of humic acid polymer and humic acid-like substances from cells lysis/decay. The cake layer of S-AnMBR was thicker than that of E-AnMBR. This was due to higher bEPS and suspended sludge concentrations in S-AnMBR compared to E-AnMBR. The observation was confirmed by higher cake filtration resistance in S-AnMBR (1.69×10^{6} m^{-1}) compared to E-AnMBR (1.06×10^{6} m^{-1}).

SMP from the cake layer was dominated by proteins while SMP from the suspended sludge was mainly fulvic acid-like. This agrees with the sticky nature of proteins making them easy to adhere to the membrane surface. SMP from the cake layers in both E-AnMBR and S-AnMBR was mainly protein-like substances, agreeing with Gao *et al*. (2014) which reported that proteins were dominant in bEPS and SMP in the cake layer.

4.3.5.4. FTIR spectroscopy

The FTIR spectra (Appendix A, Figure A-4) suggest that organic substances in bEPS from the cake layer and suspended sludge in both E-AnMBR and S-AnMBR were mainly proteins and carbohydrates. The peaks associated with bEPS of both the cake layer and suspended sludge indicated the same functional groups of organic matters including esters and polysaccharide-like, primary amine I and II, C-H bond of alkanes (Gao *et al*., 2011), lactones, and protein amides (Wang *et al*., 2008; Maruyama *et al*., 2001). The functional groups of bEPS from the suspended sludge imply strong adhesive nature that is conducive to attachment to membrane surface (as the cake layer). These findings agree with the results on cake filtration resistance and bEPS concentration discussed in Subsections 4.3.3 and 4.3.4, respectively.

4.3.6. Biogas production

Daily and cumulative biogas production in both reactors is shown in Appendix A (Figure A-5). During the first 40 days of operation for both reactors, daily biogas production gradually increased corresponding to increasing SCOD removal efficiency (Appendix A, Figure A-5(a)). After that, it was relatively stable. The trends in daily biogas production led to a lower rate of cumulative biogas production increase in the first 40 days compared to the rest of the operation period (Appendix A, Figure A-5(b)).

Biogas produced by E-AnMBR and S-AnMBR contained 18-22% and 21-25% of methane, respectively. The methane production and yield were quite stable during the sampling period (last 45 days of the operation). Both E-AnMBR and S-AnMBR had lower methane production and methane yield than theoretical values: 1.00 L/d and 0.35 L CH_4/g $SCOD_{utilized}$ (Gimenez *et al*., 2012). E-AnMBR provided methane production of 0.23±0.02 L/d and methane yield of 0.08±0.01 L CH_4/g $SCOD_{utilized}$, while S-AnMBR had methane production of 0.28±0.03 L/d and methane yield of 0.10±0.01 L CH_4/g $SCOD_{utilized}$. Hartley & Lant (2006) reported 38-85% of total methane produced can dissolve in water and is released with permeate. To prevent methane dissolution in water and increase methane recovery rate, operation at high temperature is required (Yue *et al.*, 2015; Gimenez *et al*., 2012; Martinez-Sosa *et al*., 2011). However, this research task intended to operate at ambient temperature because increasing temperature (27.4±0.6 °C) to achieve higher methane recovery rate will result in higher operation costs that are against an inherent research goal, reduction of costs associated with fouling.

The methane production of S-AnMBR in this research task is slightly lower compared to other research (Table 4-2). This is likely because the OLR used in this research task was only about half of those research (Yue *et al*., 2015; Ho *et al*., 2010). The methane production of E-AnMBR

is comparable to those in other research on biofilm-AnMBRs (Gao *et al*., 2014; Kim *et al*., 2014). E-AnMBR was operated at a lower F/M ratio, 3-14 times lower, compared to biofim-AnMBRs (Table 4-2), but achieved comparable methane production. This observation is possible because of sufficient substrate transfer throughout gel matrix and high cell mass achievable through the entrapment technique (Juntawang *et al*., 2017a; Pramanik & Khan, 2008). In biofilm-AnMBRs, cell mass is limited by available media surface (Laspidou & Rittmann, 2004).

4.3.7. Bacteria communities

Bacterial communities in the cake layers of E-AnMBR and S-AnMBR and their relative abundances are shown in Figure 4-5. The cake layer in E-AnMBR contained mainly *Proteobacteria* (60.6%), *Chloroflexi* (15.3%), *Bacteroidetes* (10.2%), *Acidobacteria* (2.1%) and *Firmicutes* (1.5%) while that in S-AnMBR was made up of *Proteobacteria* (38.9%), *Bacteroidetes* (35.4%), *Acidobacteria* (9.7%), *Chloroflexi* (5.3%) and *Verrucomicrobia* (1.4%). *Proteobacteria*, *Chloroflexi*, *Bacteroidetes*, and *Acidobacteria* were the four most dominant bacterial phyla in the cake sludge of both MBRs. All these dominated phyla contain a number of genera which are well known for their involvement in key anaerobic process steps including acidogenesis, acetogenesis and methanogenesis (Ma *et al*., 2013; Calderon *et al*., 2011; Gao *et al*., 2010). The other phyla contributed less than 6% of the abundance.

Bacteroidetes, which is known as the key phylum contributing to membrane fouling (Ma *et al*., 2013; Gao *et al*., 2010), was detected at relatively high abundance in both MBRs. Gao *et al*. (2010) reported that *Bacteroidetes* colony formation on the membrane surface is favorable because more proteinaceous EPS release. Therefore, the three times higher relative abundance of *Bacteroidetes* in the cake layer of S-AnMBR compared to E-AnMBR (35.4% in S-AnMBR and 10.2% in E-AnMBR), possibly contributed to higher cake filtration resistance in S-AnMBR as

discussed in Subsection 4.3.3. *Chloroflexi* which is frequently identified as another dominant bacterial phylum involved in the cake layer was also observed at high relative abundance in both systems with a higher level in E-AnMBR. However, their role in the cake layer formation in AnMBR is unclear (Ni *et al.*, 2010). *Chloroflexi* is known for having an ability to degrade and utilize microbial products derived from dead biomass (Miura *et al.*, 2007; Okabe *et al.*, 2005). Therefore, *Chloroflexi* in the cake layer might prevent the accumulation of foulants (bEPS and SMP) on the membrane surface and reduce the cake resistance in E-AnMBR. The relative abundance of bacteria community in the cake layer between E-AnMBR and S-AnMBR was substantially different. The cell entrapment likely influenced the relative abundance of bacteria in E-AnMBR, because both systems (E-AnMBR and S-AnMBR) had the same seeding source and operating conditions.

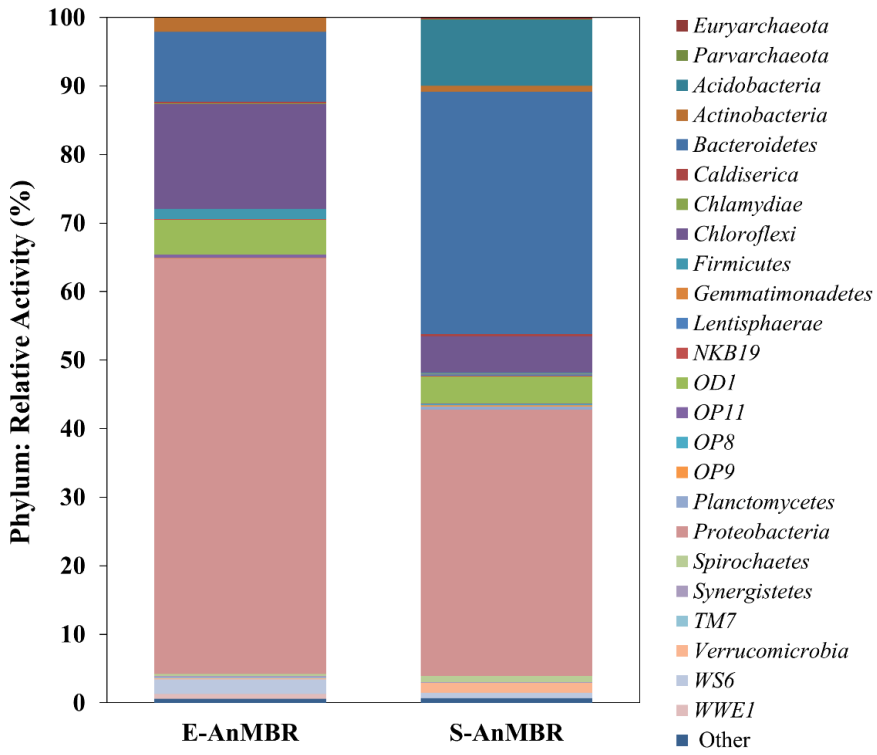

Figure 4-5: Relative abundance of bacteria in cake sludge of E-AnMBR and S-AnMBR classified by phylum. The data label "Other" represents any operational taxonomic unit representative sequences which cannot be specifically assigned to any bacterial phyla.

4.4. Summary

Application of E-AnMBR for domestic wastewater treatment lowered suspended biomass, bEPS and SMP resulting in less fouling compared to S-AnMBR. E-AnMBR provided longer operation time than S-AnMBR before chemical cleaning was required. Less frequent chemical cleaning for E-AnMBR will extend membrane life-span, and reduce chemical requirement and cost. The cake sludge in E-AnMBR and S-AnMBR was dominated by *Proteobacteria, Chloroflexi*, *Bacteroidetes* and *Acidobacteria*. However, their relative abundances were substantially different between E-AnMBR and S-AnMBR suggesting influence of cell entrapment to the bacterial community. This research task provides a scheme that effectively reduces fouling in AnMBR while maintaining the treatment performance.

CHAPTER 5: RESEARCH TASK III - ENTRAPPED-CELLS-BASED ANAEROBIC FORWARD OSMOSIS MEMBRANE BIOREACTOR TREATING MEDIUM-STRENGTH DOMESTIC WASTEWATER: FOULING CHARACTERIZATIONS AND PERFORMANCE EVALUATION

5.1. Introduction

Combining FO and MBR has led to an alternative wastewater treatment process, FOMBR. FOMBRs provide better biodegradation and better effluent quality than traditional MBR (Qin *et al*., 2010; Achilli *et al*., 2009; Cornelissen *et al*., 2008) mainly because of an ability to effectively retain small particles and inorganic contaminants by high rejection FO membrane (Qiu *et al*., 2016; Goh *et al.*, 2013; Cornelissen *et al*., 2008). Unlike conventional MBRs, permeate is not a sole component of the product of the FO process as it is blended with draw solution. To separate permeate from the diluted draw solution, an additional treatment unit such as reverse osmosis and nanofiltration is required (Tang & Ng, 2014).

In FOMBR, wastewater flows across a selectively permeable membrane due to the osmotic pressure difference between the bioreactor and the draw solution from low osmotic pressure to higher osmotic pressure (Wang *et al.*, 2016; Yuan *et al.*, 2015; Holloway *et al*., 2014). When comparing to conventional MBR, FOMBR experiences much less fouling and much less energy requirement due to the use of osmotic pressure instead of hydraulic pressure as the driving force (Lutchmiah *et al*., 2014; Qiu & Ting, 2014; Yap *et al*., 2012; Achilli *et al*., 2009). However, FOMBR provides less permeate flux, 2-5 LMH, compared to conventional MBR, 10-20 LMH (Judd, 2010; Achilli *et al*., 2009). Most of available studies on FOMBR have focused on finding a

new draw solution with higher osmotic pressure and less reverse salt flux, to obtain higher permeate flux and to reduce salt stress to bacteria in the bioreactor (Qiu *et al*., 2016; Yuan *et al*., 2015; Qiu & Ting, 2014).

One of the drawbacks associated with FOMBR is salt accumulation in the bioreactor from reverse salt flux (Luo *et al*., 2018; Yap *et al.*, 2012). During the FOMBR operation, because of an intrinsic property of FO membrane, salt in the concentrated draw solution can go across the membrane to the bioreactor side resulting in reduction of the osmotic pressure differences and the permeate flux (Hou *et al*., 2017; Hancock & Cath, 2009). Accumulation of reverse salt within the bioreactor of FOMBR causes changes in the activity and properties of bacterial sludge resulting in lowered treatment performances. In addition, the salt accumulation can increase bEPS and SMP releases leading to more biofouling on the membrane surface (Wang *et al*., 2017; Qiu & Ting, 2014). Wang *et al.* (2014) found that lowering the solids retention time and incorporating microfiltration membrane to FOMBR can reduce salt accumulation and reduce flux decline in FOMBR.

Aerobic FOMBR has demonstrated its high organic matter removal efficiency, less fouling and less energy requirement compared to the traditional MBR (Yap *et al.*, 2012; Qin *et al*., 2010; Achilli *et al*., 2009). High operation costs from aeration and sludge handling are the main drawback of aerobic FOMBR. In order to minimize the aeration cost, Chen *et al*. (2014) proposed anaerobic FOMBR and reported satisfactory removal efficiency with lower biomass yield. Tang & Ng (2014) operated anaerobic FOMBR using two different draw solutions (NaCl and Na_2SO_4). With Na_2SO_4 as a draw solution lower salt accumulation and higher permeate flux were obtained compared to those delivered by NaCl as a draw solution. Gu *et al.* (2015) studied anaerobic FOMBR treating low-strength wastewater under mesophilic conditions. The study reported high effluent quality

achieved by prolonged retention time, which allows longer exposure time for biological removal. Zhang *et al.* (2017) demonstrated that electric field could reduce reverse salt flux rate and concentrations of bEPS and SMP, in turn reducing salt accumulation and fouling, in anaerobic FOMBR. Nevertheless, reverse salt accumulation and low permeate flux remain the major drawbacks associated with FOMBRs compared to MBRs (Zhang *et al*., 2017; Gu *et al*., 2015; Chen *et al*., 2014; Tang & Ng, 2014).

Cell entrapment within a polymeric matrix is a relatively new technique for wastewater treatment. When comparing to suspended cells, entrapped cells are more resistant to undesirable environmental conditions such as inappropriate pH, temperature and shock organic loading due to higher cell concentrations and protection by the gel matrix (Pramanik & Khan, 2008). PVA is one of the common polymeric cell matrices for cell entrapment. Research tasks in Chapters 3 and 4 successfully developed entrapped cells-based aerobic and anaerobic MBR processes using PVA as an entrapment matrix and examined their ability to treat domestic wastewater (Juntawang *et al*., 2017a,b). The results from the tasks suggested that entrapped cells played a vital role in reduced fouling in both aerobic MBR and anaerobic MBR processes due to less production of bEPS and SMP.

Previous studies have identified bacteria contributing to membrane fouling for the suspended sludge and cake layer of AnMBRs and anaerobic FOMBR including *Proteobacteria*, *Bacteroides* and *Firmicutes* (Juntawang *et al*., 2017b; Ding *et al*., 2016; Ma *et al*., 2013; Yu *et al*., 2012). Qiu *et al.* (2016) and Ding *et al*. (2016) performed a microbial community analysis in their anaerobic FOMBR studies. Qiu *et al*. (2016) indicated that the abundance of *Bacteroidetes* in a mesophilic anaerobic FOMBR was much higher than that in an ambient anaerobic FOMBR. Ding *et al*. (2016) reported that at the phylum level, *Proteobacteria* and *Bacteroidetes* dominated over

other phyla. However, up to now, the knowledge on the microbial community of suspended sludge in anaerobic FOMBR is still limited. Microbial community structure is a significant factor responsible for the microbial metabolites, which influence fouling development in FOMBRs (Wu *et al*., 2017; Ding *et al*., 2016).

The objective of this research task was to develop a novel wastewater treatment process, entrapped-cells-based anaerobic FOMBR (E-FOMBR) and investigate its performances and fouling in comparison with suspended-cells-based anaerobic FOMBR (S-FOMBR). The two widely used draw solutions, NaCl and $(NH_4)_2SO_4$, were applied in this research task to observe system performances, fouling and sludge characteristics of E-FOMBR and S-FOMBR. For system performances, SCOD removal, biogas production, biogas composition and permeate flux were examined. Flux decline test, scanning electron microscopy (SEM) with energy dispersive X-ray spectroscopy (EDX), and bEPS and SMP measurements were performed to investigate fouling conditions. Sludge was characterized based on PSD, GPC, FTIR, 3DEEM. Illumina high-throughput sequencing of 16S rRNA genes was used to examine the microbial community structures in both FOMBRs.

5.2. Materials and methods

5.2.1. Synthetic wastewater and chemicals

Synthetic wastewater was prepared according to the formula listed in Subsection 3.2.1.

5.2.2. Preparation of entrapped cells

The preparation of entrapped cells followed the procedure in Subsection 4.2.2.

5.2.3. Anaerobic forward osmosis membrane bioreactor setup and operation

Laboratory scale E-FOMBR and S-FOMBR with working volume of 3 L were set up and operated under the same conditions. E-FOMBR was inoculated with the prepared entrapped cells while S-FOMBR was inoculated with anaerobic sludge taken from an anaerobic digester tank of the Moorhead wastewater treatment facility (Minnesota, USA). A thin film composite (TFC) FO flat sheet membrane (Aquaporin Inside, Denmark) with an effective surface area of 42 cm^2 was placed inside a CFO42D test cell (Sterlitech, USA). The TFC FO flat sheet membrane has a water permeability of 7 LMH (1 M NaCl as a draw solution), NaCl reverse flux of 2 $g/m^2/h$, membrane thickness of 110 µm, 0.2 µm pore size on support layer and mixed nanoscale pore size on active layer. Two peristaltic pumps (Model 7554-90, Thermo Fisher Scientific, USA) were operated at a 50 mL/min flowrate on the feed solution side and at a 3 mL/min flowrate on the draw solution side to continuously circulate both sides of the test cell as shown in Figure 5-1.

The reactors were fed with the synthetic wastewater. Two types of widely used draw solutions, NaCl and $(NH_4)_2SO_4$, at the same conductivity of 93.5 mS/cm (1 M $(NH_4)_2SO_4$ and 1.5 M NaCl) were tested. The operation time was 60 days after a 30-day startup period to reach steady state (when the daily SCOD removal varied less than 10%). The permeate flux was monitored throughout the operation period, which was divided into 4 operation cycles, 15 days for each cycle. At the end of each operation cycle (days 15, 30, 45, and 60 after reaching steady state), the system osmotic pressure difference of both E-FOMBR and S-FOMBR was adjusted to the startup value on day 0 after reaching steady state (93.5 mS/cm) by providing fresh draw solutions. A type 7200 stir light mixer (Thermolyne, USA) was used to provide complete mixing in the bioreactors and

the draw solution tanks. In order to ensure anaerobic conditions, the systems were initially purged by purified N_2 gas and DO was measured periodically. Operational conditions of E-FOMBR and S-FOMBR are summarized in Table 5-1.

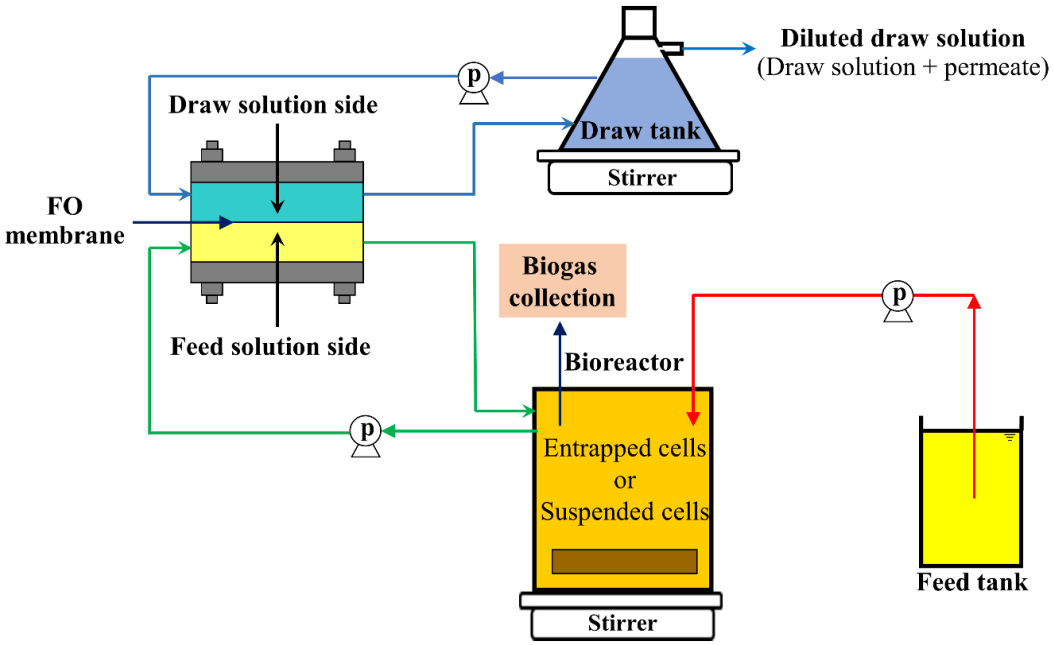

Figure 5-1: Schematic diagrams of E-FOMBR and S-FOMBR.

Table 5-1: E-FOMBR and S-FOMBR operational conditions.

Parameters	Draw solution			
	NaCl		$(NH_4)_2SO_4$	
	E-FOMBR	S-FOMBR	E-FOMBR	S-FOMBR
Influent soluble organic (mg SCOD/L)	542±9	542±9	540± 17	540± 17
Organic loading rate (kg SCOD/ m^3·d)	0.35	0.35	0.35	0.35
Hydraulic retention time (h)	36	36	36	36
Temperature (°C)	25.42 ± 0.52	25.42 ± 0.52	25.11 ± 0.92	25.11 ± 0.92
Ph	7.40 ± 0.15	7.11 ± 0.12	7.13 ± 0.15	6.91 ± 0.15
TSS (mg/L)	82 ± 10	420 ± 20	87 ± 6	422 ± 29
Oxidation reduction potential (mV)	-312 ± 8	-285 ± 15	-325 ± 11	-295 ± 12

5.2.4. Characterizations of feed, reactor fluid, permeate, sludge, bEPS, and SMP

5.2.4.1. Feed, reactor fluid, and permeate characterizations

The methods of feed, reactor fluid, and permeate characterizations are described in Subsection 4.2.4.1. However, in this research task, all parameters were monitored every 3 days instead of every 4 days mentioned in Subsection 4.2.4.1.

5.2.4.2. Particles size distribution

Particle size distribution was determined according to the procedure described in Subsection 3.2.4.2.

5.2.4.3. bEPS and SMP characterizations

5.2.4.3.1. Extraction and quantification

The methods for bEPS and SMP extractions and quantification are described in Subsection 3.2.4.3.1.

5.2.4.3.2. Gel permeation chromatography

The procedure for gel permeation chromatography is described in Subsection 3.2.4.3.2.

5.2.4.3.3. Three-dimension fluorescence excitation emission matrix spectroscopy

For 3DEEM spectroscopy, the procedure was the same as that listed in Subsection 3.2.4.3.3.

5.2.4.3.4. Fourier transform infrared spectroscopy

The method for FTIR analysis is described in Subsection 3.2.4.3.4.

5.2.5. Scanning electron microscopy with energy dispersive X-ray spectroscopy

The fouled FO membranes of E-FOMBR and S-FOMBR were taken from the CFO42D test cells at the end of the experiment (after 4 cycles of operation or 60 days after reaching steady state) and cut with a new razor blade into 2 square (1 cm × 1 cm) pieces representing samples of active layer and support layer. Samples were attached to cylindrical aluminum mounts with

double-stick carbon adhesive tabs and then sputter coated (Cressington 108 auto, Redding CA, USA) with a conductive layer of gold. Images were obtained by using a JEOL JSM-6490LV scanning electron microscope (JEOL Inc., Peabody MA, USA). The elements in the fouled FO membrane were analyzed by EDX using Nanotrace energy, a NORVAR light-element window, and a Noran six imaging system (Thermo Fisher Scientific, Madison WI, USA) at an accelerating voltage of 15 kV. For EDX, all samples were measured three times by repeating the process over one sample.

5.2.6. Flux decline test

According to Achilli *et al*. (2009) and Wang *et al*. (2014), flux decline due to the membrane fouling could be obtained from the difference between the initial permeate flux of new FO membrane and the permeate flux of fouled membrane. A new FO membrane with a workable area of 42 cm^2 was installed in the CFO42D test cell to obtain the initial water flux (F_i). Final water flux (F_f) was obtained by filtering DI water through a fouled membrane (fouling criterion is permeate flux less than 1.2 LMH). The fouled FO membrane was taken from the CFO42D test cell to conduct the test. When the flux was below 1.2 LMH, physical cleaning followed by chemical cleaning of the membrane, was applied. Physical cleaning involved removing a cake layer attached to the membrane surface by DI water flushing while in chemical cleaning the FO membrane was immersed in a 200 ppm NaOCl solution for at least 5 h and then a 5 g/L citric acid solution for another 5 h. The water flux, F_{w1}, was obtained by filtering DI water through the fouled membrane after DI water flushing while F_{w2} was obtained by filtering DI water through the fouled membrane after chemical cleaning. The difference between the F_i and F_f was regarded as flux decline due to membrane fouling, while flux decline which was computed from the difference between F_i and

F_{w1} was associated with reversible membrane fouling. Lastly, flux decline based on the difference between F_i and F_{w2} was attributed to irreversible membrane fouling. The flux decline was calculated using the following equations (Achilli *et al*., 2009; Wang *et al*., 2014):

$$L_f = (F_i - F_f)/F_i \times 100\%$$

$$L_{in1} = (F_i - F_{w1})/F_i \times 100\%$$

$$L_{in2} = (F_i - F_{w2})/F_i \times 100\%$$

Where L_f is the flux decline due to membrane fouling (%), L_{in1} is the flux decline due to reversible membrane fouling (%), L_{in2} is the flux decline due to irreversible membrane fouling (%), F_i is the flux of the new FO membrane (LMH), F_f is the flux of the fouled FO membrane (LMH), F_{w1} is the flux of the fouled FO membrane after the cake layer was removed and washed with DI water (LMH) and F_{w2} is the flux of the fouled FO membrane after chemical cleaning (LMH). The flux decline test was conducted once.

5.2.7. Biogas monitoring and analysis

For biogas production and composition, the procedure was the same as that listed in Subsection 4.2.6. However, in this research task, biogas was sampled for composition analysis monthly, day 30 and day 60, after the system reached steady state.

5.2.8. Bacteria community

The procedure for bacteria community analysis in suspended sludge of E-FOMBR and S-FOMBR is described in Subsection 4.2.7.

5.2.9. Statistical analysis

For statistical analysis, a *t*-test was performed according to the details in Subsection 3.2.6.

5.3. Results and discussion

5.3.1. System performances

With NaCl as a draw solution (D_1), influent SCOD concentration for both E-FOMBR and S-FOMBR was 542±9 mg/L (same feed tank) corresponding to OLR of 0.35 kg SCOD/m^3·d. The SCOD removal efficiencies of E-FOMBR and S-FOMBR after reaching steady state were 77.6±0.6% and 75.8±0.7%, respectively (Figure 5-2). With $(NH_4)_2SO_4$ as a draw solution (D_2), influent SCOD concentration for both E-FOMBR and S-FOMBR was 540±17 mg/L. The SCOD removal efficiencies of E-FOMBR and S-FOMBR were 80.8±0.7% and 78.8±0.9%, respectively. Yap *et al.* (2012) reported that salt accumulation in a FOMBR bioreactor causes cell dehydration leading to reduced cell activity and organic removal efficiency. Therefore, slightly higher SCOD removal efficiencies in E-FOMBR compared to S-FOMBR might be due to reduced effects of salt stress on the cells in E-FOMBR due to protection by the PVA gel matrix.

The diffusion model described in Appendix B (Appendix B, Subsection B.1) provides a better understanding on how entrapped cells experienced a reduced salt stress compared to suspended cells. The diffusion equation in Subsection B.1 (equation B1) suggests that the gel matrix delayed and/or lessened contact between salts and cells. This was attributed to lower diffusion of salts induced by high biomass concentrations and internal structure (porosity and tortuosity) inside the gel matrix compared to the bulk liquid phase (Massalha *et al*., 2010; Chen *et al*., 2002). The less salt stress likely led to higher SCOD removal in E-FOMBR than that in S-FOMBR for both draw solution types.

According to Zhang *et al*. (2017), reduction of substrate utilization is one of the possible effects of salt accumulation on bacteria in S-FOMBR. Higher SCOD removal efficiency in E-FOMBR compared to S-FOMBR for both types of draw solution (p = 0.003) supports the

deduction of higher substrate utilization in E-FOMBR over S-FOMBR. The type of draw solution played a role in system performances of both FOMBRs as confirmed by significant differences of SCOD removal efficiencies of E-FOMBR between D_1 and D_2 (p = 0.004), and of S-FOMBR between D_1 and D_2 (p = 0.004).

5.3.2. Permeate flux

Permeate flux was measured from the overflow volume of diluted draw solution (from the draw solution tank). The permeate flux, with D_1, decreased from 2.42 to 1.79 LMH (day 0 and day 15 after reaching steady state) for E-FOMBR and from 2.35 to 1.49 LMH for S-FOMBR (Figure 5-3(a)). Similarly, the permeate flux, with D_2, dropped from 2.59 to 1.85 LMH for E-FOMBR, and from 2.25 to 1.14 LMH for S-FOMBR (Figure 5-3(b)). The permeate flux of E-FOMBR was significantly higher than that of S-FOMBR for both types of draw solution (p = 0.002). After that, the osmotic pressure of both systems was adjusted back to the initial value of 740 psi by providing a new draw solution. The water flux after adjusting osmotic pressure with D_1, increased to 2.00 LMH for E-FOMBR and to 1.85 LMH for S-FOMBR. When D_2 was used as a draw solution, the flux increased to 2.20 LMH for E-FOMBR and to 1.95 LMH for S-FOMBR. The reduction of flux after adjusting osmotic pressure compared to the initial flux values (day 0 after reaching steady state) indicated fouling conditions in both E-FOMBR and S-FOMBR. The FO membrane of both E-FOMBR and S-FOMBR had not only a cake layer attached on the support layer (feed solution side) but also inorganic scaling attached on the active layer (draw solution side). The elemental precipitation on the FO membrane surface, inorganic scaling, on the draw solution side increases the transfer resistance of water which lowers the permeate flux (Gu *et al*., 2015; Tang & Ng, 2014).

As shown in Figure 5-3a and 5-3b, variations of flux and osmotic pressure in E-FOMBR were similar to those in S-FOMBR. Permeate flux reduction in FOMBR was attributed to the reduction of osmotic pressure difference and fouling (Zhang *et al*., 2017; Wang *et al*., 2014; Achilli *et al*., 2009). However, for the same osmotic pressure, E-FOMBR had higher flux than S-FOMBR, indicating more severe fouling in S-FOMBR.

Based on the conductivity, the salt accumulations in the bioreactors associated with D_1 were higher than those associated with D_2 for both E-FOMBR (p = 0.004) and S-FOMBR (p = 0.004). Achilli *et al*. (2010) reported that draw solutions containing larger-sized hydrated anion exhibit lower reverse salt diffusion. D_2 has larger-sized hydrated anion compared to D_1, 400×10^{-12} m for D_2 and 300×10^{-12} m for D_1, resulting in lower reverse salt diffusion of D_2 (3.6 g/m^2 h) compared to that of D_1 (9.1 g/m^2 h) (Achilli *et al*., 2010). With D_1, the conductivities in the bioreactors of E-FOMBR and S-FOMBR were 3.85 and 3.52 mS/cm, respectively, at the end of the operation cycle (day 15 after reaching steady state). With D_2, the corresponding values were 2.93 and 2.75 mS/cm. The salt accumulation in the bioreactor side of FOMBR not only reduces osmotic pressure difference but also affects bacteria in the bioreactor resulting in cell dehydration and growth inhibition (Luo *et al*., 2016; Lay *et al*., 2010; Achilli *et al*., 2009).

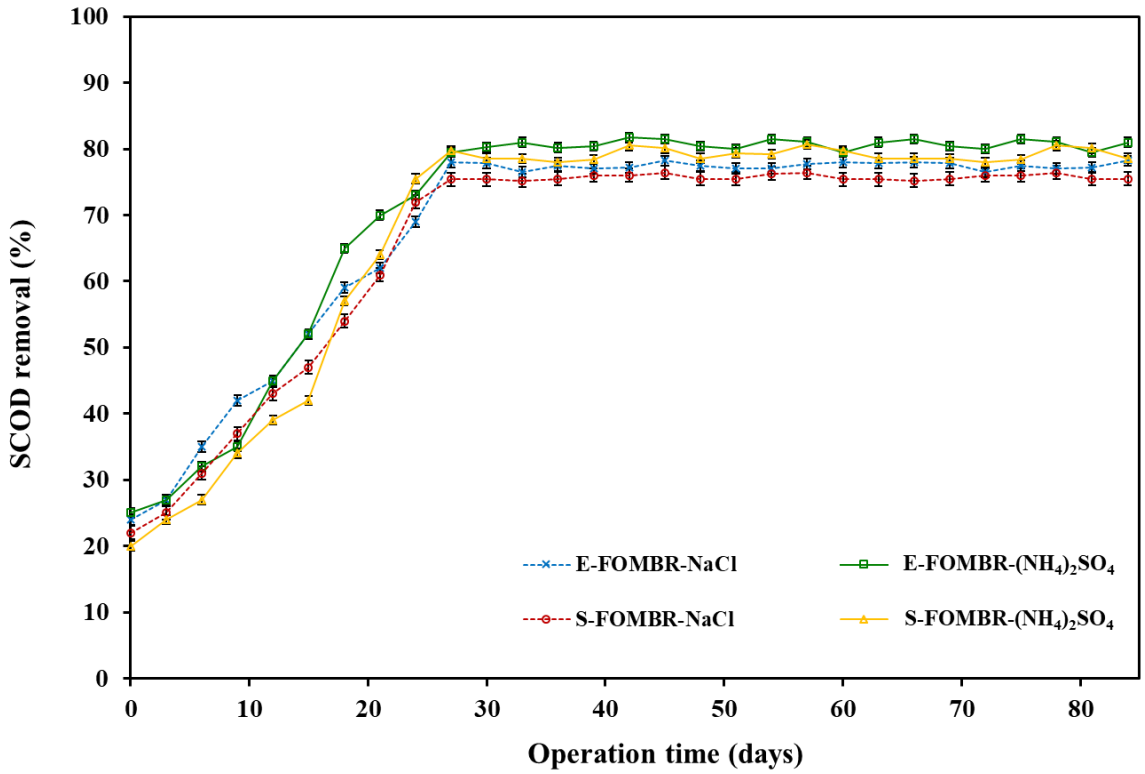

Figure 5-2: SCOD removal efficiencies of E-FOMBR and S-FOMBR using NaCl and $(NH_4)_2SO_4$ as draw solutions.

5.3.3. Foulant composition

The EDX results of FOMBR with D_1 indicated C, O, Na, S, and Cl on the membrane active layer and C, O, Na, S, Cl, Mg, Al, Si, P, K, Ca, and Fe on the membrane support layer (Table 5-2). The fouled membrane contained high C, O, Na, S and Cl and less of Mg, Al, Si and P on both sides. Na, S and Cl were detected on the active layer due to high rejection property of the active layer (Ge *et al*., 2012). The SEM images of the fouled membrane surfaces suggested the presence of a foulant layer on both sides of the membrane. Moreover, less fouling on the active layer of the membrane compared to the support layer of the membrane was observed (Appendix B, Figure B-1).

The EDX results of FOMBR using D_2 suggested C, O, P, S, Ca, Fe and Al on the active layer and C, O, P, S, Ca, Fe, Al, and Si on the support layer (Table 5-2). C, O and S were the main elements on both sides. The SEM images suggested less fouling on the active layer than the support layer (Appendix B, Figure B-2). The EDX results of the support layer (bioreactor side) indicated the co-existence of biofouling and inorganic fouling on the membrane surface, as suggested by the elements detected (Table 5-2) (Steiner *et al*., 2010; Mi & Elimelech, 2010).

5.3.4. Flux decline test

The decline of permeate flux was enhanced by the membrane fouling and lower osmotic difference between the draw solution and feed solution (bioreactor) sides. The flux decline levels, L_t, L_f, L_{in1} and L_{in2}, for E-FOMBR and S-FOMBR are summarized in Figure 5-4. L_t and L_f of S-FOMBR were more severe compared to E-FOMBR. This higher severity corresponded with lower flux in S-FOMBR compared to E-FOMBR (Figure 5-3). The flux decline test results suggested that S-FOMBR experienced more fouling than E-FOMBR for both draw solutions. Flux decline in S-FOMBR was higher than that in E-FOMBR regardless of the draw solution type. With D_1, the flux decreased from 2.42 to 1.79 LMH for E-FOMBR and from 2.35 to 1.49 LMH for S-FOMBR within 15 days. With D_2, the flux decreased from 2.59 to 1.85 LMH for E-FOMBR and from 2.25 to 1.14 LMH for S-FOMBR within 15 days. The trend of flux decline in this research task agrees with research on anaerobic FOMBR performed by Zhang *et al.* (2017) that reported a flux decrease from 3.53 to 1.09 LMH within 11 days. With D_2, a better recovery rate after physical and chemical cleaning compared to D_1 was obtained. This corresponds with lower flux decline due to irreversible fouling in E-FOMBR and S-FOMBR with D_2 than with D_1 (Figure 5-4).

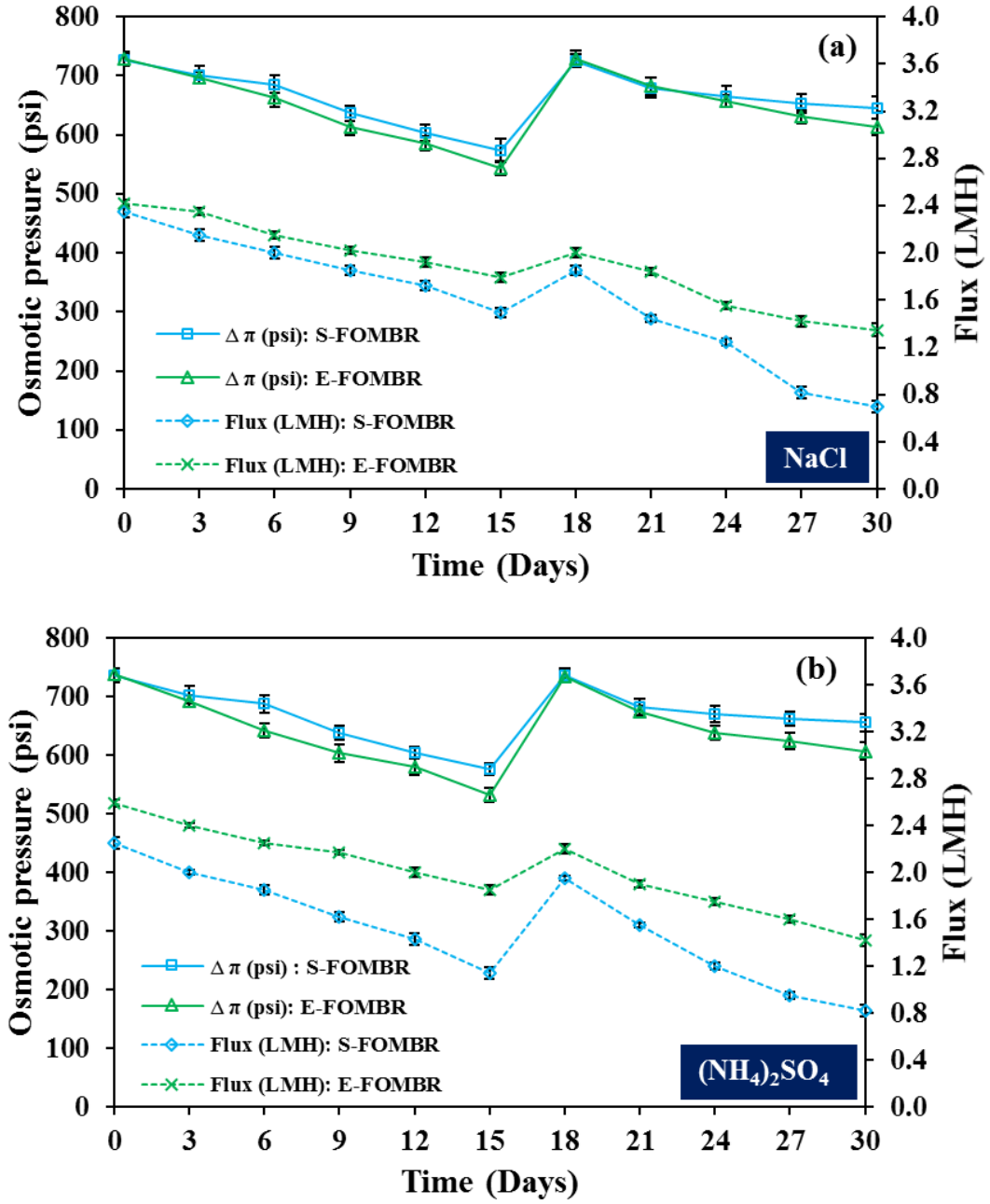

Figure 5-3: Variations of water flux (LMH) and osmotic pressure (psi) during the operations of E-FOMBR and S-FOMBR: (a) NaCl as a draw solution and (b) $(NH_4)_2SO_4$ as a draw solution.

Table 5-2: Elemental composition of foulants on the active and support layers for different draw solutions (NaCl and $(NH_4)_2SO_4$).

Element	Atomic (%)							
	NaCl draw solution				$(NH_4)_2SO_4$ draw solution			
	Active layer		Support layer		Active layer		Support layer	
	*E	**S	E	S	E	S	E	S
C	83.59	84.22	66.84	75.40	79.44	77.99	84.26	79.15
O	9.66	10.37	9.79	10.91	13.02	16.38	14.94	12.54
Na	1.21	0.84	10.74	1.24	-	-	-	-
S	4.30	3.69	0.85	0.47	4.11	4.89	0.29	6.78
Cl	1.24	0.88	9.95	1.46	-	-	-	-
Mg	-	-	0.17	0.04	-	-	-	-
Al	-	-	0.32	0.50	-	0.01	0.04	0.10
Si	-	-	0.96	0.57	-	-	0.16	0.70
P	-	-	0.19	1.22	1.28	0.23	0.14	0.12
K	-	-	0.08	0.08	-	-	-	-
Ca	-	-	0.02	0.76	0.13	0.05	0.05	0.09
Fe	-	-	0.09	7.35	2.02	0.45	0.12	0.52

*E= E-FOMBR; **S= S-FOMBR

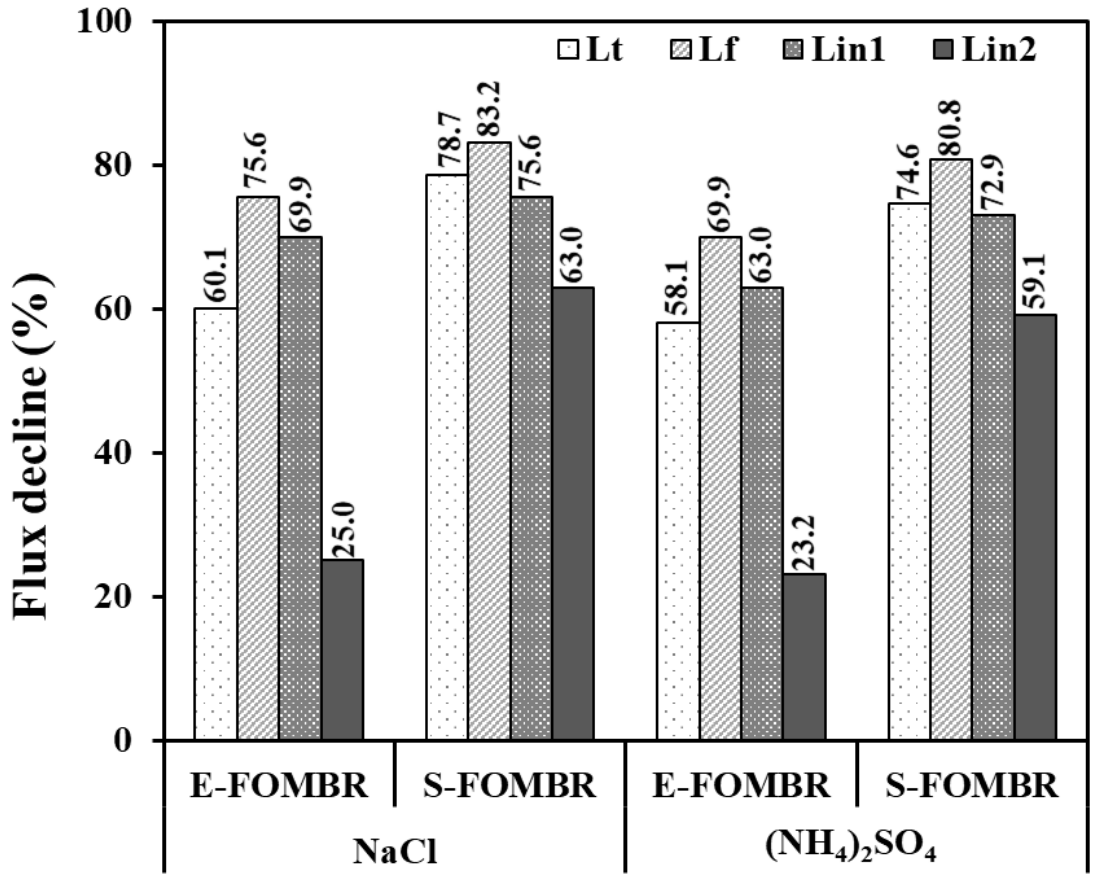

L_t = Total flux decline in the FOMBR (%), L_f = Flux decline due to membrane fouling (%), L_{in1} = Flux decline due to reversible fouling (%), L_{in2} = Flux decline due to irreversible fouling (%)

Figure 5-4: Flux decline of FO membrane due to L_t, L_f, L_{in1} and L_{in2} in E-FOMBR and S-FOMBR.

5.3.5. bEPS and SMP concentrations in E-FOMBR and S-FOMBR

bEPS and SMP are the main substances associated with membrane fouling in MBRs (Ding *et al.*, 2016; Luna *et al.*, 2014). The bEPS and SMP concentrations measured as protein and carbohydrate concentrations in the bioreactors of E-FOMBR and S-FOMBR are shown in Figure 5-5. The results suggested that with D_1, E-FOMBR had less bEPS and SMP than S-FOMBR (35% less bEPS and 65% less SMP) while with D_2, E-FOMBR had 13% less bEPS and 68% less SMP than S-FOMBR. The bEPS and SMP concentrations measured as protein and carbohydrate in E-FOMBR were significantly less than those in S-FOMBR for both types of draw solutions (p =

0.004). Furthermore, the protein and carbohydrate concentrations in E-FOMBR and S-FOMBR with D_1 were significantly higher than with D_2 (p = 0.013 for E-FOMBR and p = 0.034 for S-FOMBR). Salt stress not only reduced treatment performance as mentioned in Subsection 5.3.1 but also increased the production of bEPS and SMP (Zhang *et al*., 2017; Tang & Ng, 2014). As discussed above under system performances subsection (Subsection 5.3.1), the cells inside the gel matrix of E-FOMBR experienced lower salt stress compared to the cells in the bulk liquid of S-FOMBR. Consequently, lower bEPS and SMP concentrations were observed in E-FOMBR compared to S-FOMBR regardless of the type of draw solution.

Previous research reported that SMP is a main contributor of pore blocking (Cho & Fane, 2002), while the cake layer resistance is tied to bEPS (Ahmed *et al*., 2007). Fan *et al.* (2006) and Geng & Hall (2007) reported that SMP was the most significant substance associated with membrane fouling. For both E-FOMBR and S-FOMBR, protein concentrations in bEPS and SMP were much higher than carbohydrate concentrations. The SMP and bEPS concentrations in E-FOMBR and S-FOMBR correspond well with the flux decline test results (Figure 5-4). S-FOMBR had higher SMP than E-FOMBR resulting in higher flux decline due to irreversible fouling (pore blocking). With D_1, the conductivity in the feed solution (bioreactor) side increased from 0.72 to 3.85 mS/cm for E-FOMBR and from 0.74 to 3.52 mS/cm for S-FOMBR while with D_2, the conductivity in the feed solution side rose from 0.80 to 2.93 mS/cm for E-FOMBR and from 0.78 to 2.75 for S-FOMBR. The increases of salinity (conductivity as a surrogate parameter) from the reverse salt flux in the bioreactors led to higher protein and carbohydrate concentrations associated with bEPS and SMP. This observation agrees with a batch study of Wang & Zhang (2010) that

reported stimulation of SMP production by salinity. Chen *et al*. (2014) observed higher production of bEPS by bacteria under higher salt stress. The bEPS and SMP rises under salt stress were more pronounced in S-FOMBR compared to E-FOMBR.

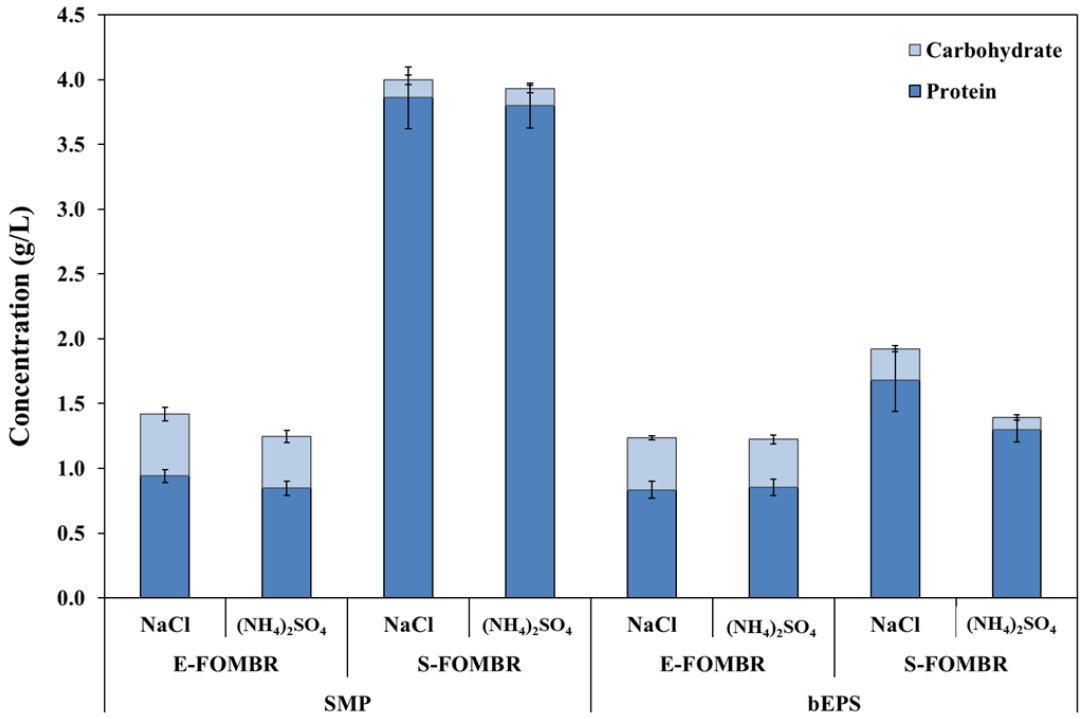

Figure 5-5: Concentrations of bEPS and SMP during the steady state operation of E-FOMBR and S-FOMBR.

5.3.6. Sludge characterizations

5.3.6.1 Particles size distribution

The mean particle sizes of sludge from both E-FOMBR and S-FOMBR were over 1 µm (Appendix B, Figure B-3). In addition, suspended sludge in S-FOMBR had larger mean particle sizes than E-FOMBR for both draw solutions (Appendix B, Figure B-3). The smaller sludge particles in E-FOMBR compared to those in S-FOMBR were due to collisions between sludge particles and entrapment matrix (Huang *et al*., 2008) and should lead to higher cake filtration resistance compared to S-FOMBR. However, that was not the case due to much higher suspended sludge concentration in S-FOMBR compared to E-FOMBR (Table 5-1).

5.3.6.2. Molecular weight distribution

When the bEPS sample went through the chromatography gel pores, large MW molecules were detected earlier than smaller MW molecules as shown in Appendix B, Figure B-4. In this research task, the MWD of bEPS in E-FOMBR and S-FOMBR can be categorized into 2 groups: (1) MW higher than 10 kDa and (2) MW less than 1,000 Da (Appendix B, Figure B-4). The organic substances with MW higher than 10 kDa, suggested the existence of carbohydrate and protein functional groups (Guo *et al*., 2011). The MW in a range of 500 - 3,000 Da corresponds with refractory organic materials, such as humic substances while the MW less than 200 Da represents low MW organic compounds, such as glucose and acetate. The GPC results suggested the presence of proteins, carbohydrates, humic substances and acetate in both systems.

With D_1, the organic substances in bEPS of E-FOMBR had higher MW than S-FOMBR. On the contrary, with D_2, the organic substances in bEPS of S-FOMBR had higher MW than E-FOMBR. However, peaks of MW shown in Appendix B (Figure B-4) indicated that the MW of bEPS in E-FOMBR remained relatively constant between D_1 and D_2 while the MW of bEPS in S-FOMBR was different between D_1 and D_2. This agrees with Mw/Mn, dispersity index, which is the ratio of Mw and Mn obtained in this research task. The Mw/Mn ratio of bEPS in E-FOMBR was 12 for both D_1 and D_2, while those of bEPS in S-FOMBR were 10 for D_1 and 14 for D_2. The MW peaks and Mw/Mn ratios suggested that the type of draw solution plays a significant role to MWD of bEPS in S-FOMBR while its effect was less pronounced on MWD of bEPS in E-FOMBR.

5.3.6.3. 3DEEM spectroscopy

The 3DEEM of SMP in E-FOMBR with D_1 indicated an aromatic protein, a protein-like compound containing tryptophan, and a hydrophobic acid (Appendix B, Figure B-5(a)). The fluorescence spectra of SMP in S-FOMBR with D_1 suggested an aromatic protein, a protein-like substance containing tryptophan, and a hydrophobic acid (Appendix B, Figure B-5(b)). Based on the fluorescence spectra, SMP in E-FOMBR with D_2 consisted of an aromatic protein and a protein-like substance containing tryptophan (Appendix B, Figure B-5(c)). SMP in S-FOMBR with D_2 was made up of an aromatic protein, a protein-like substance containing tryptophan, a humic acid-like substance and fluvic acid (Appendix B, Figure B-5(d)). Organic substances in SMP in E-FOMBR and S-FOMBR were mainly protein functional groups. The results indicated that protein-like substances played a significant role in membrane fouling in both FOMBR systems agreeing with a study by Wang *et al*. (2009).

Besides proteins in both systems, SMP in E-FOMBR contained a hydrophobic acid and SMP in S-FOMBR consisted of humic and fluvic acids. This difference between these two systems might be from retarded/protective effects of salt accumulation by gel matrix in the bioreactor of E-FOMBR. The intensity of humic acid-like substances of S-FOMBR was higher compared to that of E-FOMBR (Appendix B, Figure B-5). Higher suspended biomass concentrations in S-FOMBR compared to E-FOMBR, along with salt accumulation resulted in higher accumulation of humic acid-like substances from cells lysis/decay (Appendix B, Figure B-5 (b) and (d)) (Chen *et al*., 2003; Juntawang *et al*., 2017a,b).

5.3.6.4. FTIR spectroscophy

The FTIR spectrum of bEPS, with D_1 (Appendix B, Figure B-6 (a)), exhibits a peak at 2,927-2,924 cm^{-1}, suggesting the stretching of a C-H bond of alkyl (Gao *et al*., 2011). Peaks in a range of 1,655-1,409 cm^{-1} represent protein secondary structures, namely amide I and amide II (Maruyama *et al*., 2001; Wang *et al*., 2008). The peaks unique to E-FOMBR are at 3,389 cm^{-1} and 1,108 cm^{-1} which indicate the stretching of a N-H bond in amines and carbohydrate-like compounds, respectively (Croué *et al*., 2003). There are two peaks unique to S-FOMBR, the peak at 1,238 cm^{-1} likely due to the presence of $-CH_3$ and C-H bond (Maruyama *et al*., 2001) and the peak at 1,033 cm^{-1} attributed to carbohydrate or carbohydrate-like substances (Croué *et al*., 2003). The results specified that proteins and carbohydrates were major functional groups for bEPS in both systems. However, specific organic substances in bEPS from E-FOMBR and S-FOMBR were different. This suggests that entrapped cells in E-FOMBR influenced substrate degradation and cell lysis in E-FOMBR.

With D_2, the FTIR spectra show similarities of organic substances in bEPS from suspended sludge in E-FOMBR and S-FOMBR (Appendix B, Figure B-6(b)). Peaks at 1,658 cm^{-1} and 1,402 cm^{-1} are corresponding to the secondary structures of amide I and amide II, respectively (Wang *et al*., 2008; Maruyama *et al*., 2001). Peaks in a range of 1,112-1,109 cm^{-1} which are based on the C-O-C vibrations, associated with polysaccharides or polysaccharides-like substances (Croué *et al*., 2003). The peak that is unique to E-FOMBR is at 3,389 cm^{-1} indicating a N-H bond which represents ammonium ions. The peaks unique to S-FOMBR are at 3,235 cm^{-1}, assigned to the stretching of an O-H bond in hydroxyl functional groups representing phenols (Meng *et al*., 2006) and at 2,928 cm^{-1} suggesting C-H bonds associated with alkanes (Gao *et al*., 2011). The bEPS in E-FOMBR had more unidentified organic compounds compared to that in S-FOMBR. This

observation is tied to the environment/condition in the bioreactor. Suspended bacteria in S-FOMBR had more exposure to salinity compared to entrapped bacteria in E-FOMBR (due to protection from gel matrix). Therefore, the salinity exerted more adverse effect on the ability of suspended bacteria in S-FOMBR than that of entrapped bacteria in E-FOMBR to degrade organic compounds both on the type and concentration.

Based on the FTIR spectra results, organics in bEPS of E-FOMBR and S-FOMBR were dominated by proteins and carbohydrates regardless of the draw solution type. Compounds with protein functional groups, are recognized for its adhesive property and can increase the attachment between bacteria and the membrane surface (Meng *et al.*, 2009) lead to fouling. However, the cake layer on FO membrane surface was not as dense as those in traditional MBRs due to osmotic pressure instead of hydraulic/suction pressure as a driving force (Lutchmiah *et al*., 2014; Qiu & Ting, 2014; Yap *et al*., 2012; Achilli *et al*., 2009).

5.3.7. Biogas production

For biogas produced by E-FOMBR with D_1, the methane content was 20.94 and 19.67% in the first and second months, respectively. The content of methane in biogas produced by S-FOMBR was 21.12 and 13.05% in the first and second months, respectively. With D_2, the biogas produced by E-FOMBR contained 20.59 and 20.42% of methane while methane made up 24.84 and 20.99% of the biogas generated by S-FOMBR in the first and second months, respectively. For FOMBR systems with D_1, the methane yields were 0.06±0.01 L CH_4/g $SCOD_{utilized}$ for E-FOMBR and 0.05±0.01 L CH_4/g $SCOD_{utilized}$ for S-FOMBR. For FOMBR systems with D_2 the methane yields were 0.07±0.0004 L CH_4/g $SCOD_{utilized}$ for E-FOMBR and 0.06±0.009 L CH_4/g $SCOD_{utilized}$ for S-FOMBR.

The methane production results suggested that the type of draw solution plays a more vital role in S-FOMBR than E-FOMBR. The methane contents in first and second months of E-FOMBR between D_1 and D_2 were rather consistent (20.94 and 19.67% for D_1, and 20.59 and 20.42% for D_2), while D_2 provided higher methane contents in S-FOMBR than D_1 (21.12 and 13.05% for D_1, and 24.84 and 20.99% for D_2). This is likely because the application of entrapped cells provided a condition that protected/reduced effect of salt stress. This observation is supported by previous studies by Wu *et al.* (2017) and Chen *et al*. (2014) that indicated inhibition of methanogenesis by high salinity leading to declining methane production.

5.3.8. Bacteria communities

The relative abundances of bacterial communities in the suspended sludge of E-FOMBR and S-FOMBR with D_1 and D_2 are shown in Figure 5-6. The relative abundance of bacteria community in the suspended sludge between E-FOMBR and S-FOMBR was substantially different. With D_1, the suspended sludge of E-FOMBR had higher relative abundances of *Proteobacteria* (37% vs. 23%), *Firmicutes* (34% vs. 32%), *Bacteroidetes* (19% vs. 13%), *Chloroflexi* (3% vs. 2%) and *Actinobacteria* (2% vs. 1%) than the suspended sludge of S-FOMBR. With D_2, the suspended sludge of E-FOMBR had higher relative abundances of *Proteobacteria* (48% vs. 37%), *Bacteroidetes* (24% vs. 18%) and *Chloroflexi* (12% vs. 4%) than the suspended sludge of S-FOMBR, but had lower relative abundances of *Firmicutes* (5% vs. 31%).

The above phyla are the most commonly found bacterial taxa in AnMBRs (Juntawang *et al*., 2017b; Sun *et al*., 2014) and anaerobic FOMBRs (Qiu *et al*., 2016; Ding *et al*., 2016). All these dominated phyla contain a number of genera which are well known for their involvement in key anaerobic process steps including acidogenesis, acetogenesis and methanogenesis (Ma *et al*., 2013; Calderon *et al*., 2011; Gao *et al*., 2010). The suspended sludge samples were dominated by

Proteobacteria which agrees with previous studies of bacterial communities from suspended sludge in AnMBRs (Zhang *et al*., 2014, 2012; Lim *et al*., 2012). *Firmicutes* is known to be involved in biofouling in AnMBRs (Yu *et al*., 2012; Calderon *et al*., 2011; Gao *et al*., 2010). With D_2, 6 times higher *Firmicutes* in bulk sludge of S-FOMBR compared to E-FOMBR could be responsible for higher fouling in S-FOMBR. Previous studies reported that microorganisms deposited on the membrane surface originated mainly from bulk sludge (Ma *et al*., 2013; Yu *et al*., 2012). *Chloroflexi* is known for having an ability to degrade and utilize microbial products derived from dead biomass (Miura *et al*., 2007; Okabe *et al*., 2005). Therefore, the higher *Chloroflexi* in the bacterial community of the suspended sludge in E-FOMBR with both types of draw solution would possibly improve permeate flux and promote fouling mitigation.

The microbial community of the suspended sludge in E-FOMBR and S-FOMBR was dominated by *Proteobacteria*, *Firmicutes*, *Chloroflexi*, *Bacteroidetes* and *Actinobacteria*. However, the relative abundances of these phyla between E-FOMBR and S-FOMBR were substantially different due to effects of cell entrapment and/or lower salt stress to entrapped cells in E-FOMBR compared to those suspended cells in S-FOMBR as discussed in Subsections 5.3.1 and 5.3.5. In this research task, E-FOMBR and S-FOMBR were set up and operated under the same conditions (Table 5-1), except that E-FOMBR was inoculated with the prepared entrapped cells while S-FOMBR was inoculated with suspended anaerobic sludge. Thus, cells that later suspended in the bulk liquid of E-FOMBR mainly originated from the outer layer of the gel matrix. Cell loss from the out layer of the entrapment matrix to the bulk liquid was reported in previous studies (Barbotin *et al.,* 1990; Hill & Khan, 2008). Thus, the phyla difference between E-FOMBR and S-FOMBR was because of the entrapment (Juntawang *et al*., 2017b) and/or salt stress to cells. *Proteobacteria* dominated in both FOMBRs but was more abundant in E-FOMBR suggesting the

phylum as a possible agent for fouling mitigation. The results presented here provide a comprehensive understanding of bacteria communities in FOMBRs which is essential for developing fouling control strategies (promotion/enrichment a phylum that mitigates fouling and reduction/elimination of a phylum that enhances fouling).

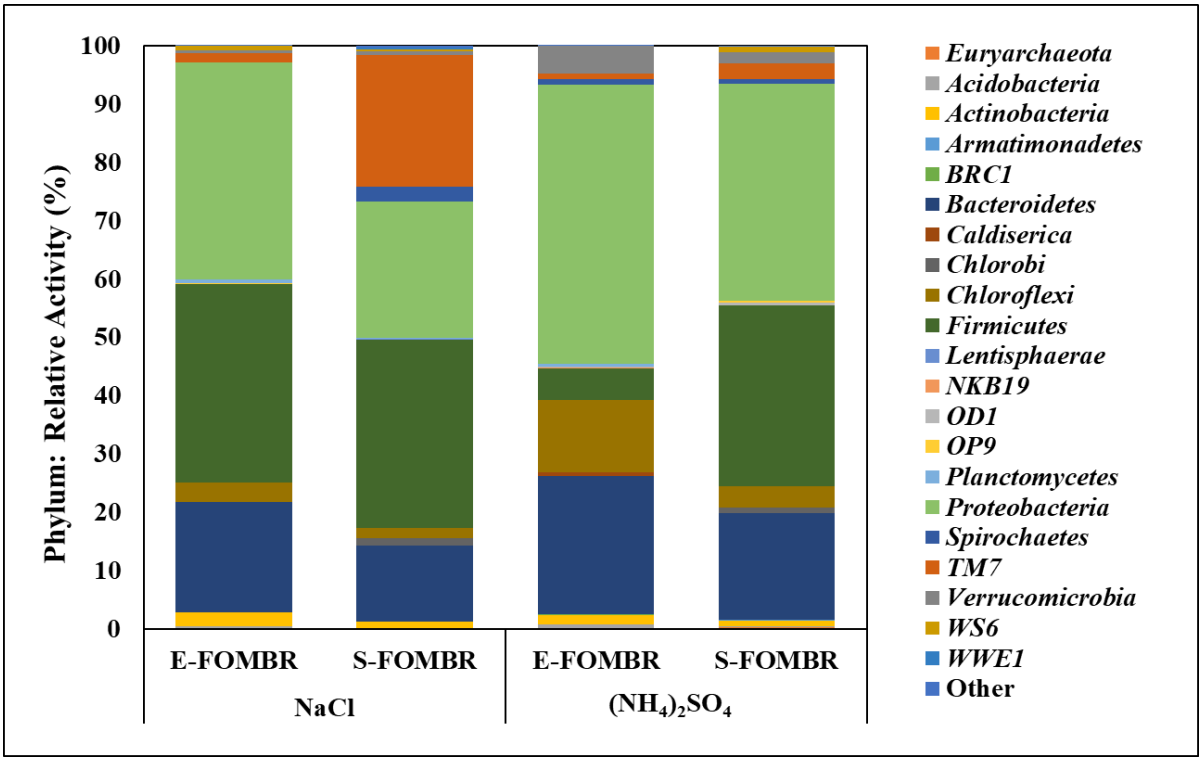

Figure 5-6: Relative abundance of bacteria in suspended sludge of E-FOMBR and S-FOMBR with NaCl and $(NH_4)_2SO_4$ as draw solution classified by phylum. The data label "Other" represents any operational taxonomic unit representative sequences which cannot be specifically assigned to any bacterial phyla.

5.4. Summary

In this research task, the application of entrapped cells based E-FOMBR for domestic wastewater treatment was investigated in comparison with suspended cells based S-FOMBR, focusing on system performances, fouling condition and sludge characteristics. For both draw solutions tested, NaCl and $(NH_4)_2SO_4$, the permeate flux monitoring and flux decline test showed that S-FOMBR experienced more severe fouling than E-FOMBR. More severe fouling in S-

FOMBR was due to higher bEPS and SMP generated compared to E-FOMBR. The salt accumulations in the bioreactors of the two systems were comparable. However, E-FOMBR was more tolerant to salt accumulation leading to higher and more stable system performances throughout the experimental period. During the operation period, the methane content in the biogas dropped substantially for S-FOMBR with both types of draw solutions especially with NaCl while it did not for E-FOMBR. In addition, E-FOMBR provided higher permeate flux regardless of the type of draw solution. Salt stress in the bioreactors of both systems led to different relative abundances of major phyla between E-FOMBR and S-FOMBR. *Proteobacteria* was the most abundant phylum in both FOMBRs but was higher in E-FOMBR, suggesting their possible role as a fouling mitigation bacterial group. This research task provides a novel entrapped-cells-based FOMBR process with reliable treatment performances, less fouling, higher flux, longer operation time and more tolerance to salt accumulation than a traditional suspended-cells-based FOMBR process.

CHAPTER 6: CONCLUSIONS AND FUTURE WORK RECOMMENDATIONS

6.1. Conclusions

MBRs have gained popularity as a treatment process of choice for domestic wastewater due to higher effluent quality, less biomass yields and smaller footprints compared to CAS. However, one of the major drawbacks of MBRs is fouling which limits the widespread applications of the process. Fouling is a reduction of system permeate flux due to deposits of particles and organics substances on the surface and/or in the pores of the membrane module. Fouling in MBRs increases operation and maintenance costs.

In this dissertation, application of cell entrapment technique to reduce/delay fouling without compromising treatment performance in MBR and FOMBR processes has been demonstrated through 3 research tasks involving aerobic MBR (Task 1), anaerobic MBR (Task 2), and anaerobic FOMBR (Task 3), respectively. Task 3 also examined the use of cell entrapment to reduce effect of salt accumulation (in anaerobic FOMBR).

In Task 1, a MBR with entrapped cells, E-MBR, and a MBR with suspended cells, S-MBR, were operated side by side for treatment of medium-strength synthetic wastewater to investigate membrane fouling and system performances. Both E-MBR and S-MBR achieved high soluble organic removal and nitrification of ammonia nitrogen. Lower biomass concentration, and lower bEPS and SMP concentrations (in terms of proteins and carbohydrates) in E-MBR contributed to less membrane fouling than S-MBR. The membrane resistance test showed that pore blocking resistance, which is a main culprit for fouling in MBR, was greatly reduced in E-MBR. The results of PSD, GPC, 3DEEM and FTIR analyses provided a better understanding of sludge characteristics in E-MBR and S-MBR systems. The results indicated that: (1) E-MBR had smaller particle sizes compared to S-MBR; (2) The molecular sizes of bEPS indicated proteins and carbohydrates as the

main components of bEPS; (3) The 3DEEM intensity of humic acid-like substances in SMP was 4 times higher in S-MBR than E-MBR; and (4) The organic structures identified by FTIR are known to be sticky and can induce cake layer on the membrane surface, leading to fouling condition. All these sludge characterization results support the lower fouling observation in E-MBR.

In Task 2, an ability of cell entrapment to mitigate membrane fouling was tested in anaerobic MBR. Similar to Task 1, E-AnMBR and S-AnMBR were tested at a laboratory scale for treatment of medium-strength synthetic wastewater. The results showed no significant difference between E-AnMBR and S-AnMBR systems in terms of the organic removal efficiency. E-AnMBR experienced less fouling than S-AnMBR. E-AnMBR achieved lower production of bEPS, SMP and biomass, thereby reducing membrane fouling. E-AnMBR sustained a longer service duration of 11 days while S-AnMBR reached a fouling point (55 kPa) in 7 days at the permeate flux of 10.63 LMH. The results of GPC, 3DEEM and FTIR analyses for suspended sludge and cake layer of E-AnMBR and S-AnMBR suggested that proteins and carbohydrates were the major organic substances in both systems. Due to higher production of bEPS and SMP, the concentrations of proteins and carbohydrates were much higher in S-AnMBR compared to those in E-AnMBR. The cake sludge in E-AnMBR and S-AnMBR was dominated by *Proteobacteria*, *Chloroflexi*, *Bacteroidetes* and *Acidobacteria*. However, their relative abundances were substantially different between E-AnMBR and S-AnMBR suggesting influence of cell entrapment to the bacterial community.

A novel E-FOMBR process was developed and its feasibility for treating medium-strength domestic wastewater was examined in Task 3. Laboratory scale E-FOMBR and S-FOMBR were operated side by side under the same operating conditions using NaCl and $(NH_4)_2SO_4$ as draw

solutions. An increase in the salinity due to reverse solute flux and retained inorganic matters by FO membrane enhanced the accumulations of bEPS and SMP in the bioreactors, especially bEPS in S-FOMBR when using NaCl as a draw solution. The permeate flux monitoring and flux decline test showed that S-FOMBR experienced more severe fouling than E-FOMBR. FTIR results suggested more variety of organic substances in S-FOMBR compared to E-FOMBR, which were likely due to the influence of salt accumulation on substrate degradation and cell decay in the bioreactors. The effect of salt accumulation on sludge characteristics in the bioreactors resulted in more severe membrane fouling and lower system performances in S-FOMBR compared to E-FOMBR. E-FOMBR was more tolerant to salt accumulation leading to satisfactory system performances throughout the experimental period. It had higher permeate flux regardless of the draw solution.

This dissertation research demonstrates successful applications of entrapped cells in aerobic and anaerobic MBRs, and anaerobic FOMBR. The findings show that entrapped cells can reduce the production of bEPS and SMP – the main causes of fouling. The entrapment mitigates the exposure of cells to salt stress in the bioreactor. The comprehensive characterizations of sludge provided better understandings on the behaviors and activities of entrapped cells in MBR and FOMBR. This research lays the groundwork for applications of entrapped cells for biofouling mitigation which can be extended beyond wastewater treatment as membrane processes are common in many industries.

6.2. Future work recommendations

Although the results of this dissertation research demonstrated the successful applications of entrapped cells in both MBRs and FOMBR, there are numbers of topics/issues on entrapped cells-based-MBR and entrapped cells-based-FOMBR that are recommended for future research.

(1) A study optimizing entrapment bead size, density and porosity to maximize simultaneously system performance and fouling reduction should be conducted. These factors can influence the physiology of bacteria such as cell growth and decay, and substrate utilization which are tied directly to organic contaminant removal and in turn affect metabolic products including bEPS and SMP, the main causes of membrane fouling.

(2) In situ levels of oxygen, pH, temperature, and substrate should play vital roles to bacteria inside the gel matrix rather than the environmental conditions surrounding the entrapment. The influences of environmental conditions inside the entrapment on the production of bEPS and SMP and the membrane fouling should be further investigated.

(3) Mechanisms governing less production bEPS and SMP by entrapped cells in different MBR systems should be investigated. High-throughput sequencing for tracking the dynamic changes of bacteria during the fouling development should be conducted. By tracking changes of bacteria in each stage of entrapped cells MBR and suspended cells MBR, specific type(s) of bacteria that promote and mitigate fouling can be identified.

REFERENCES

Achilli, A., Cath, T. Y., Childress, A. E. 2010. Selection of inorganic-based draw solutions for forward osmosis applications. *Journal of Membrane Science*, 364(1), 233-241.

Achilli, A., Cath, T. Y., Marchand, E. A., Childress, A. E. 2009. The forward osmosis membrane bioreactor: a low fouling alternative to MBR processes. *Desalination*, 239(1), 10-21.

Ahmed, Z., Cho, J., Lim, B.R., Song, K.G., Ahn, K.H. 2007. Effects of sludge retention time on membrane fouling and microbial community structure in a membrane bioreactor. *Journal of Membrane Science,* 287, 211–218.

Akram, A., Stuckey, D. C. 2008. Flux and performance improvement in a submerged anaerobic membrane bioreactor (SAMBR) using powdered activated carbon (PAC). *Process Biochemistry,* 43(1), 93-102.

Al-Juboori, R. A., Yusaf, T. 2012. Biofouling in RO system: mechanisms, monitoring and controlling. *Desalination*, 302, 1-23.

Al-Malack, M. H. 2006. Determination of biokinetic coefficients of an immersed membrane bioreactor. *Journal of Membrane Science*, 271(1), 47-58.

Alturki, A., McDonald, J., Khan, S. J., Hai, F. I., Price, W. E., Nghiem, L. D. 2012. Performance of a novel osmotic membrane bioreactor (OMBR) system: flux stability and removal of trace organics. *Bioresource Technology*, 113, 201-206.

APHA, AWWA, WEF, 2005. Standards Methods for the Examination of Water and Wastewater. APHA-AWWA-WEF, Washington D.C.

American Membrane Technology Association, 2013. Membrane Bio-Reactors (MBR): FS-13.

Arabi, S., Nakhla, G. 2010. Impact of molecular weight distribution of soluble microbial products on fouling in membrane bioreactors. *Separation and Purification Technology*, 73(3), 391–396.

Bai, H., Liu, Z., Sun, D. D. 2011. Highly water soluble and recovered dextran coated Fe_3O_4 magnetic nanoparticles for brackish water desalination. *Separation and Purification Technology*, 81(3), 392-399.

Baker, J. S., Dudley, L. Y. 1998. Biofouling in membrane systems-a review. *Desalination*, 118(1), 81-89.

Barbotin, J. N., Nava Saucedo, J. E., Thomasset, B. 1990. Morphological observations on immobilized cells. *Physiology of Immobilized Cells*, 487-498.

Bouhabila, E. H., Aïm, R. B., Buisson, H. 2001. Fouling characterisation in membrane bioreactors. *Separation and Purification Technology*, 22, 123-132.

Bowden, K. S., Achilli, A., Childress, A. E. 2012. Organic ionic salt draw solutions for osmotic membrane bioreactors. *Bioresource Technology*, 122, 207-216.

Brepols, C., Drensla, K., Janot, A., Trimborn, M., Engelhardt, N. 2008. Strategies for chemical cleaning in large scale membrane bioreactors. *Water Science and Technology*, 57(3), 457-463.

Burton, F. L., Stensel, H. D., Tchobanoglous, G. 2003. Wastewater engineering: treatment and reuse. McGraw Hill.

Calderón, K., Rodelas, B., Cabirol, N., González-López, J., Noyola, A. 2011. Analysis of microbial communities developed on the fouling layers of a membrane-coupled anaerobic bioreactor applied to wastewater treatment. *Bioresource Technology*, 102(7), 4618-4627.

Cath, T. Y., Childress, A. E., Elimelech, M. 2006. Forward osmosis: principles, applications, and recent developments. *Journal of Membrane Science*, 281(1), 70-87.

Charfi, A., Amar, N.B., Harmand, J. 2012. Analysis of fouling mechanisms in anaerobic membrane bioreactors. *Water Research*, 46 (8), 2637-2650.

Charfi, A., Yang, Y., Harmand, J., Amar, N. B., Héran, M., Grasmick, A. 2015. Soluble microbial products and suspended solids influence in membrane fouling dynamics and interest of punctual relaxation and/or backwashing. *Journal of Membrane Science*, 475, 156-166.

Chen, K. C., Lin, Y. F. 1994. Immobilization of microorganisms with phosphorylated polyvinyl alcohol (PVA) gel. *Enzyme and Microbial Technology*, 16(1), 79-83.

Chen, K. C., Lin, Y. H., Chen, W. H., Liu, Y. C. 2002. Degradation of phenol by PAA-immobilized Candida tropicalis. *Enzyme and Microbial Technology*, 31(4), 490-497.

Chen, L., Gu, Y., Cao, C., Zhang, J., Ng, J. W., Tang, C. 2014. Performance of a submerged anaerobic membrane bioreactor with forward osmosis membrane for low-strength wastewater treatment. *Water Research*, 50, 114-123.

Chen, W., Westerhoff, P., Leenheer, J. A., Booksh, K. 2003. Fluorescence excitation-emission matrix regional integration to quantify spectra for dissolved organic matter. *Environmental Science and Technology*, 37(24), 5701-5710.

Cho, B., Fane, A. 2002. Fouling transients in nominally sub-critical flux operation of a membrane bioreactor. *Journal of Membrane Science*, 209, 391-403.

Chon, K., KyongShon, H., Cho, J. 2012. Membrane bioreactor and nanofiltration hybrid system for reclamation of municipal wastewater: removal of nutrients, organic matter and micropollutants. *Bioresource Technology*, 122, 181-188.

Chu, L., Li, S. 2006. Filtration capability and operational characteristics of dynamic membrane bioreactor for municipal wastewater treatment. *Separation and Purification Technology*, 51(2), 173-179.

Chung, T. S. N. 2008. Fabrication of Hollow-Fiber Membranes by Phase Inversion. *Advanced Membrane Technology and Applications*, 821-839.

Chung, T. S., Zhang, S., Wang, K. Y., Su, J., Ling, M. M. 2012. Forward osmosis processes: yesterday, today and tomorrow. *Desalination*, 287, 78-81.

Cornel, P., Wagner, M., Krause, S. 2003. Investigation of oxygen transfer rates in full scale membrane bioreactors. *Water Science and Technol*ogy, 47(11), 313-319.

Cornelissen, E. R., Harmsen, D., De Korte, K. F., Ruiken, C. J., Qin, J. J., Oo, H., Wessels, L. P. 2008. Membrane fouling and process performance of forward osmosis membranes on activated sludge. *Journal of Membrane Science*, 319(1), 158-168.

Côté, P., Buisson, H., Praderie, M. 1998. Immersed membranes activated sludge process applied to the treatment of municipal wastewater. *Water Science and Technology*, 38(4), 437-442.

Croué, J. P., Benedetti, M. F., Violleau, D., Leenheer, J. A. 2003. Characterization and copper binding of humic and nonhumic organic matter isolated from the South Platte River: evidence for the presence of nitrogenous binding site. *Environmental Science and Technology*, 37(2), 328-336.

De Wever, H., Van Roy, S., Dotremont, C., Müller, J., Knepper, T. 2004. Comparison of linear alkylbenzene sulfonates removal in conventional activated sludge systems and membrane bioreactors. *Water Science and Technology*, 50(5), 219-225.

Delrue, F., Stricker, A.E., Mietton-Peuchot, M., Racault, Y. 2011. Relationships between mixed liquor properties, operating conditions and fouling on two full-scale MBR plants. *Desalination,* 272 (1), 9–19.

Deng, L., Guo, W., Ngo, H.H., Zuthi, M.F.R., Zhang, J., Liang, S., Zhang, X. 2015. Membrane fouling reduction and improvement of sludge characteristics by bioflocculant addition in submerged membrane bioreactor. *Separation and Purification Technol*ogy, 156 (2015), 450–458.

Dereli, R. K., Heffernan, B., Grelot, A., van Der Zee, F. P., van Lier, J. B. 2015. Influence of high lipid containing wastewater on filtration performance and fouling in AnMBRs operated at different solids retention times. *Separation and Purification Technology,* 139, 43-52.

Di Trapani, D., Di Bella, G., Mannina, G., Torregrossa, M., Viviani, G. 2014. Comparison between moving bed-membrane bioreactor (MB-MBR) and membrane bioreactor (MBR) systems: influence of wastewater salinity variation. *Bioresource Technology*, 162, 60-69.

Ding, Y., Tian, Y., Liu, J., Li, N., Zhang, J., Zuo, W., Li, Z. 2016. Investigation of microbial structure and composition involved in membrane fouling in the forward osmosis membrane bioreactor treating anaerobic bioreactor effluent. *Chemical Engineering Journal*, 286, 198-207.

Ding, Y., Tian, Y., Li, Z., Zuo, W., Zhang, J. 2015. A comprehensive study into fouling properties of extracellular polymeric substance (EPS) extracted from bulk sludge and cake sludge in a mesophilic anaerobic membrane bioreactor. *Bioresource Technology,* 192, 105-114.

Erickson, H. P. 2009. Size and shape of protein molecules at the nanometer level determined by sedimentation, gel filtration, and electron microscopy. *Biological Procedures Online*, 11(1), 32.

Fan, F., Zhou, H., Husain, H. 2006. Identification of wastewater sludge characteristics to predict critical flux for membrane bioreactor processes. *Water Research*, 40(2), 205-212.

Galil, N. I., Malachi, K. B. D., Sheindorf, C. 2009. Biological nutrient removal in membrane biological reactors. *Environmental Engineering Science*, 26(4), 817-824.

Gander, M. A., Jefferson, B., Judd, S. J. 2000. Membrane bioreactors for use in small wastewater treatment plants: membrane materials and effluent quality. *Water Science and Technology*, 41(1), 205-211.

Gao, D.W., Hu, Q., Yao, C., Ren, N.Q., Wu, W.M. 2014. Integrated anaerobic fluidized bed membrane bioreactor for domestic wastewater treatment. *Chemical Engineering Journal*, 240, 362–368.

Gao, M., Yang, M., Li, H., Yang, Q., Zhang, Y. 2004. Comparison between a submerged membrane bioreactor and a conventional activated sludge system on treating ammonia-bearing inorganic wastewater. *Journal of Biotechnology*, 108(3), 265-269.

Gao, W. J., Lin, H. J., Leung, K. T., Liao, B. Q. 2010. Influence of elevated pH shocks on the performance of a submerged anaerobic membrane bioreactor. *Process Biochememistry*, 45(8), 1279-1287.

Gao, W.J., Lin, H.J., Leung, K.T., Schraft, H., Liao, B.Q. 2011. Structure of cake layer in a submerged anaerobic membrane bioreactor. *Journal of Membrane Science*,374 (1-2), 110–120.

GE Power & Water 2012. Using Membrane Bioreactors for Wastewater Treatment in Small Communities: TP1037EN.

Ge, Q., Ling, M., Chung, T. S. 2013. Draw solutions for forward osmosis processes: developments, challenges, and prospects for the future. *Journal of Membrane Science*, 442, 225-237.

Ge, Q., Su, J., Amy, G. L., Chung, T. S. 2012. Exploration of polyelectrolytes as draw solutes in forward osmosis processes. *Water Research*, 46(4), 1318-1326.

Geng, Z., Hall, E. R. 2007. A comparative study of fouling-related properties of sludge from conventional and membrane enhanced biological phosphorus removal processes. *Water Research*, 41(19), 4329-4338.

Gimenez, J.B., Martí, N., Ferrer, J., Seco, A. 2012. Methane recovery efficiency in a submerged anaerobic membrane bioreactor (SAnMBR) treating sulphate-rich urban wastewater: evaluation of methane losses with the effluent. *Bioresource Technol*ogy, 118, 67-72.

Goh, S., Zhang, J., Liu, Y., Fane, A. G. 2013. Fouling and wetting in membrane distillation (MD) and MD-bioreactor (MDBR) for wastewater reclamation. *Desalination*, 323, 39-47.

Gray, G. T., McCutcheon, J. R., Elimelech, M. 2006. Internal concentration polarization in forward osmosis: role of membrane orientation. *Desalination*, 197(1), 1-8.

Gu, Y., Chen, L., Ng, J. W., Lee, C., Chang, V. W. C., Tang, C. Y. 2015. Development of anaerobic osmotic membrane bioreactor for low-strength wastewater treatment at mesophilic condition. *Journal of Membrane Science*, 490, 197-208.

Hancock, N. T., Cath, T. Y. 2009. Solute coupled diffusion in osmotically driven membrane processes. *Environmental Science and Technology*, 43(17), 6769-6775.

Hancock, N. T., Phillip, W. A., Elimelech, M., Cath, T. Y. 2011. Bidirectional permeation of electrolytes in osmotically driven membrane processes. *Environmental Science and Technology*, 45(24), 10642-10651.

Hartley, K., Lant, P. 2006. Eliminating non-renewable CO_2 emissions from sewage treatment: An anaerobic migrating bed reactor pilot plant study. *Biotechnology and Bioengineering*, 95(3), 384-398.

Hill, C. B., Khan, E. 2008. A comparative study of immobilized nitrifying and coimmobilized nitrifying and denitrifying bacteria for ammonia removal from sludge digester supernatant. *Water, Air, and Soil Pollution*, 195, 23-33.

Ho, J., Sung, S. 2010. Methanogenic activities in anaerobic membrane bioreactors (AnMBR) treating synthetic municipal wastewater. *Bioresource Techn*ology, 101(7), 2191-2196.

Holloway, R. W., Regnery, J., Nghiem, L. D., Cath, T. Y. 2014. Removal of trace organic chemicals and performance of a novel hybrid ultrafiltration-osmotic membrane bioreactor. *Environmental Science and Technology*, 48(18), 10859-10868.

Hu, J., Ren, H., Xu, K., Geng, J., Ding, L., Yan, X., Li, K. 2012. Effect of carriers on sludge characteristics and mitigation of membrane fouling in attached-growth membrane bioreactor. *Bioresource Technology*, 122, 35-41.

Huang, X., Wei, C. H., Yu, K. C. 2008. Mechanism of membrane fouling control by suspended carriers in a submerged membrane bioreactor. *Journal of Membrane Science*, 309(1), 7-16.

Huang, Z., Ong, S. L., Ng, H. Y. 2011. Submerged anaerobic membrane bioreactor for low-strength wastewater treatment: effect of HRT and SRT on treatment performance and membrane fouling. *Water Research*, 45(2), 705-713.

Huang, L. Y., Lee, D. J., Lai, J. Y. 2015. Forward osmosis membrane bioreactor for wastewater treatment with phosphorus recovery. *Bioresource Technology*, 198, 418-423.

Judd, S. 2010. *The MBR book: principles and applications of membrane bioreactors for water and wastewater treatment*. Elsevier.

Juntawang, C., Rongsayamanont, C., Khan, E. 2017a. Fouling characterization in entrapped- cells-based membrane bioreactor treating wastewater. *Separation and Purification Technology*, 175, 321-329.

Juntawang, C., Rongsayamanont, C., Khan, E. 2017b. Entrapped cells-based-anaerobic membrane bioreactor treating domestic wastewater: Performances, fouling, and bacterial community structure. *Chemosphere*, 187, 147-155.

Karst, S.M., Albertsen, M., Kirkegaard, R.H., Dueholm, M.H., Nielsen, P.H. 2016. Molecular methods. In: van Loosdrecht, M.C.M., Nielsen, P.H., Lopez-Vazquez, C.M., Brdjanovic, D. (Eds.), Experimental Methods in Wastewater Treatment. IWA Publishing, London, UK.

Khan, S. J., Ilyas, S., Javid, S., Visvanathan, C., Jegatheesan, V. 2011. Performance of suspended and attached growth MBR systems in treating high strength synthetic wastewater. *Bioresource Technology*, 102(9), 5331-5336.

Khan, S. J., Visvanathan, C., Jegatheesan, V. 2012. Influence of biofilm carriers on membrane fouling propensity in moving biofilm membrane bioreactor. *Bioresource Technology*, 113, 161-164.

Kim, H., Kim, H., Yeom, I. T., Chae, Y. B. 2005. Application of membrane bioreactor system with full scale plant on livestock wastewater. *Water Science and Technology*, 51(6), 465-471.

Kim, J., Kim, K., Ye, H., Lee, E., Shin, C., McCarty, P.L., Bae, J. 2011. Anaerobic fluidized bed membrane bioreactor for wastewater treatment. *Environmental Science and Technology*, 45, 576-581.

Kim J., Shin J., Kim H., Lee J. Y., Yoon M. H., Won S., Song, K. G. 2014. Membrane fouling control using a rotary disk in a submerged anaerobic membrane sponge bioreactor. *Bioresource Technology*, 172, 321-327.

Klindworth, A., Pruesse, E., Schweer, T., Peplies, J., Quast, C., Horn, M., Glöckner, F. O. 2013. Evaluation of general 16S ribosomal RNA gene PCR primers for classical and next-generation sequencing-based diversity studies. *Nucleic Acids Research*, 41(1), 11-24.

Konsoula, Z., Liakopoulou-Kyriakides, M. 2006. Thermostable α-amylase production by Bacillus subtilis entrapped in calcium alginate gel capsules. *Enzyme and Microbial Technology*, 39(4), 690-696.

Kraume, M., Bracklow, U., Vocks, M., Drews, A. 2005. Nutrients removal in MBRs for municipal wastewater treatment. *Water Science and Technology*, 51(6-7), 391-402.

Kumar, M., Adham, S. S., Pearce, W. R. 2006. Investigation of seawater reverse osmosis fouling and its relationship to pretreatment type. *Environmental Science and Technology*, 40(6), 2037-2044.

Lant, P., Hartley, K. 2007. Solids characterisation in an anaerobic migrating bed reactor (AMBR) sewage treatment system. *Water Research*, 41(11), 2437-2448.

Lay, W. C., Liu, Y., Fane, A. G. 2010. Impacts of salinity on the performance of high retention membrane bioreactors for water reclamation: a review. *Water Research*, 44(1), 21-40.

Lay, W. C., Zhang, Q., Zhang, J., McDougald, D., Tang, C., Wang, R., Fane, A. G. 2011. Study of integration of forward osmosis and biological process: membrane performance under elevated salt environment. *Desalination*, 283, 123-130.

Le-Clech, P., Chen, V., Fane, T. A. 2006. Fouling in membrane bioreactors used in wastewater treatment. *Journal of Membrane Science*, 284(1), 17-53.

Lee, K. C., Rittmann, B. E. 2002. Applying a novel autohydrogenotrophic hollow-fiber membrane biofilm reactor for denitrification of drinking water. *Water Research*, 36(8), 2040-2052.

Lee, W. N., Kang, I. J., Lee, C. H. 2006. Factors affecting filtration characteristics in membrane-coupled moving bed biofilm reactor. *Water Research*, 40(9), 1827-1835.

Lesjean, B., Gnirss, R., Adam, C., Kraume, M., Luck, F. 2003. Enhanced biological phosphorus removal process implemented in membrane bioreactors to improve phosphorous recovery and recycling. *Water Science and Technology*, 48(1), 87-94.

Lew, B., Tarre, S., Beliavski, M., Dosoretz, C., Green, M. 2009. Anaerobic membrane bioreactor (AnMBR) for domestic wastewater treatment. *Desalination*, 243(1), 251-257.

Li, J., Yang, F., Liu, Y., Song, H., Li, D., Cheng, F. 2012. Microbial community and biomass characteristics associated severe membrane fouling during start-up of a hybrid anoxic–oxic membrane bioreactor. *Bioresource Technology*, 103(1), 43-47.

Li, Z. Y., Yangali-Quintanilla, V., Valladares-Linares, R., Li, Q., Zhan, T., Amy, G. 2012. Flux patterns and membrane fouling propensity during desalination of seawater by forward osmosis. *Water Research*, 46(1), 195-204.

Lim, S., Kim, S., Yeon, K. M., Sang, B. I., Chun, J., Lee, C. H. 2012. Correlation between microbial community structure and biofouling in a laboratory scale membrane bioreactor with synthetic wastewater. *Desalination*, 287, 209-215.

Lin, H., Peng, W., Zhang, M., Chen, J., Huachang, H., Zhang, Y. 2013. A review on anaerobic membrane bioreactors: applications, membrane fouling and future perspectives. *Desalination*, 314, 169-188.

Lin, H., Liao, B. Q., Chen, J., Gao, W., Wang, L., Wang, F., Lu, X. 2011. New insights into membrane fouling in a submerged anaerobic membrane bioreactor based on characterization of cake sludge and bulk sludge. *Bioresource Technology*, 102(3), 2373-2379.

Ling, M. M., Chung, T. S. 2011. Desalination process using super hydrophilic nanoparticles via forward osmosis integrated with ultrafiltration regeneration. *Desalination*, 278(1), 194-202.

Liu, J., Jia, X., Gao, B., Bo, L., Wang, L. 2016. Membrane fouling behavior in anaerobic baffled membrane bioreactor under static operating condition. *Bioresource Technology*, 214, 582-588.

Liu, Y., Chang, S., Defersha, F.M. 2015. Characterization of the proton binding sites of extracellular polymeric substances in an anaerobic membrane bioreactor. *Water Res*earch, 78, 133–143.

Liu, Y., Mi, B. 2012. Combined fouling of forward osmosis membranes: Synergistic foulant interaction and direct observation of fouling layer formation. *Journal of Membrane Science*, 407, 136-144.

Lowry, O. H., Rosebrough, N. J., Farr, A. L., Randall, R. J. 1951. Protein measurement with the Folin phenol reagent. *Journal of Biological Chemistry*, 193(1), 265-275.

Ludwig, T. G., Goldberg, H. J. 1956. The anthrone method for the determination of carbohydrates in foods and in oral rinsing. *Journal of Dental Research*, 35, 90-94.

Luna, H.J., Baeta, B.E.L., Aquino, S.F.E., Susa, M.R. 2014. EPS and SMP dynamics at different heights of a submerged anaerobic membrane bioreactor (SAMBR). *Process Biochemistry*, 49 (12), 2241–2248.

Lutchmiah, K., Verliefde, A. R. D., Roest, K., Rietveld, L. C., Cornelissen, E. R. 2014. Forward osmosis for application in wastewater treatment: a review. *Water Research*, 58, 179-197.

Ma, J., Wang, Z., Zou, X., Feng, J., Wu, Z. 2013. Microbial communities in an anaerobic dynamic membrane bioreactor (AnDMBR) for municipal wastewater treatment: Comparison of bulk sludge and cake layer. *Process Biochemistry*, 48(3), 510-516.

Martinez-Sosa, D., Helmreich, B., Netter, T., Paris, S., Bischof, F., Horn, H. 2011. Anaerobic submerged membrane bioreactor (AnSMBR) for municipal wastewater treatment under mesophilic and psychrophilic temperature conditions. *Bioresource Technology*, 102(22), 10377-10385.

Maruyama, T., Katoh, S., Nakajima, M., Nabetani, H., Abbott, T. P., Shono, A., Satoh, K. 2001. FT-IR analysis of BSA fouled on ultrafiltration and microfiltration membranes. *Journal of Membrane Science*, 192(1), 201-207.

Massalha, N., Shaviv, A., Sabbah, I. 2010. Modeling the effect of immobilization of microorganisms on the rate of biodegradation of phenol under inhibitory conditions. *Water Research*, 44(18), 5252-5259.

Maximous, N., Nakhla, G., Wan, W. 2009. Comparative assessment of hydrophobic and hydrophilic membrane fouling in wastewater applications. *Journal of Membrane Science*, 339(1), 93-99.

McCarty, P.L., Bae, J., Kim, J. 2011. Domestic wastewater treatment as a net energy producer-can this be achieved? *Environmental Science and Technology*, 45, 7100–7106.

McGinnis, R. L., Elimelech, M. 2007. Energy requirements of ammonia-carbon dioxide forward osmosis desalination. *Desalination*, 207(1), 370-382.

Meng, F., Chae, S. R., Drews, A., Kraume, M., Shin, H. S., Yang, F. 2009. Recent advances in membrane bioreactors (MBRs): membrane fouling and membrane material. *Water Research*, 43(6), 1489-1512.

Meng, F.G., Liao, B.Q., Liang, S.A., Yang, F.L., Zhang, H.M., Song, L.F. 2010. Morphological visualization, componential characterization and microbiological identification of membrane fouling in membrane bioreactors (MBRs). *Journal of Membrane Science*, 361 (1-2), 1-14.

Meshram, P., Dave, R., Joshi, H., Dharani, G., Kirubagaran, R., Venugopalan, V.P. 2016. A fence that eats the weed: alginate lyase immobilization on ultrafiltration membrane for fouling mitigation and flux recovery. *Chemosphere*, 165, 144-151.

Metzger, U., Le-Clech, P., Stuetz, R. M., Frimmel, F. H., Chen, V. 2007. Characterisation of polymeric fouling in membrane bioreactors and the effect of different filtration modes *Journal of Membrane Science*, 301(1), 180-189.

Mi, B., Elimelech, M. 2008. Chemical and physical aspects of organic fouling of forward osmosis membranes. *Journal of Membrane Science*, 320(1), 292-302.

Miura, Y., Watanabe, Y., Okabe, S. 2007. Significance of Chloroflexi in performance of submerged membrane bioreactors (MBR) treating municipal wastewater. *Environmental Science and Technology*, 41, 7787-7794.

Monti, A., Hall, E. R., Dawson, R. N., Husain, H., Kelly, H. G. 2006. Comparative study of biological nutrient removal (BNR) processes with sedimentation and membrane-based separation. *Biotechnology and Bioengineering*, 94(4), 740-752.

Morão, A. M., Nunes, J. C., Sousa, F., de Amorim, M. T. P., Escobar, I. C., Queiroz, J. A. 2011. Ultrafiltration of supercoiled plasmid DNA: modeling and application. *Journal of Membrane Science*, 378(1), 280-289.

Nagaoka, H. 1999. Nitrogen removal by submerged membrane separation activated sludge process. *Water Science and Technology*, 39(8), 107-114.

Nawaz, M. S., Gadelha, G., Khan, S. J., Hankins, N. 2013. Microbial toxicity effects of reverse transported draw solute in the forward osmosis membrane bioreactor (FO-MBR). *Journal of Membrane Science*, 429, 323-329.

Ni, S.Q., Lee, P.H., Fessehaie, A., Gao, B.Y., Sung, S. 2010. Enrichment and biofilm formation of Anammox bacteria in a non-woven membrane reactor. *Bioresource Technology*, 101 (6), 1792-1799.

Nissinen, T. K., Miettinen, I. T., Martikainen, P. J., Vartiainen, T. 2001. Molecular size distribution of natural organic matter in raw and drinking waters. *Chemosphere*, 45(6), 865-873.

Ng, A. N., Kim, A. S. 2007. A mini-review of modeling studies on membrane bioreactor (MBR) treatment for municipal wastewaters. *Desalination*, 212(1), 261-281.

Ng, K. K., Lin, C. F., Lateef, S. K., Panchangam, S. C., Hong, P. K. A., Yang, P. Y. 2010. The effect of soluble microbial products on membrane fouling in a fixed carrier biological system. *Separation and Purification Technology*, 72(1), 98-104.

Ng, K. K., Lin, C. F., Panchangam, S. C., Hong, P. K. A., Yang, P. Y. 2011. Reduced membrane fouling in a novel bio-entrapped membrane reactor for treatment of food and beverage processing wastewater. *Water Research*, *45*(14), 4269-4278.

Ng, K. K., Shi, X., Tang, M. K. Y., Ng, H. Y. 2014. A novel application of anaerobic bio-entrapped membrane reactor for the treatment of chemical synthesis-based pharmaceutical wastewater. *Separation and Purification Technology*, 132, 634-643.

Ng, K. K., Wu, C. J., You, L. Y., Kuo, C. S., Lin, C. F., Hong, A. P. K., Yang, P. Y. 2012. Bio-entrapped membrane reactor for organic matter removal and membrane fouling reduction. *Desalination and Water Treatment*, 50 (1-3), 59-66.

Ni, B. J., Zeng, R. J., Fang, F., Xie, W. M., Sheng, G. P., Yu, H. Q. 2010. Fractionating soluble microbial products in the activated sludge process. *Water Research*, 44(7), 2292-2302.

Ni, S. Q., Lee, P. H., Fessehaie, A., Gao, B. Y., Sung, S. 2010. Enrichment and biofilm formation of Anammox bacteria in a non-woven membrane reactor. *Bioresource Technology*, 101(6), 1792-1799.

Okabe, S., Kindaichi, T., Ito, T. 2005. Fate of 14C-labeled microbial products derived from nitrifying bacteria in autotrophic nitrifying biofilms. *Apply Environmental Microbiology*, 71, 3987-3994.

Ozgun, H., Dereli, R. K., Ersahin, M. E., Kinaci, C., Spanjers, H., van Lier, J. B. 2013. A review of anaerobic membrane bioreactors for municipal wastewater treatment: integration options, limitations and expectations. *Separation and Purification Technology*, 118, 89-104.

Patel, J., Nakhla, G., Margaritis, A. 2005. Optimization of biological nutrient removal in a membrane bioreactor system. *Journal of Environmental Engineering*, 131(7), 1021-1029.

Pramanik, S., Khan, E. 2008. Effects of cell entrapment on growth rate and metabolic activity of mixed cultures in biological wastewater treatment. *Enzyme and Microbial Technology*, 43(3), 245-251.

Qin, J. J., Kekre, K. A., Oo, M. H., Tao, G., Lay, C. L., Lew, C. H., Ruiken, C. J. 2010. Preliminary study of osmotic membrane bioreactor: effects of draw solution on water flux and air scouring on fouling. *Water Science and Technology*, 62(6), 1353-1360.

Qiu, G., Ting, Y. P. 2013. Osmotic membrane bioreactor for wastewater treatment and the effect of salt accumulation on system performance and microbial community dynamics. *Bioresource Technology*, 150, 287-297.

Qiu, G., Ting, Y. P. 2014. Short-term fouling propensity and flux behavior in an osmotic membrane bioreactor for wastewater treatment. *Desalination*, 332(1), 91-99.

Qiu, G., Zhang, S., Raghavan, D. S. S., Das, S., Ting, Y. P. 2016. The potential of hybrid forward osmosis membrane bioreactor (FOMBR) processes in achieving high throughput treatment of municipal wastewater with enhanced phosphorus recovery. *Water Research*, 105, 370-382.

Ramphao, M., Wentzel, M. C., Merritt, R., Ekama, G. A., Young, T., Buckley, C. A. 2005. Impact of membrane solid–liquid separation on design of biological nutrient removal activated sludge systems. *Biotechnology and Bioengineering*, 89(6), 630-646.

Reid, E., Liu, X., Judd, S. J. 2008. Sludge characteristics and membrane fouling in full-scale submerged membrane bioreactors. *Desalination*, 219(1), 240-249.

Ren, N., Chen, Z., Wang, A., Hu, D. 2005. Removal of organic pollutants and analysis of MLSS–COD removal relationship at different HRTs in a submerged membrane bioreactor. *International Biodeterioration and Biodegradation*, 55(4), 279-284.

Rodríguez-Hernández, L., Esteban-García, A. L., Tejero, I. 2014. Comparison between a fixed bed hybrid membrane bioreactor and a conventional membrane bioreactor for municipal wastewater treatment: A pilot-scale study. *Bioresource Technology*, 152, 212-219.

Rosenberger, S., Laabs, C., Lesjean, B., Gnirss, R., Amy, G., Jekel, M., Schrotter, J. C. 2006. Impact of colloidal and soluble organic material on membrane performance in membrane bioreactors for municipal wastewater treatment. *Water Research*, 40(4), 710-720.

Salazar-Peláez, M. L., Morgan-Sagastume, J. M., Noyola, A. 2011. Influence of hydraulic retention time on fouling in a UASB coupled with an external ultrafiltration membrane treating synthetic municipal wastewater. *Desalination*, 277(1), 164-170.

She, Q., Wang, R., Fane, A. G., Tang, C. Y. 2016. Membrane fouling in osmotically driven membrane processes: A review. *Journal of Membrane Science*, 499, 201-233.

Shen, L. G., Lei, Q., Chen, J. R., Hong, H. C., He, Y. M., Lin, H. J. 2015. Membrane fouling in a submerged membrane bioreactor: Impacts of floc size. *Chemical Engineering Journal*, 269, 328-334.

Siripattanakul, S., Wirojanagud, W., McEvoy, J., Khan, E. 2008. Effect of cell-to-matrix ratio in polyvinyl alcohol immobilized pure and mixed cultures on atrazine degradation. *Water, Air, and Soil Pollution: Focus*, 8(3-4), 257-266.

Smith, A.L., Skerlos, S.J., Raskin L. 2013. Psychrophilic anaerobic membrane bioreactor treatment of domestic wastewater. *Water Res*earch, 47, 1655-1665.

Smith, S., Judd, S., Stephenson, T., Jefferson, B. 2003. Membrane bioreactors-Hybrid activated sludge or a new process? *Membrane Technology*, 12, 5-8.

Steiner, Z., Rapaport, H., Oren, Y., Kasher, R. 2010. Effect of surface-exposed chemical groups on calcium-phosphate mineralization in water-treatment systems. *Environmental Science and Technology*, 44(20), 7937-7943.

Stephenson, T. 2000. *Membrane bioreactors for wastewater treatment* (pp. 6-8). London: IWA.

Stuckey, D.C. 2012. Recent developments in anaerobic membrane reactors. *Bioresource Technology*, 122, 137-148.

Su, X., Tian, Y., Sun, Z., Lu, Y., Li, Z. 2013. Performance of a combined system of microbial fuel cell and membrane bioreactor: wastewater treatment, sludge reduction, energy recovery and membrane fouling. *Biosensors and Bioelectronics*, 49, 92-98.

Sun, C., Leiknes, T., Fredriksen, R. H., Riviere, E. 2012. Comparison of membrane filtration performance between biofilm-MBR and activated sludge-MBR. *Desalination and Water Treatment*, 48(1-3), 285-293.

Sun, Y., Shen, Y. X., Liang, P., Zhou, J., Yang, Y., Huang, X. 2014. Linkages between microbial functional potential and wastewater constituents in large-scale membrane bioreactors for municipal wastewater treatment. *Water Research*, 56, 162-171.

Tang, C. H., Ng, H. Y. 2010. A novel hybrid forward osmosis-nanofiltration (FO-NF) process for seawater desalination: draw solution selection and system configuration. *Desalination and Water Treatment*, 13(1-3), 356-361.

Tang, C. Y., She, Q., Lay, W. C., Wang, R., Fane, A. G. 2010. Coupled effects of internal concentration polarization and fouling on flux behavior of forward osmosis membranes during humic acid filtration. *Journal of Membrane Science*, 354(1), 123-133.

Tardieu, E., Grasmick, A., Geaugey, V., Manem, J. 1999. Influence of hydrodynamics on fouling velocity in a recirculated MBR for wastewater treatment. *Journal of Membrane Science*, 156(1), 131-140.

Tchobanoglous, G., Franklin, L.B., Stensel, H.D. 2003 Wastewater Engineering: Treatment and Reuse, fourth ed., McGraw-Hill, New York, USA.

Tsen, J.H., Lin, Y.P., King, V.A.E. 2004. Fermentation of banana media by using carrageenan immobilized Lactobacillus acidophilus. *International Journal of Food Microbiology*, 91(2),215–220.

Ujang, Z., Salim, M. R., Khor, S. L. 2002. The effect of aeration and non-aeration time on simultaneous organic, nitrogen and phosphorus removal using an intermittent aeration membrane bioreactor. *Water and Wastewater Management for Developing Countries*, 46(9), 193-200.

Van Dijk, L., Roncken, G. C. G. 1997. Membrane bioreactors for wastewater treatment: the state of the art and new developments. *Water Science and Technology*, 35(10), 35-41.

Verrecht, B., Maere, T., Benedetti, L., Nopens, I., Judd, S. 2010. Model-based energy optimisation of a small-scale decentralised membrane bioreactor for urban reuse. *Water Research*, 44(14), 4047-4056.

Waheed, H., Xiao, Y., Hashmi, I., Stuckey, D., Zhou, Y. 2017. Insights into quorum quenching mechanisms to control membrane biofouling under changing organic loading rates. *Chemosphere*, 182, 40-47.

Verrecht, B., Maere, T., Benedetti, L., Nopens, I., Judd, S. 2010. Model-based energy optimization of a small-scale decentralised membrane bioreactor for urban reuse. *Water Research*, 44(14), 4047-4056.

Wang, H., Ding, A., Gan, Z., Qu, F., Cheng, X., Bai, L., Guo, S., Li, G., Liang, H. 2017. Fluorescent natural organic matter responsible for ultrafiltration membrane fouling: fate, contributions and fouling mechanisms. *Chemosphere*, 182, 183-192.

Wang, X., Chen, Y., Yuan, B., Li, X., Ren, Y. 2014. Impacts of sludge retention time on sludge characteristics and membrane fouling in a submerged osmotic membrane bioreactor. *Bioresource Technol*ogy, 161, 340-347.

Wang, Z., Mei, X., Ma, J., Grasmick, A., Wu, Z. 2013. Potential foulants and fouling indicators in MBRs: a critical review. *Separation Science and Technology,* 48(1), 22-50.

Wang, Z., Wu, Z., Tang, S. 2009. Extracellular polymeric substances (EPS) properties and their effects on membrane fouling in a submerged membrane bioreactor. *Water Research*, 43(9), 2504-2512.

Wang, Z., Wu, Z., Yin, X., Tian, L. 2008. Membrane fouling in a submerged membrane bioreactor (MBR) under sub-critical flux operation: membrane foulant and gel layer characterization. *Journal of Membrane Science*, 325(1), 238-244.

Wang, Z. P., Zhang, T. 2010. Characterization of soluble microbial products (SMP) under stressful conditions. *Water Res*earch, 44(18), 5499-5509.

Wen, C., Huang, X., Qian, Y. 1999. Domestic wastewater treatment using an anaerobic bioreactor coupled with membrane filtration. *Process Biochemistry*, 35(3), 335-340.

Wisniewski, C., Grasmick, A. 1998. Floc size distribution in a membrane bioreactor and consequences for membrane fouling. *Colloids and Surfaces A: Physicochemical and Engineering Aspects*, 138(2), 403-411.

Xing, C. H., Tardieu, E., Qian, Y., Wen, X. H. 2000. Ultrafiltration membrane bioreactor for urban wastewater reclamation. *Journal of Membrane Science*, 177(1), 73-82.

Yamamura, H., Kimura, K., Watanabe, Y. 2007. Mechanism involved in the evolution of physically irreversible fouling in microfiltration and ultrafiltration membranes used for drinking water treatment. *Environmental Science and Technology*, 41(19), 6789-6794.

Yang, Q., Wang, K. Y., Chung, T. S. 2009. A novel dual-layer forward osmosis membrane for protein enrichment and concentration. *Separation and Purification Technology*, 69(3), 269-274.

Yang, S., Yang, F., Fu, Z., Lei, R. 2009. Comparison between a moving bed membrane bioreactor and a conventional membrane bioreactor on organic carbon and nitrogen removal. *Bioresource Technology*, 100(8), 2369-2374.

Yap, W. J., Zhang, J., Lay, W. C., Cao, B., Fane, A. G., Liu, Y. 2012. State of the art of osmotic membrane bioreactors for water reclamation. *Bioresource Technology*, 122, 217-222.

Yeom, I. T., Nah, Y. M., Ahn, K. H. 1999. Treatment of household wastewater using an intermittently aerated membrane bioreactor. *Desalination*, 124(1), 193-203.

Yu, Z., Wen, X., Xu, M., Huang, X. 2012. Characteristics of extracellular polymeric substances and bacterial communities in an anaerobic membrane bioreactor coupled with online ultrasound equipment. *Bioresource Technology*, 117, 333-340.

Yuan, B., Wang, X., Tang, C., Li, X., Yu, G. 2015. In situ observation of the growth of biofouling layer in osmotic membrane bioreactors by multiple fluorescence labeling and confocal laser scanning microscopy. *Water Research*, 75, 188-200.

Yue, X., Koh, Y.K.K., Ng, H. Y. 2015. Effects of dissolved organic matters (DOMs) on membrane fouling in anaerobic ceramic membrane bioreactors (AnCMBRs) treating domestic wastewater. *Water Research*, 86, 96-107.

Yun, M. A., Yeon, K. M., Park, J. S., Lee, C. H., Chun, J., Lim, D. J. 2006. Characterization of biofilm structure and its effect on membrane permeability in MBR for dye wastewater treatment. *Water Research*, 40(1), 45-52.

Zanetti, F., De Luca, G., Sacchetti, R. 2010. Performance of a full-scale membrane bioreactor system in treating municipal wastewater for reuse purposes. *Bioresource technology*, 101(10), 3768-3771.

Zhang, H., Jiang, W., Cui, H. 2017. Performance of anaerobic forward osmosis membrane bioreactor coupled with microbial electrolysis cell (AnOMEBR) for energy recovery and membrane fouling alleviation. *Chemical Engineering Journal*, 321, 375–383.

Zhang, Q., Jie, Y. W., Loong, W. L. C., Zhang, J., Fane, A. G., Kjelleberg, S., McDougald, D. 2014. Characterization of biofouling in a lab-scale forward osmosis membrane bioreactor (FOMBR). *Water Research*, 58, 141-151.

Zhang, T., Shao, M. F., Ye, L. 2012. 454 Pyrosequencing reveals bacterial diversity of activated sludge from 14 sewage treatment plants. *The ISME Journal*, 6(6), 1137-1147.

Zhang, L. S., Wu, W. Z., Wang, J. L. 2007. Immobilization of activated sludge using improved polyvinyl alcohol (PVA) gel. *Journal of Environmental Sciences*, 19(11), 1293-1297.

Zhang, S., Van, Houten, R., Eikelboom, D. H., Doddema, H., Jiang, Z., Fan, Y., Wang, J. 2003. Sewage treatment by a low energy membrane bioreactor. *Bioresource Technology*, 90(2), 185-192.

Zhao, S., Zou, L., Tang, C. Y., Mulcahy, D. 2012. Recent developments in forward osmosis: opportunities and challenges. *Journal of Membrane Science*, 396, 1-21.

APPENDIX A: SUPPLEMENTARY DATA FOR RESEARCH TASK 2 (CHAPTER 4)

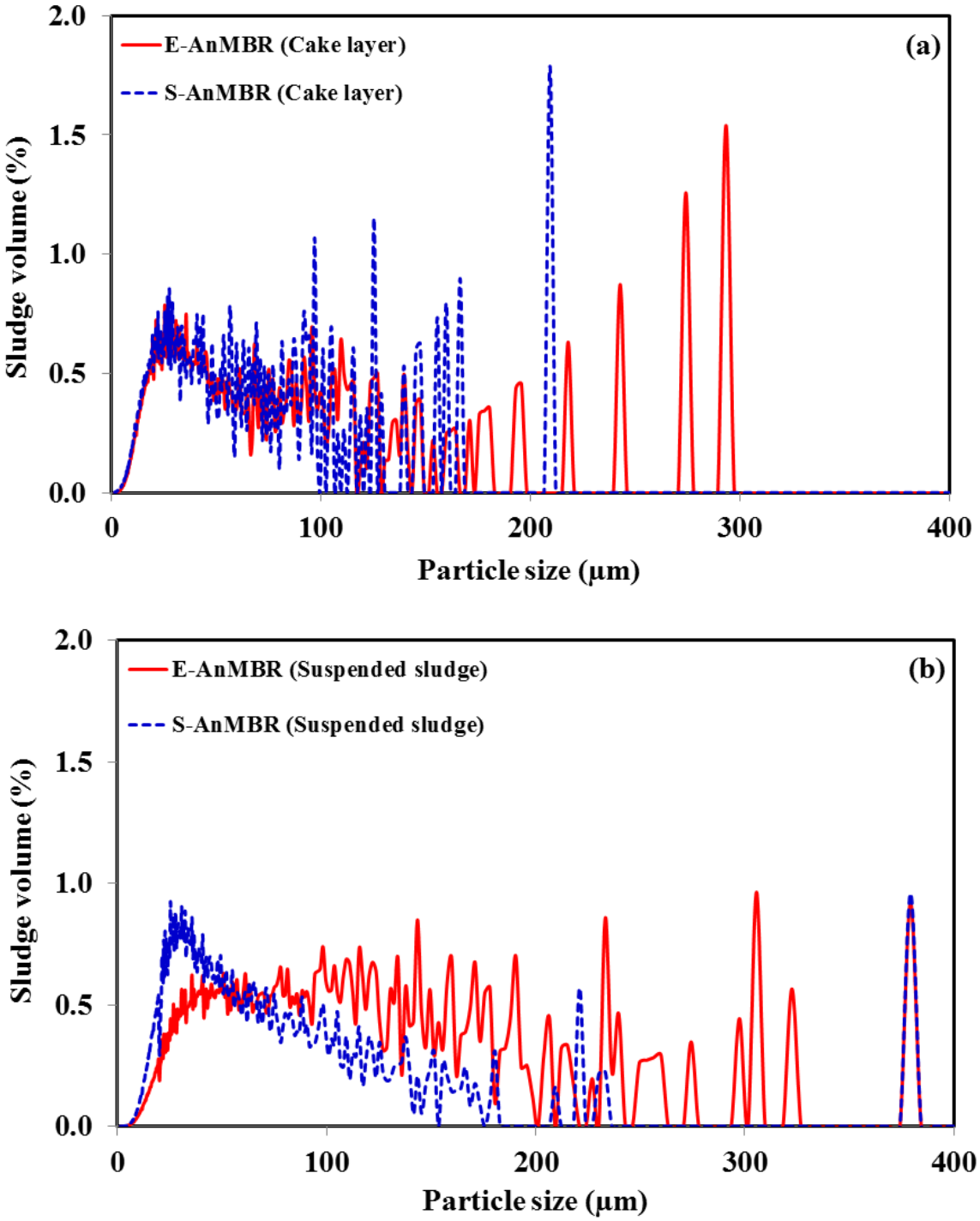

Figure A-1: Particles size distribution in E-AnMBR and S-AnMBR: (a) cake layer (1–400 µm) and (b) suspended sludge (1–400 µm).

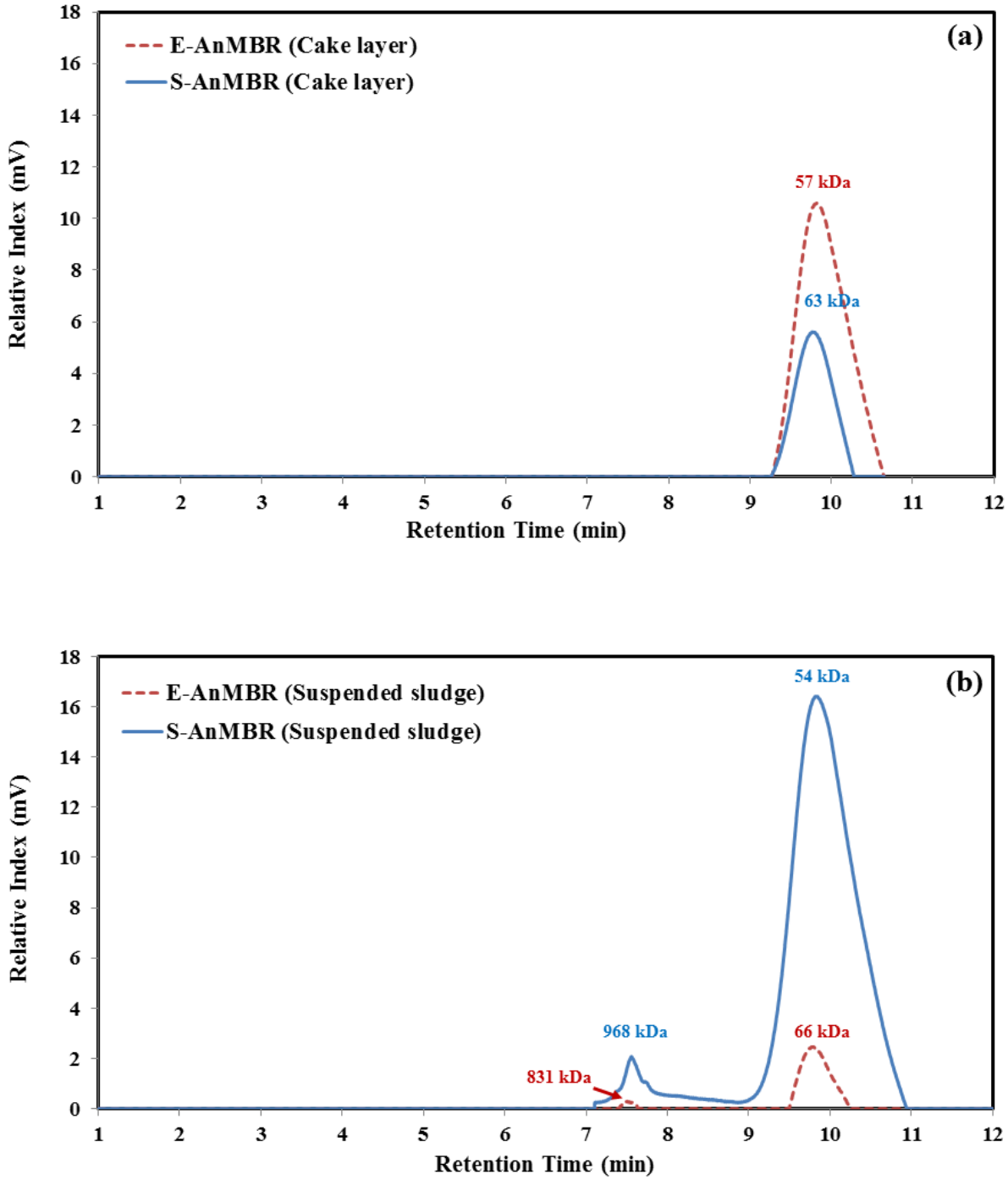

Figure A-2: Molecular weight distribution of bEPS from E-AnMBR and S-AnMBR: (a) cake layer and (b) suspended sludge.

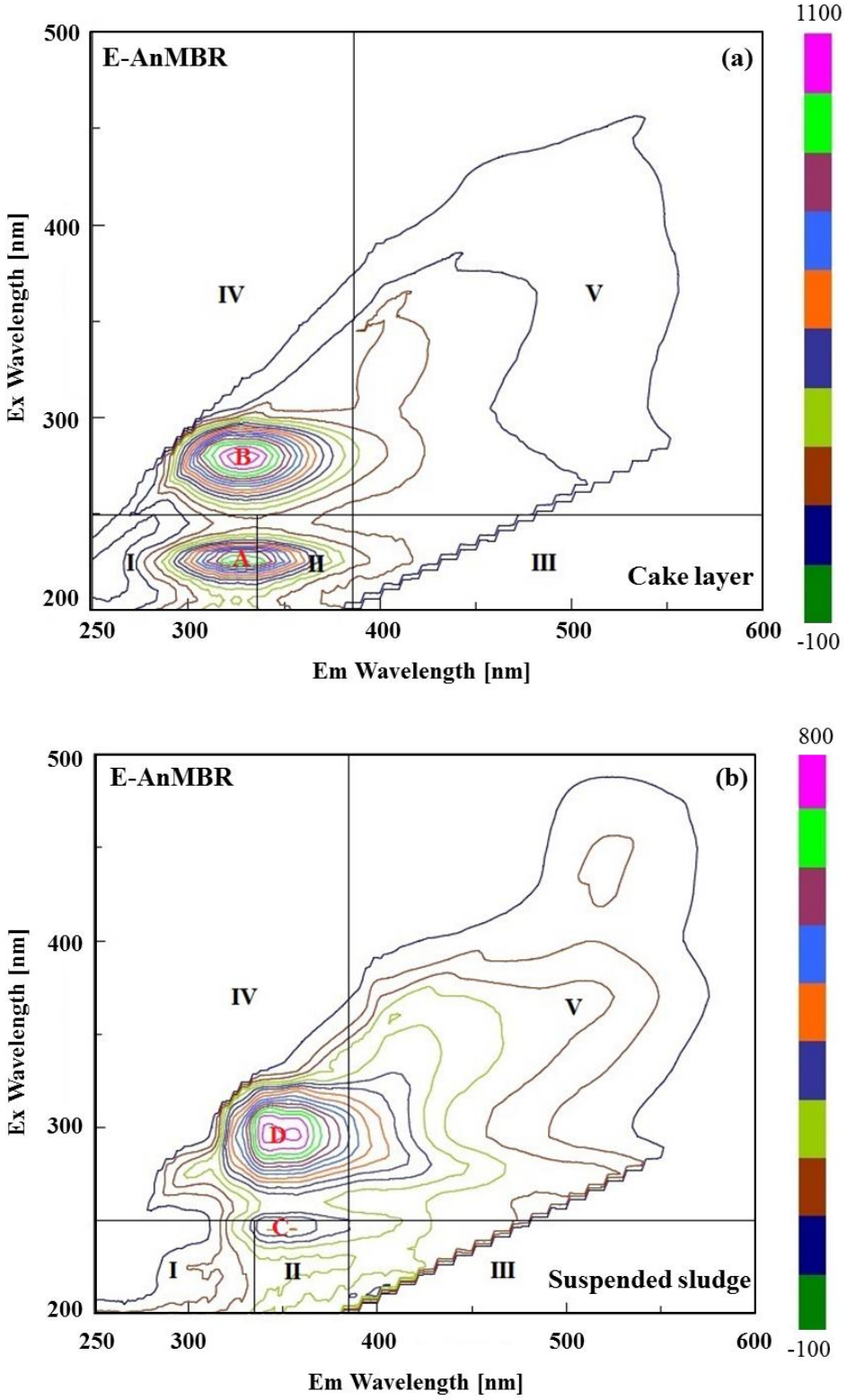

Figure A-3: EEMs of SMP from (a) cake layer of E-AnMBR, (b) suspended sludge of E-AnMBR, (c) cake layer of S-AnMBR, and (d) suspended sludge of S-AnMBR.

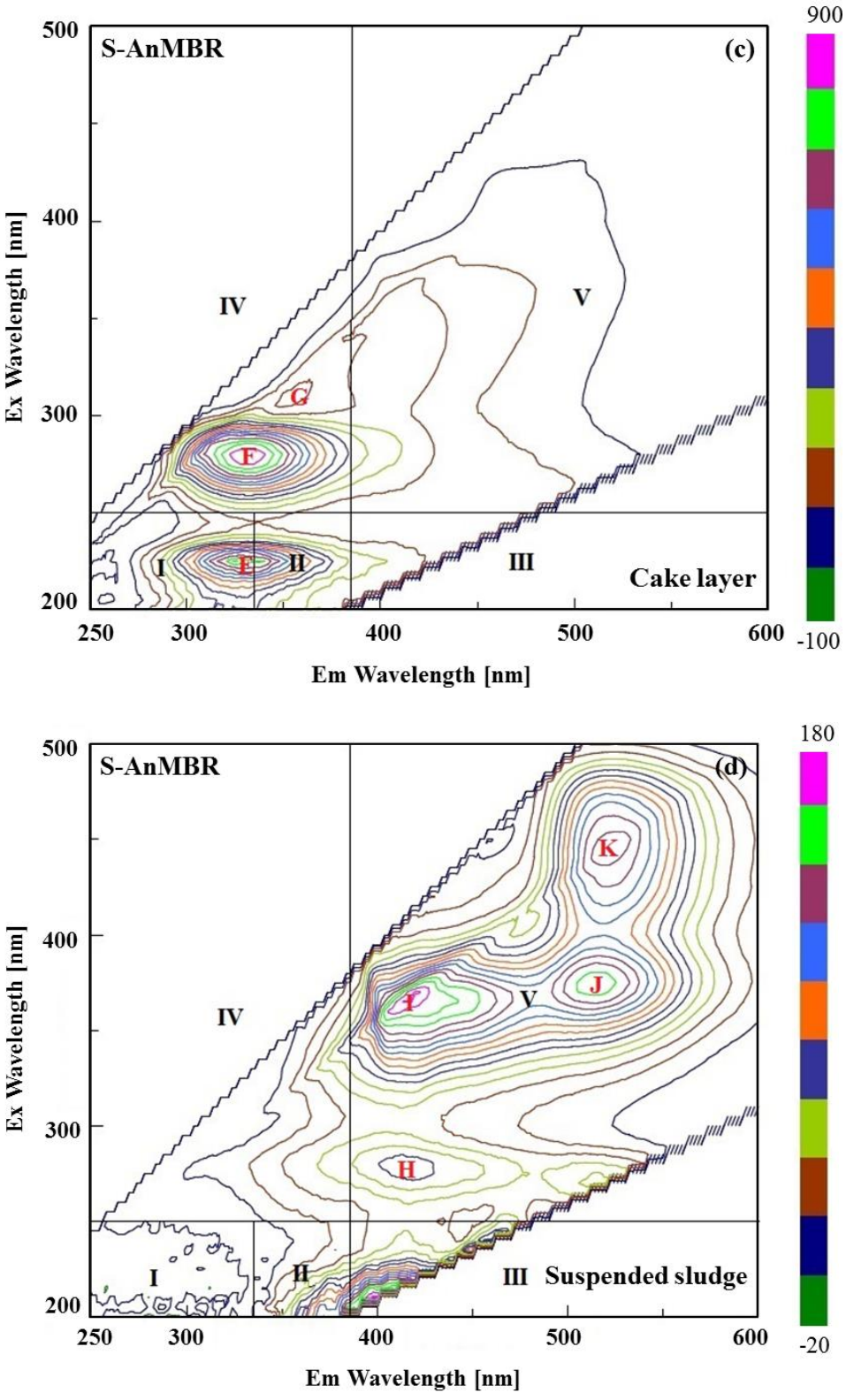

Figure A-3: EEMs of SMP from (a) cake layer of E-AnMBR, (b) suspended sludge of E-AnMBR, (c) cake layer of S-AnMBR, and (d) suspended sludge of S-AnMBR. (continued)

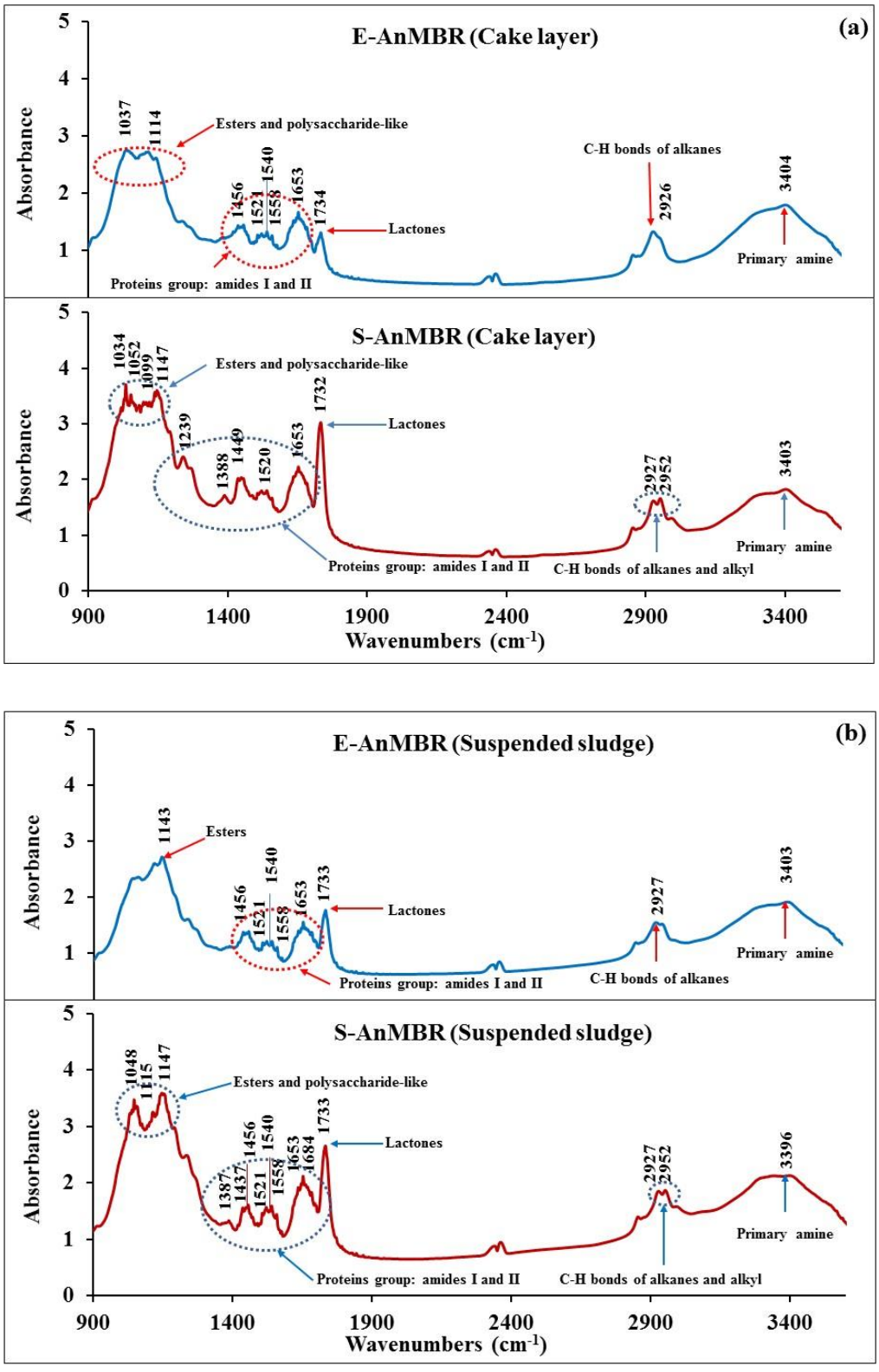

Figure A-4: FTIR spectra of bEPS from E-AnMBR and S-AnMBR: (a) cake layer and (b) suspended sludge.

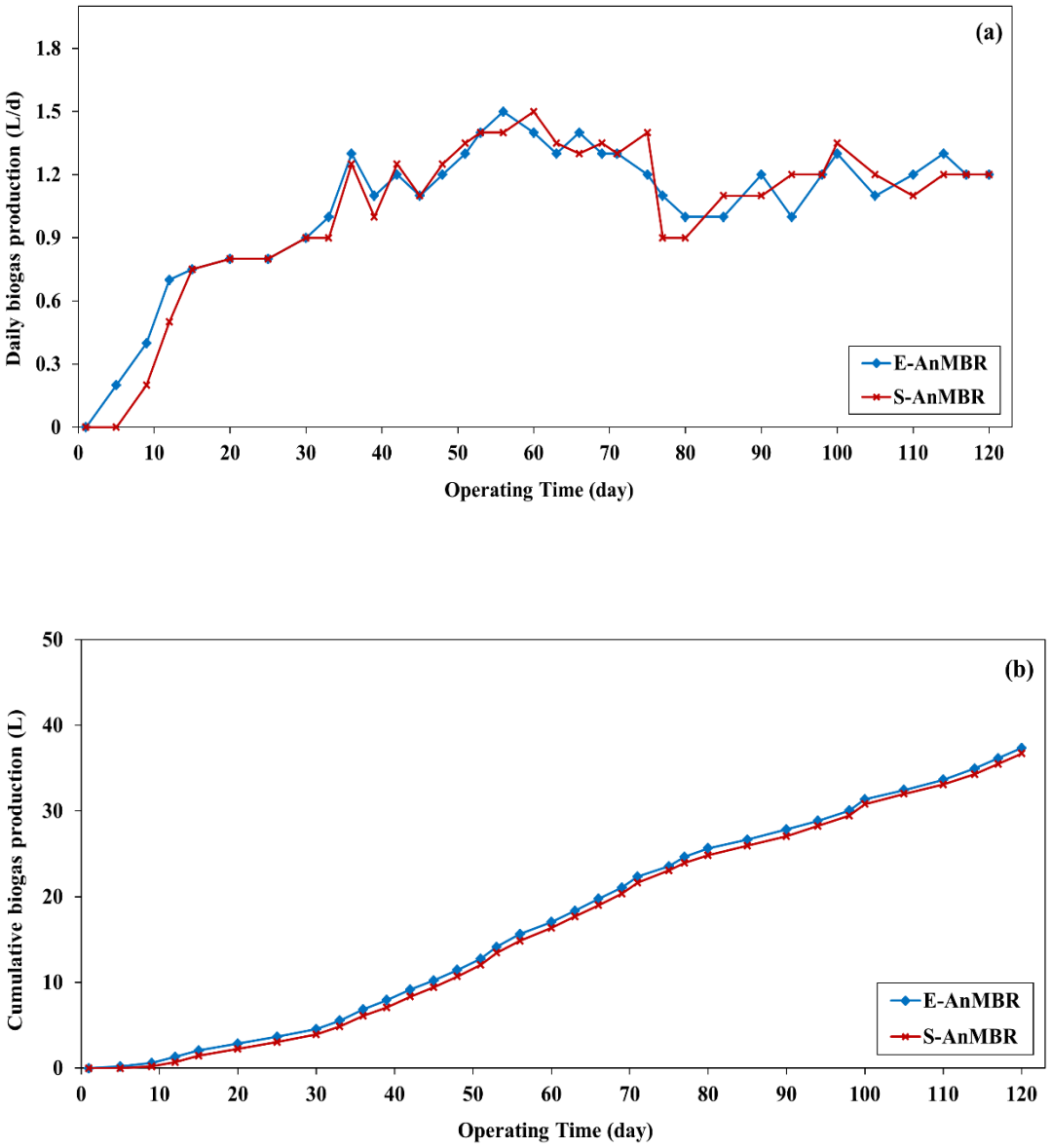

Figure A-5: (a) Daily biogas production of E-AnMBR and S-AnMBR, and (b) Cumulative biogas production of E-AnMBR and S-AnMBR.

APPENDIX B. SUPPLEMENTARY DATA FOR RESEARCH TASK 3 (CHAPTER 5)

B.1. Diffusion model

The physicochemical properties of cell entrapment gel influence the metabolism and substrate kinetics of cells, due to mass transfer limitation through the gel matrix (Vives *et al*., 1993). Bacteria growth depends on diffusion of the substrate within entrapment gel/polymer (i.e., alginate, *k*-carrageenan and PVA) and may affect cell physiology (Barbotin *et al*., 1990). The equation governing substrate diffusion and utilization for entrapped cells is:

$$\frac{d^2S}{dr^2} = \frac{\frac{\mu}{Y_{xs}}X(t) + mX(t)\left(\frac{S}{K_S + S}\right)}{D_e} - \frac{2}{r}\frac{dS}{dr} \qquad \text{(B1)}$$

Where S is substrate concentration (mol. m^{-3}), r is distance from the center of the bead to outer layer (m), μ is specific growth rate (s^{-1}), Y_{xs} is yield coefficient (kg. mol^{-1}), X is biomass concentration (kg. m^{-3}), t is time (s), m is the maintenance coefficient (mol. kg^{-1}. s^{-1}), K_s is Monod constant (mol. m^{-3}) and D_e is effective diffusion coefficient (m^2. s^{-1}). This equation suggests that substrate utilization depends on bacteria growth and substrate diffusion coefficient. When biomass concentration reaches the maximum value, the substrate utilization by the bacteria may be used for metabolism or the bacteria may continue to grow and move out of the gel/polymer matrix. Izadi and Rashedi (2015) and Wang *et al*. (2010) reported that increases in substrate diffusion result in higher substrate utilizations. These studies indicated that the transfer of substrate from bulk liquid to the entrapped cells depends on substrate utilization and diffusion coefficient of substrate in the entrapment gel/polymer.

B.2. References

Barbotin, J. N., Nava Saucedo, J. E., Thomasset, B. 1990. Morphological observations on immobilized cells. *Physiology of Immobilized Cells*, 487-498.

Izadi, A., Rashedi, H. 2015. Substrate Diffusion Analysis in Immobilized Spherical Cell-Support Aggregate by Using of Least Square Method. *Journal of Applied Biotechnology Reports,* 2(2), 245-250.

Vives, C., Casas, C., Gòdia, F., Solà, C. 1993. Determination of the intrinsic fermentation kinetics of Saccharomyces cerevisiae cells immobilized in Ca-alginate beads and observations on their growth. *Applied Microbiology and Biotechnology*, 38(4), 467-472.

Wang, Y. Z., Liao, Q., Zhu, X., Tian, X., Zhang, C. 2010. Characteristics of hydrogen production and substrate consumption of Rhodopseudomonas palustris CQK 01 in an immobilized-cell photobioreactor. *Bioresource Technology*, 101(11), 4034-4041.

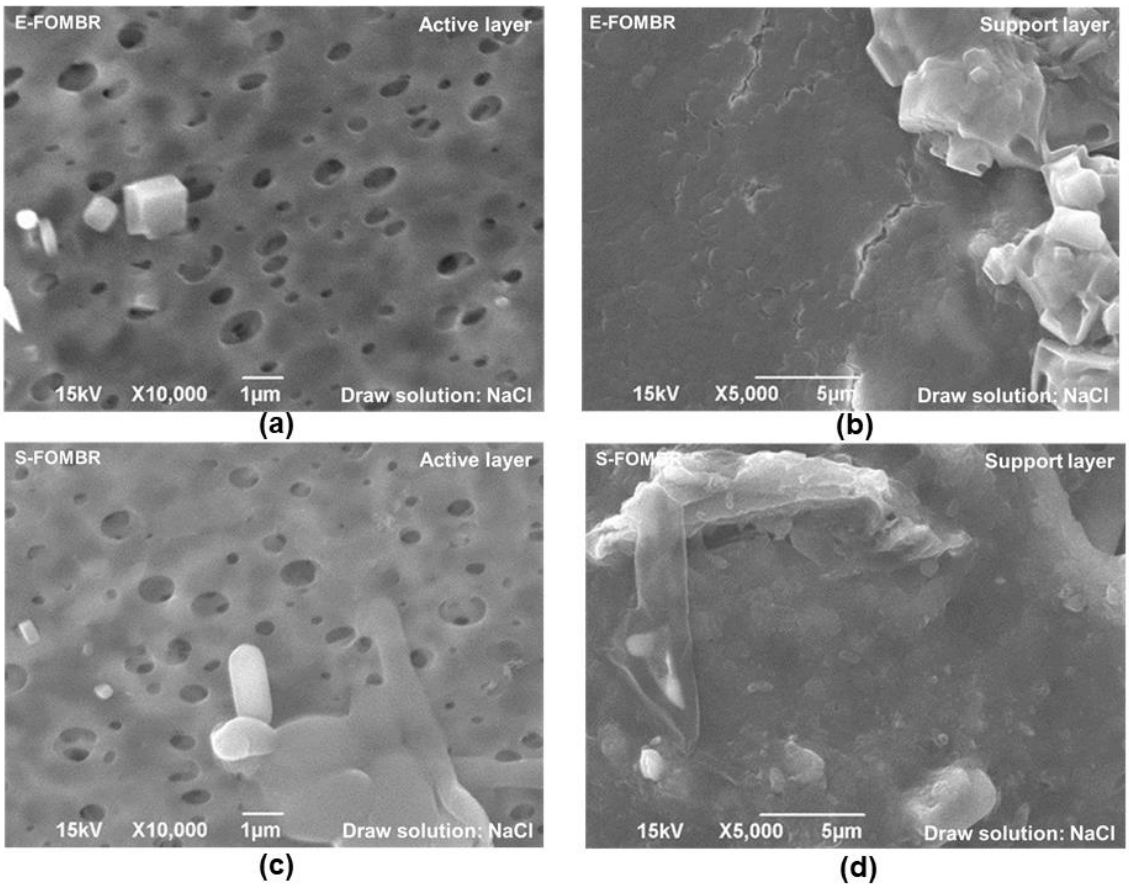

Figure B-1: SEM images of fouled FO membrane in E-FOMBR and S-FOMBR with NaCl as a draw solution: (a) Active layer of fouled FO membrane in E-FOMBR: 10,000× magnification, (b) Support layer of fouled FO membrane in E-FOMBR: 5,000× magnification, (c) Active layer of fouled FO membrane in S-FOMBR: 10,000× magnification, and (d) Support layer of fouled FO membrane in S-FOMBR: 5,000× magnification.

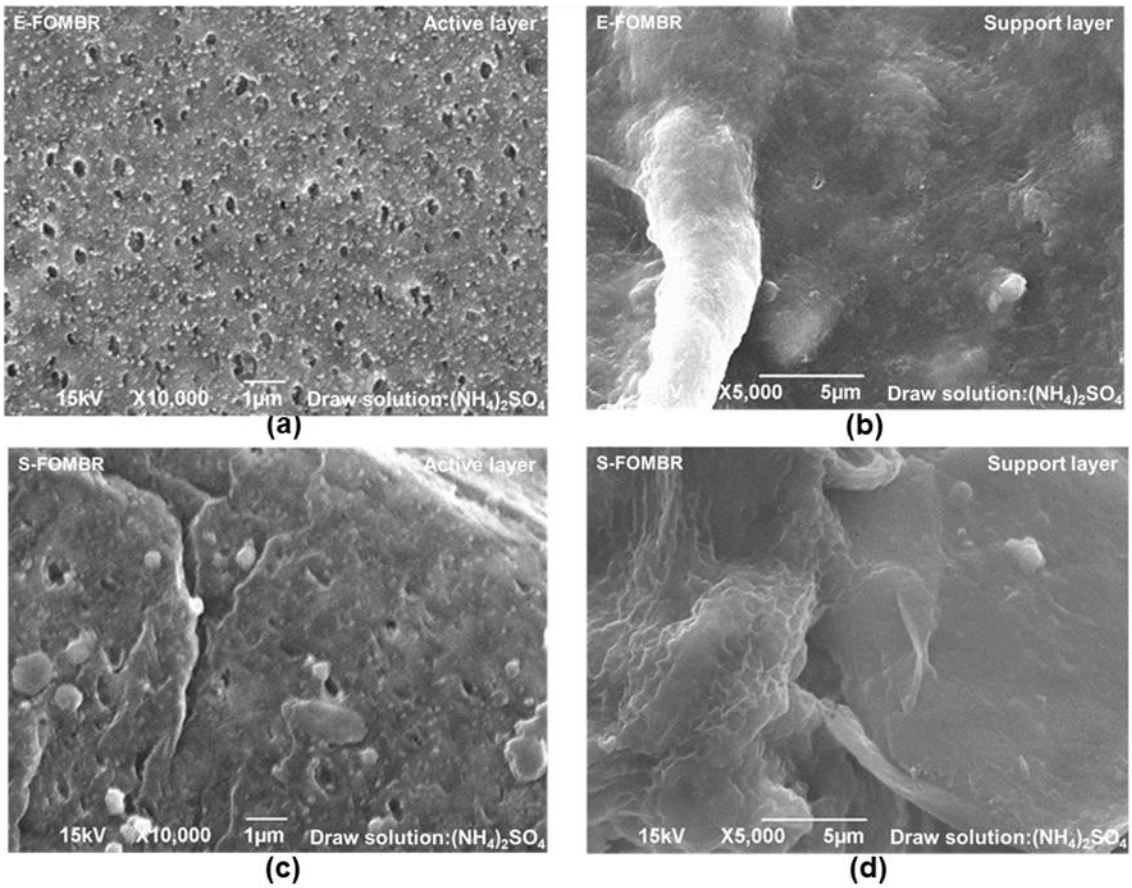

Figure B-2: SEM images of fouled FO membrane in E-FOMBR and S-FOMBR with $(NH_4)_2SO_4$ as a draw solution: (a) Active layer of fouled FO membrane in E-FOMBR: 10,000× magnification, (b) Support layer of fouled FO membrane in E-FOMBR: 5,000× magnification, (c) Active layer of fouled FO membrane in S-FOMBR: 10,000× magnification, and (d) Support layer of fouled FO membrane in S-FOMBR: 5,000× magnification.

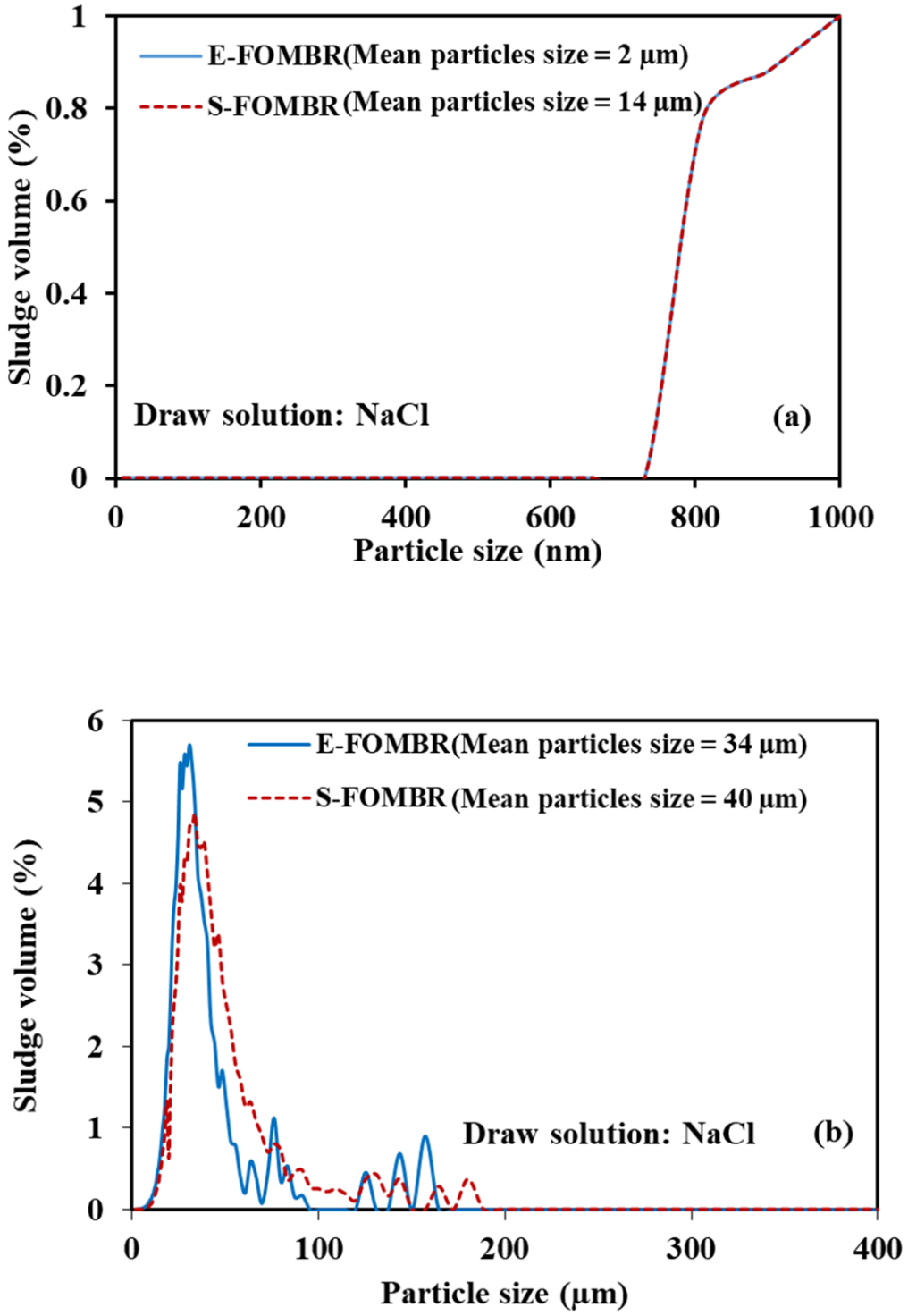

Figure B-3: Particles size distribution during the steady state operation of E-FOMBR and S-FOMBR: (a) A particle size range of 1 nm – 1 µm with NaCl as a draw solution, (b) A particle size range of 1 µm – 400 µm with NaCl as a draw solution, (c) A particle size range of 1 nm – 1 µm with $(NH_4)_2SO_4$ as a draw solution, and (d) A particle size range of 1 µm – 400 µm with $(NH_4)_2SO_4$ as a draw solution.

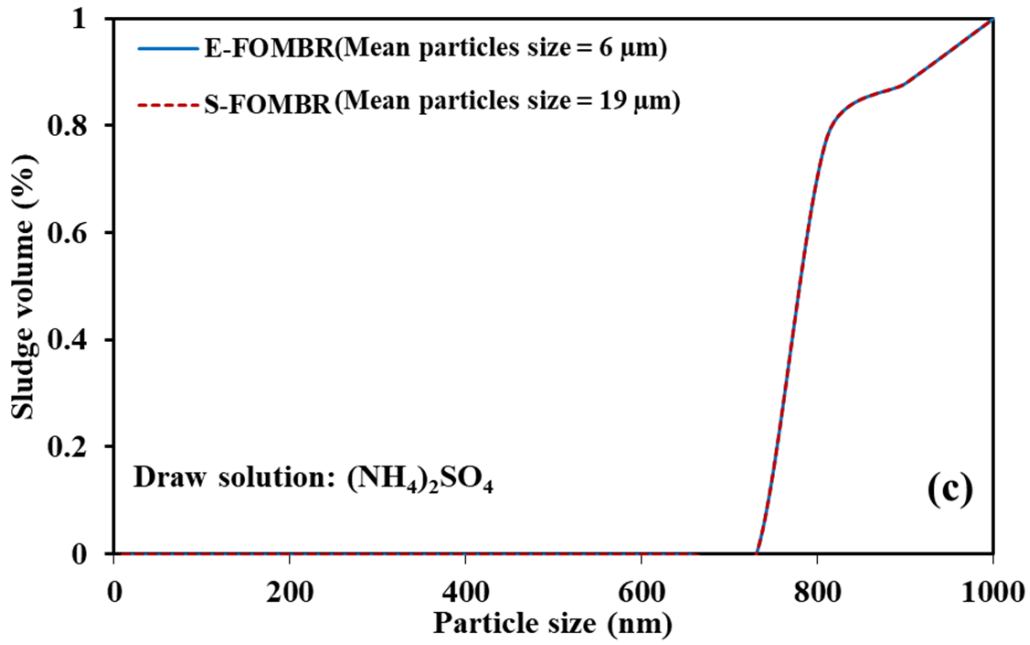

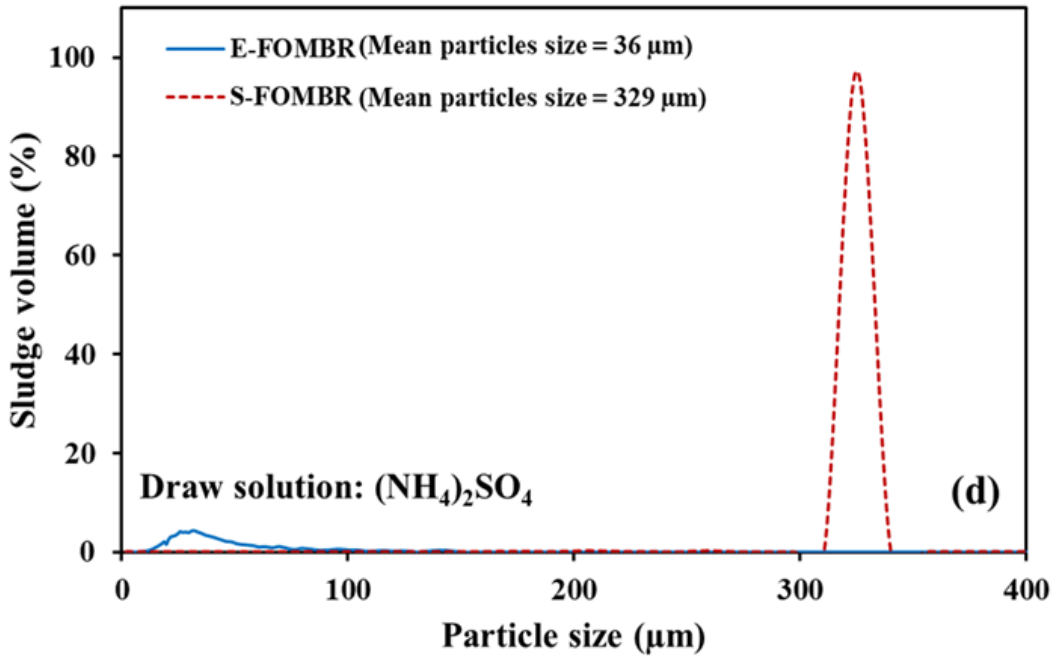

Figure B-3: Particles size distribution during the steady state operation of E-FOMBR and S-FOMBR: (a) A particle size range of 1 nm – 1 µm with NaCl as a draw solution, (b) A particle size range of 1 µm – 400 µm with NaCl as a draw solution, (c) A particle size range of 1 nm – 1 µm with $(NH_4)_2SO_4$ as a draw solution, and (d) A particle size range of 1 µm – 400 µm with $(NH_4)_2SO_4$ as a draw solution. (continued)

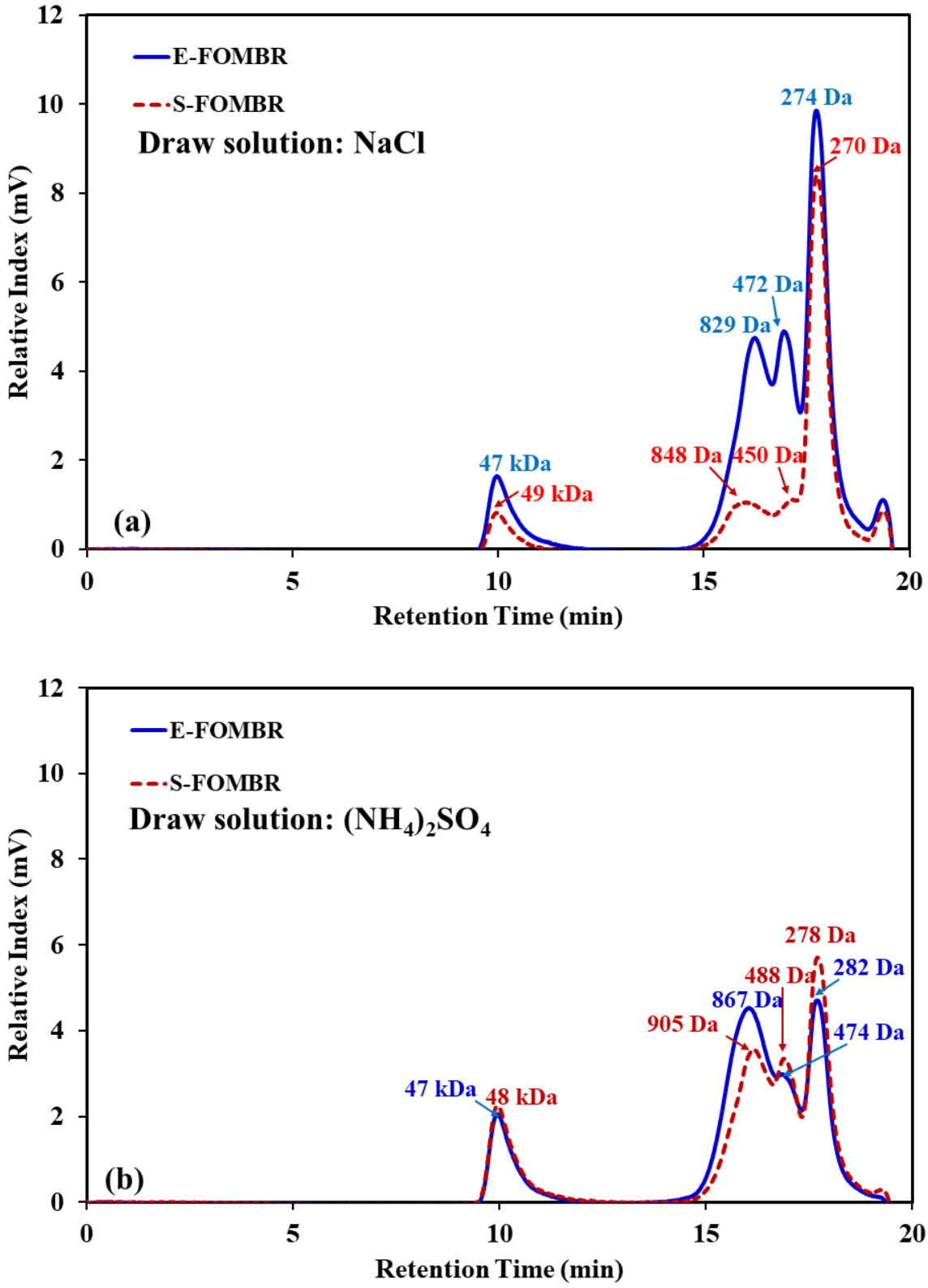

Figure B-4: Molecular weight distribution of bEPS during the steady state operation in E-FOMBR and S-FOMBR with (a) NaCl and (b) $(NH_4)_2SO_4$ as draw solutions.

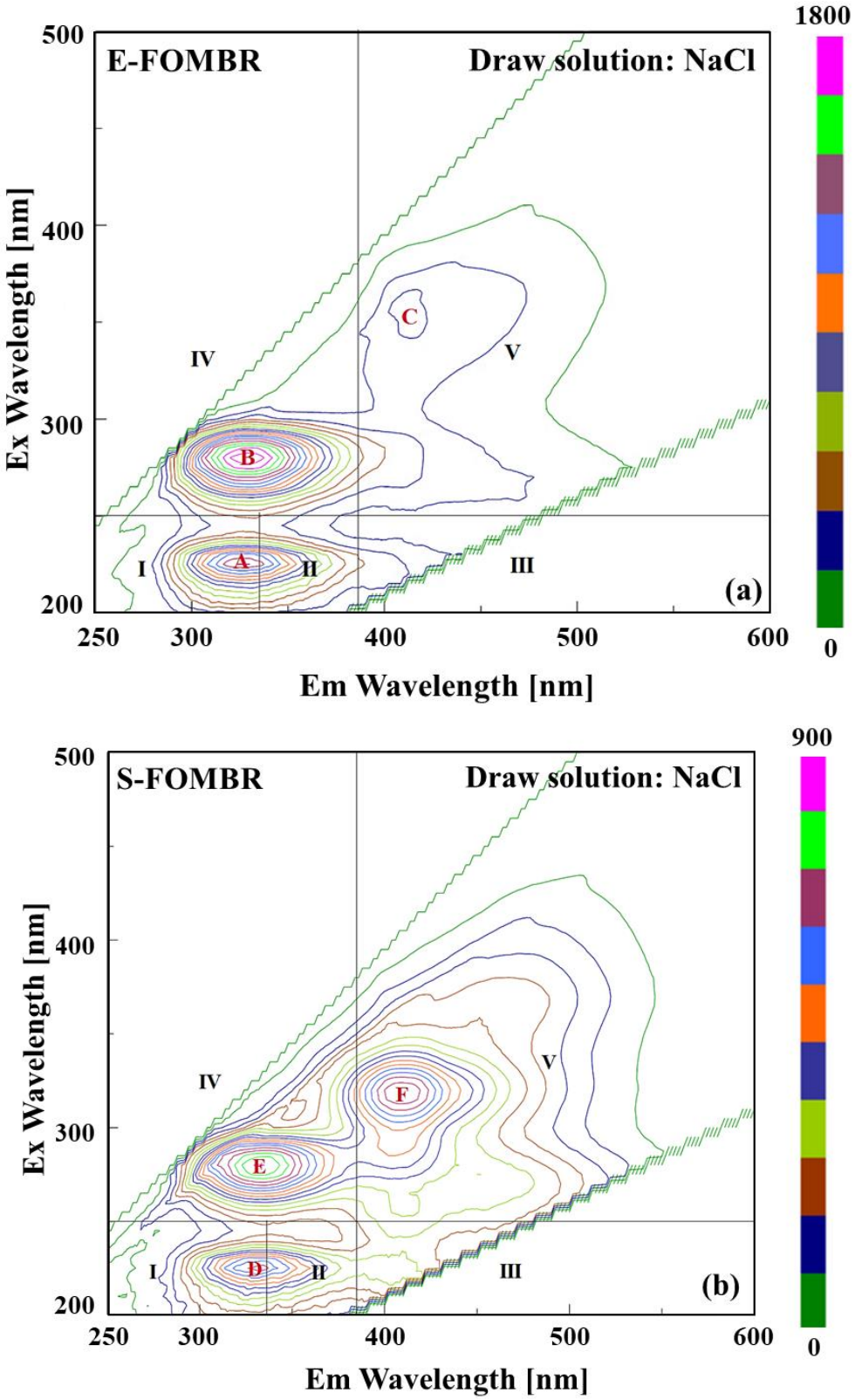

Figure B-5: Excitation emission matrix of SMP during the steady state operation: (a) E-FOMBR with NaCl as a draw solution, (b) S-FOMBR with NaCl as a draw solution, (c) E-FOMBR with $(NH_4)_2SO_4$ as a draw solution, and (d) S-FOMBR with $(NH_4)_2SO_4$ as a draw solution.

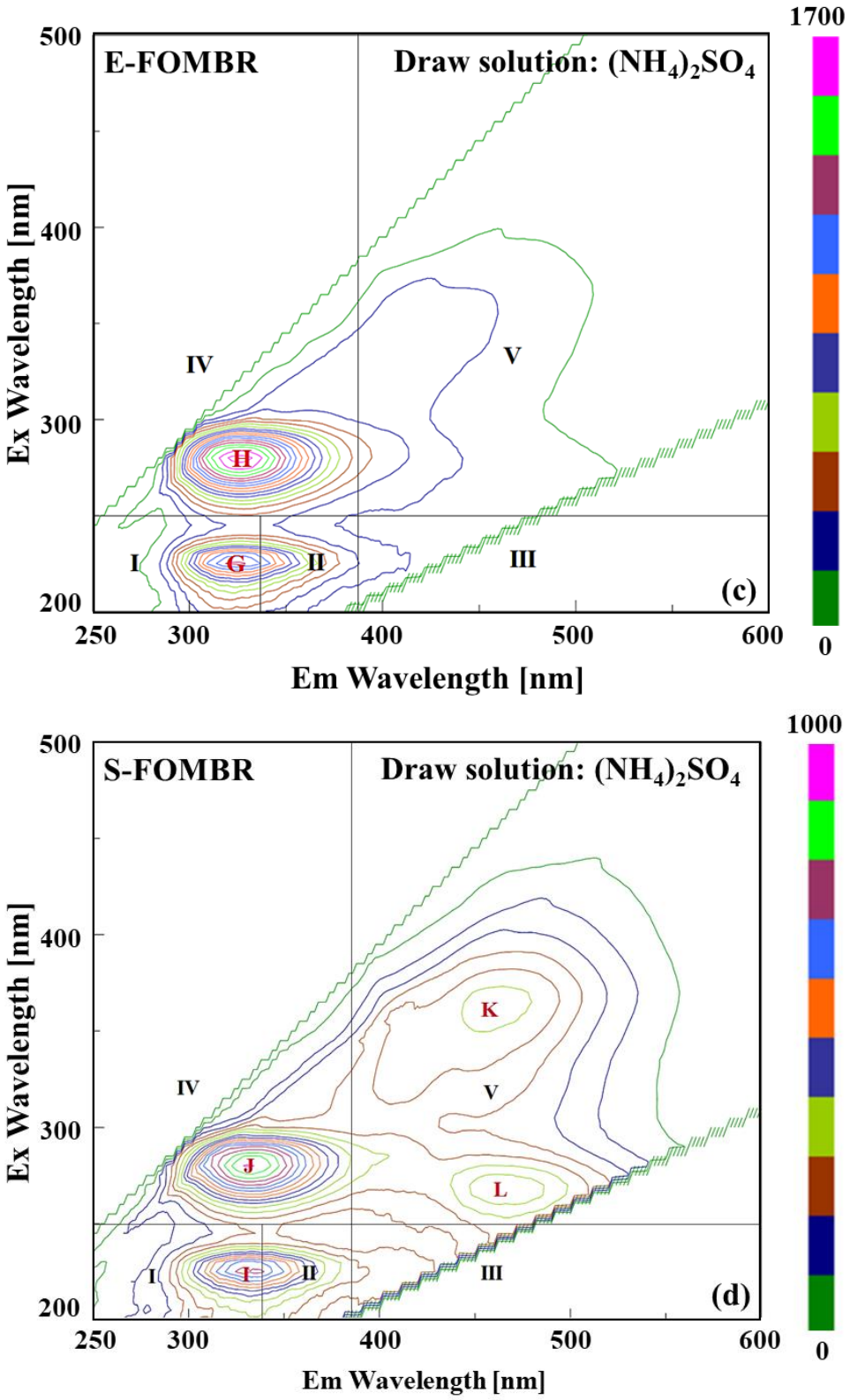

Figure B-5: Excitation emission matrix of SMP during the steady state operation: (a) E-FOMBR with NaCl as a draw solution, (b) S-FOMBR with NaCl as a draw solution, (c) E-FOMBR with $(NH_4)_2SO_4$ as a draw solution, and (d) S-FOMBR with $(NH_4)_2SO_4$ as a draw solution.(continued)

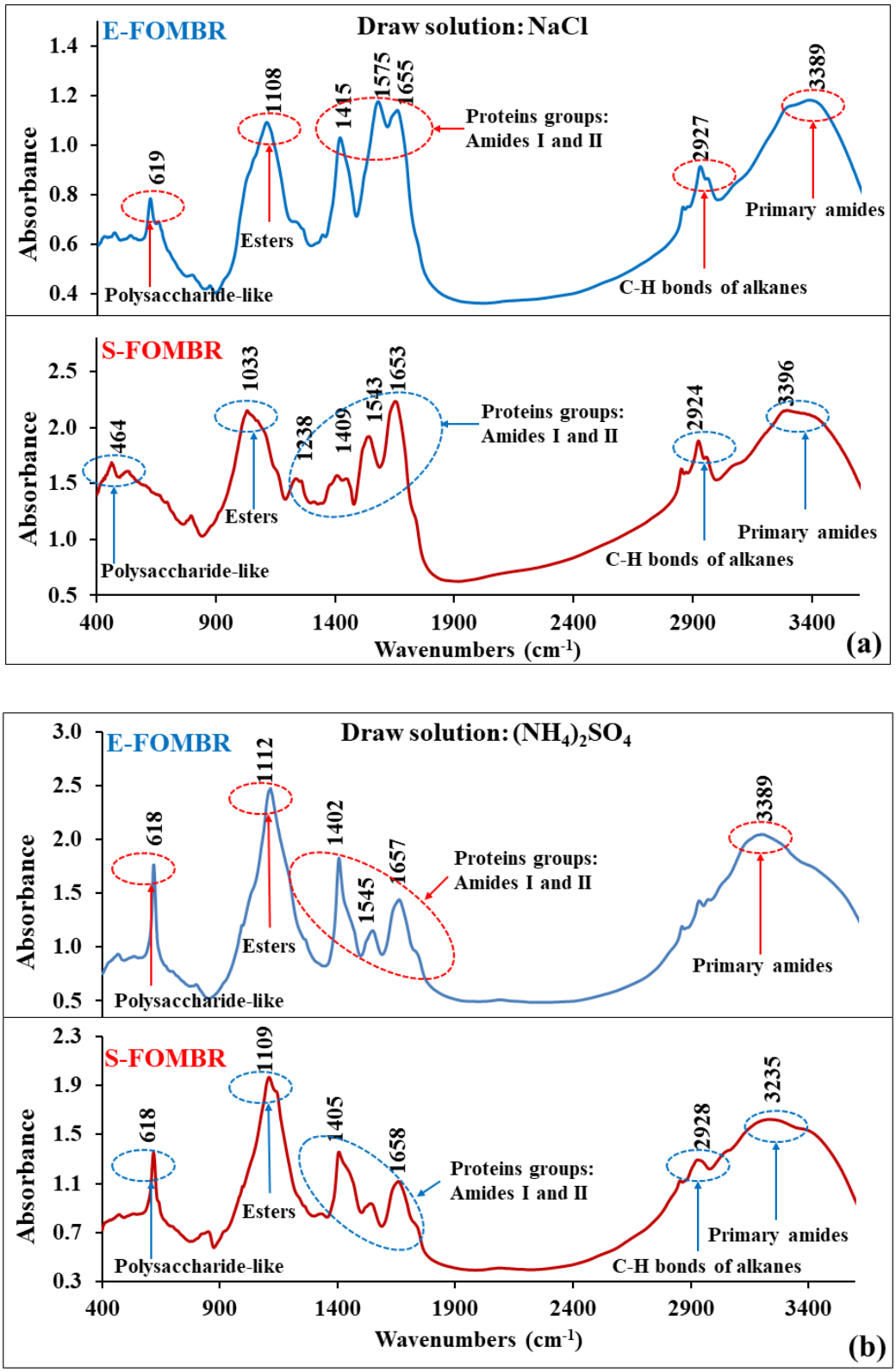

Figure B-6: FTIR spectra of bEPS during the steady state operation in E-FOMBR and S-FOMBR (a) NaCl and (b) $(NH_4)_2SO_4$ as draw solutions.